DEVELOPMENT OF FRAGILITY CURVE DATABASE FOR MULTI-HAZARD PERFORMANCE BASED DESIGN

Haseeb Tahir

Thesis submitted to the faculty of the Virginia Polytechnic Institute and State University in partial fulfillment of the requirements for the degree of

Master of Science

In

Civil and Environmental Engineering

Matthew R. Eatherton, Chair

Roberto T. Leon

Madeleine M. Flint

June 3, 2016

Blacksburg, Virginia

Keywords: Multi-hazard, Earthquake, Hurricane, Tsunami, Performance Based Design, Fragility Curves, Incremental Dynamic Analysis

DEVELOPMENT OF FRAGILITY CURVE DATABASE FOR MULTI-HAZARD PERFORMANCE BASED DESIGN

Haseeb Tahir

Abstract

There is a need to develop efficient multi-hazard performance based design (PBD) tools to analyze and optimize buildings at a preliminary stage of design. The first step was to develop a database and it is supported by five major contributions: 1) development of nomenclature of variables in PBD; 2) creation of mathematical model to fit data; 3) collection of data; 4) identification of gaps and methods for filling data in PBD; 5) screening of soil, foundation, structure, and envelope (SFSE) combinations.. A unified nomenclature was developed with the collaboration of a multi-disciplinary team to navigate through the PBD. A mathematical model for incremental dynamic analysis was developed to fit the existing data in the database in a manageable way. Three sets of data were collected to initialize the database: 1) responses of structures subjected to hazard; 2) fragility curves; 3) consequence functions. Fragility curves were critically analyzed to determine the source and the process of development of the curves, but structural analysis results and consequence functions were not critically analyzed due to lack of similarities between the data and background information respectively. Gaps in the data and the methods to fill them were identified to lay out the path for the completion of the database. A list of SFSE systems applicable to typical midrise office buildings was developed. Since the database did not have enough data to conduct PBD calculations, engineering judgement was used to screen SFSE combinations to identify the potential combinations for detailed analysis. Through these five contributions this thesis lays the foundation for the development of a database for multi- hazard PBD and identifies potential future work in this area.

DEVELOPMENT OF FRAGILITY CURVE DATABASE FOR MULTI-HAZARD PERFORMANCE BASED DESIGN

Haseeb Tahir

General Audience Abstract

There is a need to develop efficient multi-hazard performance based design (PBD) tools to analyze and optimize buildings at a preliminary stage of design. The first step was to develop a database and it is supported by five major contributions: 1) development of nomenclature of variables in PBD; 2) creation of mathematical model to fit data; 3) collection of data; 4) identification of gaps and methods for filling data in PBD; 5) screening of soil, foundation, structure, and envelope (SFSE) combinations.. A unified nomenclature was developed with the collaboration of a multi-disciplinary team to navigate through the PBD. A mathematical model for incremental dynamic analysis was developed to fit the existing data in the database in a manageable way. Three sets of data were collected to initialize the database: 1) responses of structures subjected to hazard; 2) fragility curves; 3) consequence functions. Fragility curves were critically analyzed to determine the source and the process of development of the curves, but structural analysis results and consequence functions were not critically analyzed due to lack of similarities between the data and background information respectively. Gaps in the data and the methods to fill them were identified to lay out the path for the completion of the database. A list of SFSE systems applicable to typical midrise office buildings was developed. Since the database did not have enough data to conduct PBD calculations, engineering judgement was used to screen SFSE combinations to identify the potential combinations for detailed analysis. Through these five contributions this thesis lays the foundation for the development of a database for multi- hazard PBD and identifies potential future work in this area.

ACKNOWLEDGEMENTS

I would like to express my sincere gratitude to Dr. Matthew R. Eatherton for inviting me to become part of this project and for his guidance. He taught me to thick critically about my research. I would also like to thank my committee members, Dr. Roberto T. Leon and Dr. Madeleine M. Flint, for their guidance, support and time.

I would also like to thank my family for their love and support through my education. I would also like to thank my friends for their support and encouragement.

Table of Contents

LIST OF FIGURES

LIST OF TABLES

Chapter 1 Introduction

1.1 Motivation

Earthquakes, hurricanes, and tsunamis can cause extreme damage to a building during its lifetime. Most structures are designed using the building codes of their region. Building codes are intended to prevent the collapse of structures and loss of life, but they do not explicitly limit damage during these catastrophic hazards. Performance based design (PBD) can be used to design more resilient structures and to estimate damage in the case that hazards affect the structure. Conversely, PBD can be used to relax requirements for unimportant buildings. It also helps to make decisions like whether it is more economical to spend money to construct a resilient structure or to spend money on repairs if disaster occurs. Currently, practical applications of PBD are limited to earthquakes, but researchers are working to include hurricanes and tsunamis in PBD.

The motivation for this thesis is to support the development of a framework and the means to conduct the multi-hazard performance based design of a midrise office building at an early stage of conceptual design of the building. The multi-hazard performance based assessment will then be utilized in the next part of this study to optimize the SFSE system for the building. Performance based design of buildings requires a computationally expensive nonlinear analysis to characterize the response of buildings. A database of fragility curves is also required to estimate the damage caused in the structural and non-structural components. Finally, consequence functions are required to convert the amount of damage to monetary value and life loss. A database of analyses of generic buildings, fragility curves for structural and non-structural components, and the consequence functions needs to be developed because it is inefficient for engineers to analyze all of the SFSE combinations for every single project. The relationships developed for the generic

buildings will help to optimize the SFSE combination at an early stage of design. The last point of the motivation is to identify the gaps in the collected information and recommend methods to fulfill them.

1.2 Scope

This study is the first phase of a larger NSF funded project to optimize the soil, foundation, structure, and envelope (SFSE) system of a building by multi-hazard PBD to achieve a sustainable and resilient design. The goal of this study is to develop a database that may be used to conduct a multi-hazard PBD and optimize SFSE systems. Since the FEMA P58 methodology and the PEER performance based earthquake engineering framework methodology for PBD regarding earthquakes already exists, it is reasonable to extend these methodologies to include hurricane and tsunami as hazards.

This study was partitioned into four major tasks. The first task was to develop a nomenclature of "pinch points" so that the terminologies from the structural and nonstructural disciplines could be combined. Pinch points are intersections between analyses where one analysis passes a limited number of variables to the next. Pinch point variables (here called pinch points) are generic variables that describe the type of data passed at the pinch points. In the PBEE methodology, the pinch points are: intensity measures (IMs), engineering demand parameters (EDPs), damage states (DSs), and decision variables (DVs). Intensity measure is used to define the intensity of hazard such as wind speed, water depth, and spectral acceleration etc. Engineering demand parameter measures the response of a structure when subjected to a hazard such as interstory drift ratio. Damage state explains the extent of damage suffered by a component or the whole structure. Qualitative description of damage suffered by a component such as cracking is used to define a DS, and it normally has a method of repair associated with it. The decision variable

is data used to make final decisions about the performance of the structure such as repair cost. At the same time, it was also important to set up the terminologies for the pinch point for each of the hazards.

The second task was to study the effects of hazards and the methodologies that are developed for each of the hazards i.e. (Earthquake, Hurricane, and Tsunami) to formulate a unified framework for terminology and storing data to support multi-hazard performance based design. The third task was to collect the data regarding the response of building subjected to hazards, component fragility curves and the consequence functions. The nature of these data will be described in Chapter 4, 5 and 6 respectively. Data collected regarding response of building subjected to hazard was not critically analyzed because there were not enough similarities between the data. Component fragility curves were critically reviewed to determine the quality of data used to develop theses curves. Consequence functions were just collected because no background information was found to critically review. The last task is to identify the gaps in the database and recommend the analyses and the tests that could be conducted to collect the missing data.

The development of the database led to the review of the ten structural background studies that were the basis of the FEMA P-58 structural component fragility curves. The complications faced by the authors of the background studies and the comparison of the background studies provided the foundation for the recommendation to improve the development of the fragility curves. A bilinear mathematical model was also proposed to categorize the IDA curves in order to reduce the computational expense associated with performing PBD.

1.3 Organization

This thesis includes eight chapters. The second chapter reviews the existing performance based engineering methodologies for earthquake, hurricane and tsunami. Chapter 3 discusses the selection of soil, foundation, structural and envelope systems. It also discusses the development of the framework for this study and the unified nomenclature for the pinch points. Chapter 4 explains the collection of the IM to DS and IM to EDP curves. It also goes over the development of the bi-linear mathematical model to characterize the IDA. Chapter 5 focuses on the collection of the EDP to DS curves, and it also reviews the structural background studies performed for the development of the damage fragility curves for the FEMA-58. It also includes the critical review of these reports by comparing them and identifying the curves that are solely based on the engineering judgment. Chapter 6 focuses on the collection of the DS to DV curves. Chapter 7 identifies the gaps in the collected data and recommends techniques to fill these gaps. Chapter 8 provide conclusion and recommendations for future research.

Chapter 2 Methodologies

2.1 Introduction

This chapter provides a literature review of existing PBD methodologies for multi-hazard, earthquake, hurricane, and tsunami. These methodologies provide the steps for conducting performance based design of a structure. Performance based engineering for an earthquake is more developed as compared to other hazards. In addition to methodology, tools for conducting PBD are also available for earthquakes. Only methodologies are present for multi-hazard and hurricane. HAZUS provide fragility curves for communities for hurricane hazard. No fragility curves representing structural systems have been found in the literature. Lastly, PBD for a tsunami is under development and there is an ongoing effort to include tsunami loads in ASCE 7 2016 edition. The new guidelines developed will likely include performance based engineering methods.

2.2 Multi-hazard

There are multiple studies regarding multi-hazard design, but most of them are related to bridge design e.g. Bisadi & Padgett (2015), Kameshwar & Padgett (2014) etc. Multi-hazard performance based design methodology developed by Kareem & McCullough, (2011) is discussed below in detail because it is related to building design for coastal regions.

Kareem & McCullough, (2011) proposed a framework for a multi-hazard PBD of buildings in coastal environments. Some coastal environments are exposed to all three hazards: earthquake, hurricane, and tsunami. Therefore, this framework was specifically developed for the coastal environments otherwise, it could be applied to any location that is susceptible to multiple hazards. Kareem & McCullough, (2011) combined performance-based engineering with multi-hazard engineering to increase the robustness of the structures.

Figure 2-1 presents the design and analysis framework for combined multi-hazard engineering and PBE. The first step is to determine to which hazards a structure is exposed based on its location and history. Probabilistic distribution of maximum wind speed based on location, exposure, and elevation of the site can be used to define wind hazard at the site. Storm surge is an effect of the hurricane for which surge depth, velocity, and duration are essential variables. Hurricane storm surge could be modeled using several models available in the literature like ADCIRC (Advance circulation), STWAVE (Steady state spectral wave), SWAN (Simulating wave near shore), and SLOSH (Sea, Lake, and Overland surges for hurricanes). TSUNAMOS (NEES project) can be used to model tsunami waves similar to storm surge. Earthquake ground motions could also be developed using ground motion equations or obtained from previous earthquakes. A stochastic model of single and multiple hazards occurring during the lifetime of the structure is developed using the models developed for hazards.

After hazard and loads are defined, structural fragility analysis can be conducted. Fragility curves for structural and non-structural components developed by FEMA and HAZUS-MH can be used in these calculations. Acceptable damages for events during the life of structure can be calculated by conducting a risk analysis. Optimization of the structure can be performed until acceptable damage and monetary losses are achieved.

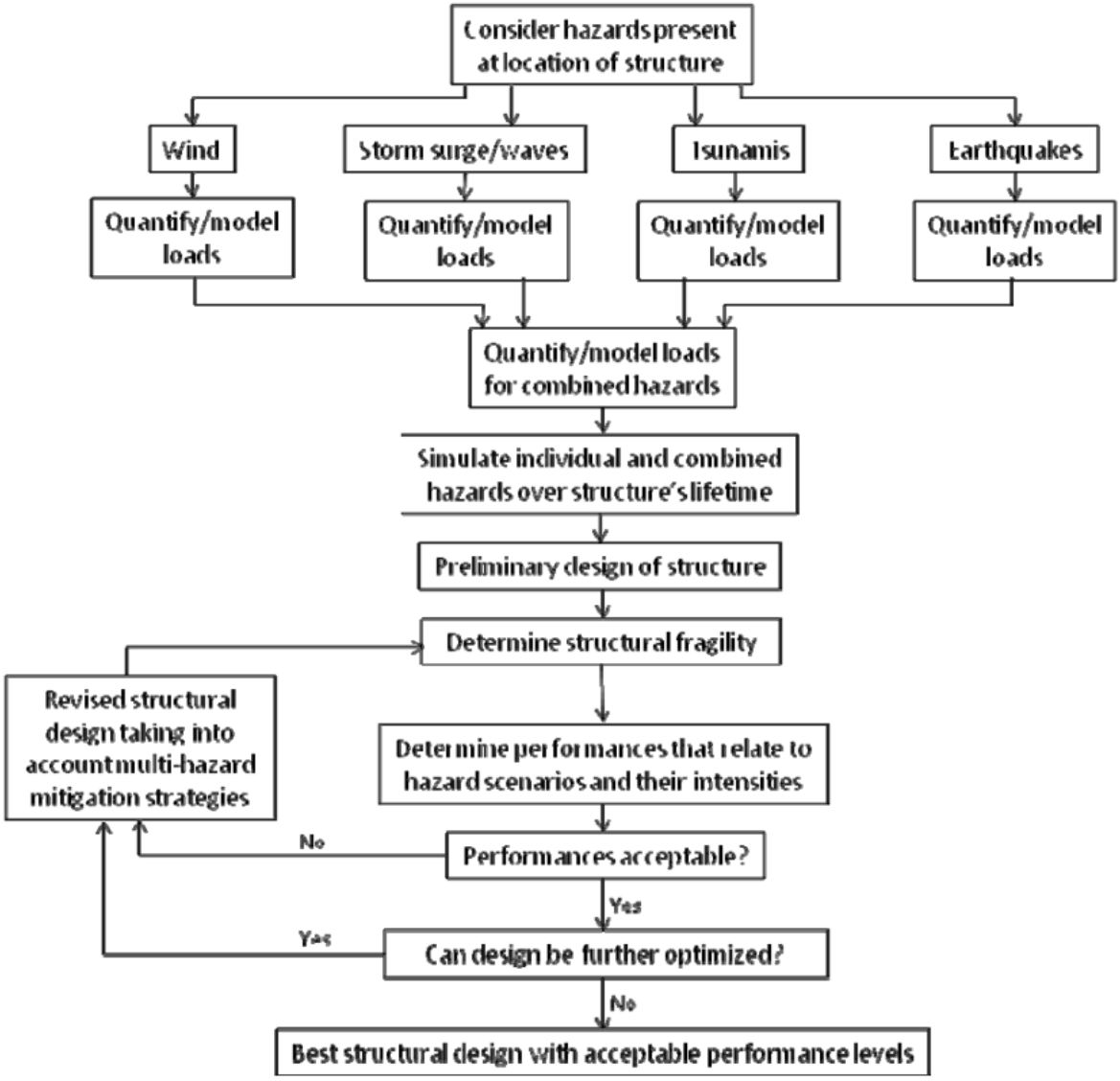

Figure 2-1. Design and analysis framework for combined multi-hazard engineering and PBE (Kareem & McCullough, 2011).

2.3 Earthquake

Earthquakes are caused by the movement of the tectonic plates under Earth's crust. Reid's Elastic Rebound theory explains the energy release during an earthquake (B. F. Howell, 1997). Tectonic plates are constantly moving at very slow rate due to which plates deform and energy is stored. Once the stored energy increases the internal strength of the plates, there is a sudden release of energy which is felt as shaking of the ground. It also explains the severity of earthquakes being directly proportional to the time between earthquakes because the longer the energy is stored the higher amount of energy will be released. There are four main aspects of earthquakes: ground motion, tsunami, liquefaction, and landslide.

Ground motion is caused by the seismic waves that propagate through soil during an event and it is measured as ground acceleration. Tsunami is an aspect of the earthquake, but it is treated as a separate hazard in this study due to its different effects on structures. Liquefaction is a phenomenon caused by earthquakes when there is loose granular saturated soil (Oommen, Drive, & Baise, 2013). Liquefaction reduces the strength and stiffness of the soil and forces ground water to move above the surface. It can cause substantial displacement and relative displacement in structures or in severe cases structures could also get buried. The last aspect is landslide which happens when a stable slope becomes unstable due to ground shaking.

FEMA P-58 (Applied Technology Council, 2012) provides methodology and tools to conduct performance based earthquake (PBEE) engineering calculations. Figure 2-2 shows the underlying probabilistic framework for FEMA P-58 (Moehle & Deierlein, 2004). It is comprised of a tool called Performance Assessment Calculation Tool (PACT), Fragility database, and supplementary tools for pre-analysis calculations. Causalities, repair time, repair cost, and unsafe placarding are used to measure the performance of a structure in this methodology. It allows users

to conduct three types of performance assessments: Intensity-based assessment, Scenario-based assessment, and Time-based assessment. Intensity-based assessment can be used to calculate the performance of a building subjected to a design spectrum which can be user defined or building code response spectrum. For buildings located near faults, scenario-based assessment can be used because it is based on an earthquake with specific magnitude and distance from the building. An earthquake can be selected from past data or future projected earthquake. Time-based assessment is used to measure the performance of a structure over a specific period of time. It considers all the earthquakes that could happen during that period of time, and it also accounts for uncertainty in magnitude, location, and intensity of motion of future earthquakes.

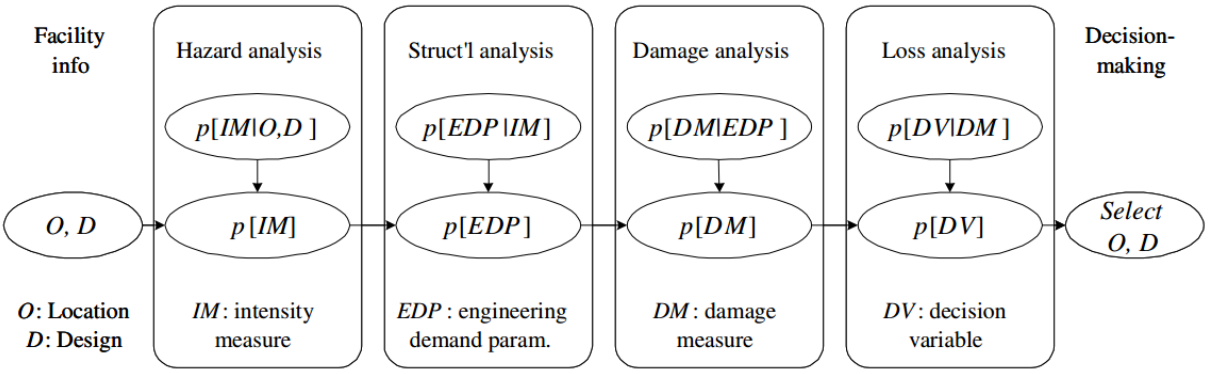

Figure 2-2. Underlying earthquake probabilistic framework (Moehle & Deierlein, 2004)

The first step of the analysis is to develop the building model. Information about structural components, non-structural components and occupancy is entered. Occupancy models for some building types are provided in this methodology that can be used to calculate casualties in case of the collapse of a building. There is a database of component fragility curves from structural and non-structural components and consequence functions of repair cost and repair time for corresponding damage states of each component available for analysis. The next step is to define hazard based on the type of assessment required. After that results from the structural analysis are

entered. Depending upon the complexity two types of analysis can be done: 1) nonlinear-response history, 2) equivalent lateral force method. Monte Carlo simulation is used for performance calculations to account for uncertainties related to seismic performance.

2.4 Hurricane

Hurricane can split into two main aspects: wind and storm surge. The Wind can have sub-aspects: wind pressure, uplift, wind-borne debris, and rain. The Storm surge can have sub-aspects: wave, scour, and water-borne debris. Recent studies of post-disaster surveys have shown it is important to analyze buildings for combined effects of these intensity measures instead of looking at them separately. Performance based hurricane engineering (PBHE) methodologies and hurricane modeling techniques are presented in this section.

Vickery et al., (2006) presented the HAZUS-MH methodology for modeling of hurricane hazard, terrain, and wind induced pressures, and debris impact probabilities. The hurricane model used in HAZUS was developed by updating the Vickery et al. (2000a,b) model. The updates included: limitation on the change in the storm heading as a function of translation speed, and relating radius to maximum wind speed to central pressure and latitude. Statistics of key parameters of a hurricane from historic data and model simulation from Gulf and Atlantic oceans of USA were used to reconfirm the model. The rainfall model is an extension of the wind model and it is used to estimate the water intrusion in the building through broken windows and doors. It is a function of rainfall rate, radius of maximum speed, radius to the point of interest, rate of change of central pressure, and asymmetric distribution of rainfall. Wind speed at lower levels is highly affected by the roughness of the terrain. HAZUS also provides a parameter roughness length based on the spacing of buildings, trees, and other obstructions to account for the difference in terrains.

Empirical equations are developed to model wind loads and uplift forces. Lastly, HAZUS also provide two models for wind debris: residential, and rooftop gravel.

A PBHE framework using total probability theorem for risk assessment is proposed by (Unnikrishnan et al., 2013). The proposed methodology accounts for the multi-hazard nature of hurricanes meaning wind speed, water depth etc. can be accounted for in three different forms: independent, interacting, and hazard chain. This study refers to these hazards as intensity measures because hurricane is one hazard and wind speed and water depth are intensity measures. Figure 2-3 shows a flowchart diagram of the framework. The framework can be segregated into five steps: hazard analysis, interaction analysis, structural analysis, damage analysis, and loss analysis.

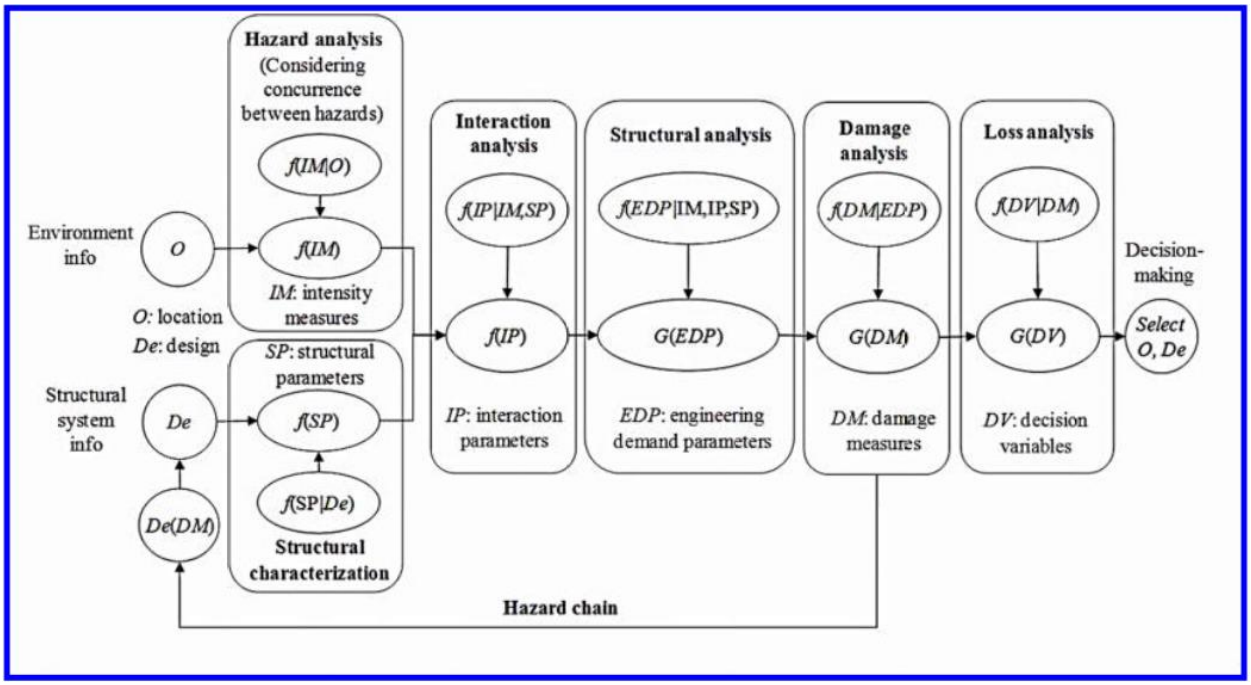

Figure 2-3. PBHE framework (Unnikrishnan et al., 2013)

2.5 Tsunami

Tsunami is caused when an earthquake occurs due to movement of plates under the ocean. There are four aspects of the tsunami: wave, scour, water-borne debris, and standing water. The intensity measures for each aspect are explained in the next chapter. There is no existing PBD framework for the tsunami in the literature, but work is going on including the design provision and tsunami loads and effects in the ASCE 7 2016 edition (Chock, Robertson, & Riggs, 2011).

According to Chock et al., (2011) tsunami load provision has not been updated since 1980's. Use of tsunami hazard maps has been limited to evacuation planning only and they are not being implemented in the structural design. Network of Earthquake Engineering Simulation (NEES) has been actively working on the development of new tsunami load provisions using large scale model testing at Oregon state university in wave basin and wave flume facility. These new provisions are intended for two types of usages: prescriptive loading conditions for building codes, and performance-based criteria for site specific hazard analysis and design of essential facilities. Equations to calculate loads on structures are developed for each of the following loading conditions in Chock et al., (2011).

1. **Hydrostatic Forces:**
   - Lateral Forces
   - Buoyant Forces
   - Additional Gravity Loads on Elevated Floors
2. **Hydrodynamic Forces:**
   - Lateral Impulsive Forces of Tsunami Bores
   - Uplift on Elevated Floors
   - Surge Forces and Damming by Waterborne Debris
3. **Debris Impact Forces:**
   - Tsunamis are capable of generating large debris strikes
4. **Scour Effects:**
   - Shear of cyclic inflow and outflow

- Transient liquefaction due to excess internal pore pressure gradient during rapid drawdown

Charvet et al., (2015) developed empirical multivariable fragility curves (IM to DS) from the damage data collected from the Kesennuma city after the 2011 Great East Japan Tsunami. Effects of flow depth, flow velocity, and debris impact are considered in the development of the fragility curves for all of the buildings, wood buildings, masonry buildings, RC buildings, and steel buildings. Charvet et al., (2015) concluded from the data collected that the collapse of the RC building and steel buildings are not entirely related to the flow depth which is contrary to the behavior of the wood and the masonry buildings. It was also noted that median values of flow depth and velocity decrease when effects of flow depth and velocity are considered as compared to just flow depth. It is important to analyze the response of buildings under combinations of multiple intensity measures because combination of intensity measures tends to be the controlling case instead of individual intensity measures. Figure 2-4 is an example of multivariate fragility curve developed by (Charvet et al., 2015). Charvet et al., (2015) also proved that empirical multivariate fragility curves based on flow velocity and flow depth reach a certain damage state at a lower value as compared to single variable flow depth fragility curves. Figure 2-5 shows the influence of intensity measure on damage state 1 to 5 which correspond to minor non-structural damage to complete collapse of the structure. The direction of the arrow shows the direction of increase of influence of the corresponding intensity measure.

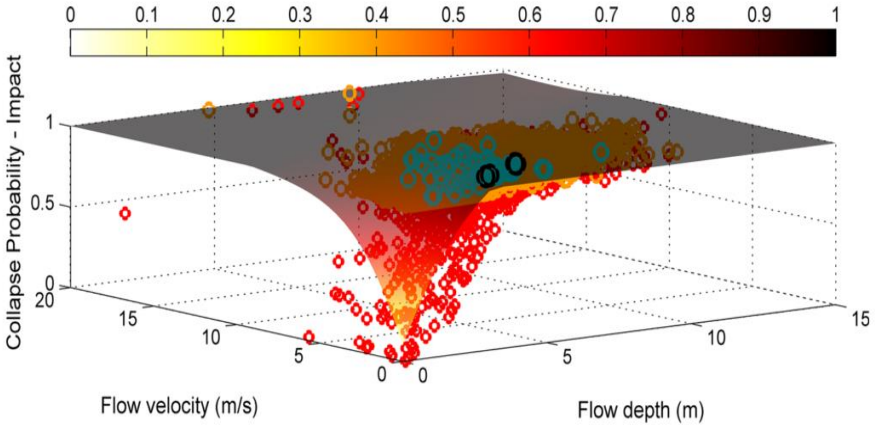

Figure 2-4. Multivariate fragility curve for tsunami (Charvet et al., 2015)

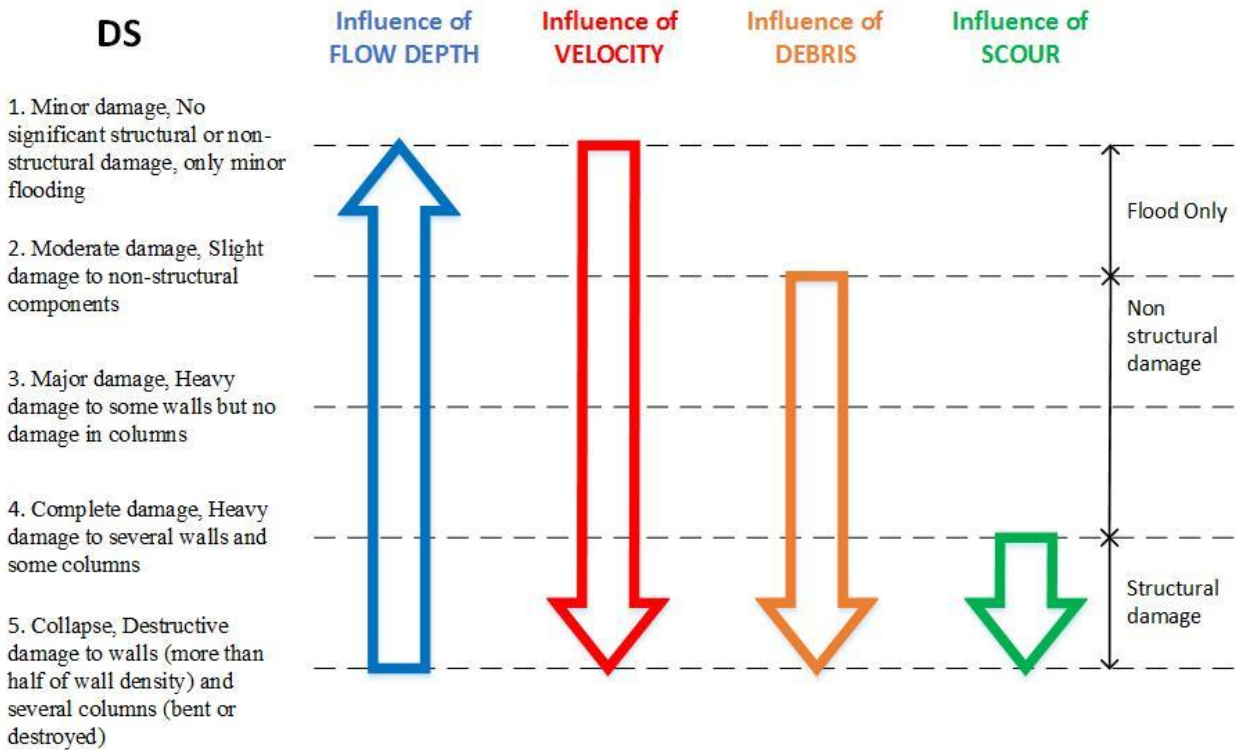

Figure 2-5. Influence of multiple intensity measures on damage states of buildings (Charvet et al., 2015)

Chapter 3 Framework

A new framework was proposed by modifying the FEMA P-58 framework. The first goal was to extend the framework to include hurricane and tsunami as hazards. Even though tsunami is an aspect of earthquakes, it is considered as a separate hazard in this study because of it extreme effects on structures. PBD can be summarized as an analysis that is done to obtain Decision variables (DV) based on a set of Intensity Measures (IM) describing one or more hazards. PBD can be partitioned into four pinch points: Intensity Measure (IM), Engineering Demand Parameter (EDP), Damage State (DS), and Decision Variable (DV). IM defines the intensity of hazards e.g. ground acceleration, wind speed etc. EDP represents the response of a structure when subjected to certain IM e.g. Inter story drift ratio. DS is used to describe the amount of damage occurring in components of the structure. DV are the end results that can be used to make a decision about the design of the building. They are normally in the form of monetary expenses, loss of life or downtime.

3.1 Nomenclature

Pinch points are defined for three hazards and to make sure all of the pinch points are included, first, each hazard was subdivided into its aspects and then the pinch points were selected. This study is part of a larger multidisciplinary project, so it was crucial to come up with a unified nomenclature. Table 3-1 includes the list of the pinch points that were selected after consensus in the teams. Appendix A has the definitions of the nomenclature terminology.

Table 3-1 was developed based on engineering judgment and then refined by the naming conventions used in the industry. It was distributed into six columns. The first column has the name of the hazard and the characteristics that are required to define it. The second field has the

Hazard Aspects. It is a supporting field which shows the relationship between the IM and the hazard. The third column has the IMs for each of the hazard aspects. The fourth column has the EDP related to the IM. The fifth column describes the general forms of damage that occur in the structure. The last column has the decision variables.

Table 3-1: Unified Nomenclature of Pinch Points for all of the Multidisciplinary Teams.

Hazard	Hazard Aspects	Intensity Measures [IM]	EDP	Damage States [DS]	Decision Variables [DV]
Hurricane: Date/Time Category Min. Distance Mean Sea Surface Elevation Tide Associated Precipitation Soil Saturation Before Event	Wind pressure	Wind velocity	Deflection	Peel/Detachment Deformation Crack/tear Deformation Breach/crack/tear Wetting Crack Displacement Collapse	Casualties, Repair Costs, Repair Time, Carbon Emission, Embodied Energy, Building Lifetime
		Exposure	Roof Drift Ratio		
	Uplift	Wind velocity	Deflection		
	Wind-borne debris	Debris class	Deflection		
		Debris velocity			
	Wind-driven rain	Wind velocity	Volume of Water		
		Rainfall intensity			
	Rain	Rainfall Intensity	Volume of Water		
	Standing Water	Standing water elevation	Deflection		
		Standing water duration	Volume of Water		
	Wave	Wave height	Deflection		
		Wave period			
		Wave velocity			
	Erosion / Scour	Wave velocity	Settlement		
			Differential Settlement		
	Water-borne debris	Debris class	Deflection		
		Debris velocity			
Earthquake: Date/Time Magnitude Number Each year Distance to Fault line Soil Conditions	Ground Motion	Ground accelerations	Inter story Drift Ratio		
			Roof Drift Ratio		
			Residual Drift		
			Floor Velocity		
			Floor Acceleration		
	Liquefaction	Ground accelerations	Settlement		
			Differential Settlement		
	Landslide	Ground accelerations	Deflection		
	Tsunami	-	-		
Tsunami: Date/Time Distance from Shore Tide Water Duration Water level Mean Sea Surface Elevation	Wave	Wave height	Deflection		
		Wave period			
		Wave velocity			
	Erosion / Scour	Wave velocity	Settlement		
			Differential Settlement		
	Water-borne debris	Debris class	Deflection		
		Debris velocity			
	Standing Water	Standing water elevation	Deflection		
		Standing water duration	Volume of Water		

3.2 Selection of SFSE systems

One of the goals of this study is to identify potential SFSE systems for a midrise office building. A set of soil, foundation, structural and envelope systems were selected to develop multiple SFSE combination. Engineering judgment and use of systems in practice were used to select three soil systems, four foundations systems, and 11 structural systems. Envelope systems have been divided into two parts: wall systems and roof systems. Researchers on the envelope team have selected 32 wall systems and work on roof systems is still ongoing.

3.2.1 Soil Systems

The following are the three soil systems selected for this study.

1. Unimproved Soil

   When no soil modification or reinforcement techniques are used on the soil it is considered as unimproved soil. Shallow footings are mainly used with unimproved soil if the soil is strong enough otherwise deep footings or soil improvement techniques are used.

2. Reinforced Soil

   Sha footings cannot be constructed on the weak soil. Therefore, reinforcement techniques like adding layers of geotextile can be used to increase the allowable soil pressure. Soil reinforcing techniques only increase the bearing strength of the soil, but do not modify the behavior of soil through characteristics such as shear velocity.

3. Modified Soil

   Soil can also be modified to improve its allowable pressure by techniques like grouting. Not only soil modification techniques improve the allowable pressure, but they also change the behavior of the soil. For example, after grouting the soil acts as a solid rock while changing properties such as shear velocity.

3.2.2 Foundation Systems

The following are the four foundation systems selected for this study.

1. Single Footing

   It is the simplest footings for individual columns. Each column has its own footing. Figure 3-1-a shows a single footing.

2. Continuous Footing

   These footings are used for load bearing walls. They are rectangular in shape, and Figure 3-1-b shows an example of Continuous footing.

3. Mat Footing

   These footings are used as combined footing for all of the columns of the building. It acts as a raft under the building. Sometimes the slab of the entire basement can also be used as a mat footing. They are normally used when single footings overlap due to low allowable pressure. Figure 3-1-c shows a Mat footing.

4. Deep Footing

   Deep foundations are used in the case of weak soil. Drilled piers are constructed by drilling holes in the ground and the filling them with reinforced concrete. Piles are vertical structural elements made up of wood, concrete or steel driven into ground e.g. steel H-pile. Deep foundations have pile cap on top of them, and the structure rests on the pile caps. Figure 3-1-d shows an example of Drilled piers/ Driven piles.

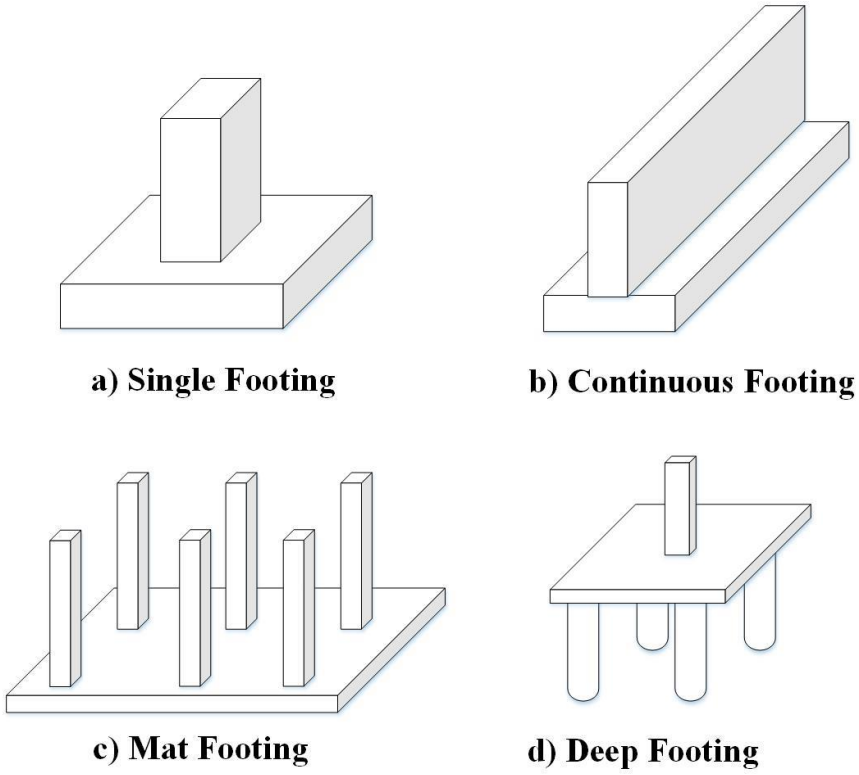

Figure 3-1: Types of Footings: a) Single Footing, b) Continuous Footing, c) Mat Footing, d) Deep Footing

3.2.3 Structural Systems

Structural systems were selected to cover four different construction materials namely concrete, steel, masonry, and wood. Structural systems were selected from the ASCE 7-10 to ensure they are consistent with current structural systems used for midrise office buildings.

1. Cold Formed Steel Shear Walls

   In this system, lateral forces are transferred by shear in the cold formed shear wall. Energy is dissipated by local buckling and yielding of the studs and yielding of nails. Damage occurs in the form of screw head pull through of sheathing, permanent rotation of sheathing, and buckling of studs (Grummel & Dolan, 2010). Figure 3-2-c shows an illustration of the shear wall system.

2. Steel Concentrically Braced Frame

In this system, lateral forces are transferred by steel members oriented diagonally in frames called braces. Energy is dissipated by yielding and buckling of the braces. Damage occurs in the form of yielding, buckling and rupture of the braces (Roeder, Lehman, & Lumpkin, 2009). Figure 3-2-a shows an illustration of steel concentrically braced system.

3. Steel Eccentrically Braced Frame

In this system, lateral forces are transferred by the combination of braces and link beams. Energy is dissipated using flexural or shear hinging of the link beams. Damage occurs in the link beams in the form of buckling and yielding of the beams (C. K. Gulec, Gibbons, Chen, & Whittaker, 2011). Figure 3-2-b shows an illustration of steel eccentrically braced system

4. Steel Buckling Restrained Braced Frames

This system is similar to steel concentrically braced frame except the braces are not allowed to buckle and energy is dissipated only by yielding of the braces. Damage occurs as yielding of braces.

5. Steel Plate Shear Walls

In this system, lateral forces are transferred by shear in steel plates. Energy is dissipated by local buckling and yielding of the web plate along tension fields. Damage occurs in the form of yielding, buckling, and rupture. Figure 3-2-c shows an illustration of the shear wall system.

6. Steel Moment Frames

In this system, lateral forces are resisted by flexure in members. Energy is dissipated by flexural hinging at the ends of the beams. Damage occurs as yielding, buckling, and rupture of beams (Deierlein & Victorsson, 2008). Figure 3-2-d shows an illustration of steel moment frame system.

7. Reinforced Concrete Moment Frames

In this system, lateral forces are transferred by flexure in members. Energy is dissipated by flexural hinging at the ends of the beams. Damage occurs as yielding of reinforcements, cracking of concrete, spalling of concrete and rupture of steel reinforcements (Lowes & Li, 2009). Figure 3-2-d shows an illustration of Concrete moment frame system.

8. Reinforced Concrete Shear Walls

Lateral forces are transferred by shear in concrete shear walls. Energy is dissipated by flexural hinging at the base of the wall. Damage occurs as yielding of reinforcement, cracking of concrete, spalling of concrete and rupture of steel reinforcement (Birely, Lowes, & Lehman, 2011).

9. Pre-Cast Concrete Shear Walls

Lateral forces are transferred by shear in shear walls made up of precast panels of concrete. Energy is dissipated by flexural hinging at the base of the wall. Damage occurs as yielding of reinforcement, cracking of concrete, spalling of concrete and rupture of steel reinforcement.

10. Wood Shear Wall

Lateral forces are transferred by shear in Wood panels. Energy is dissipated by inelastic deformations of nails from sheathing to studs. Damage occurs as cracking and

buckling of sheathing, fracture of studs, tear out of nails and sheathing tear out (Ekiert & Filiatrault, 2008).

11. Reinforced Masonry Shear Walls

Lateral forces are transferred by masonry shear walls. Energy is dissipated by flexural hinging at the base of the wall. Damage occurs as cracks in the masonry and yielding, buckling, and rupture of the reinforcement (Murcia-delso & Shing, 2009).

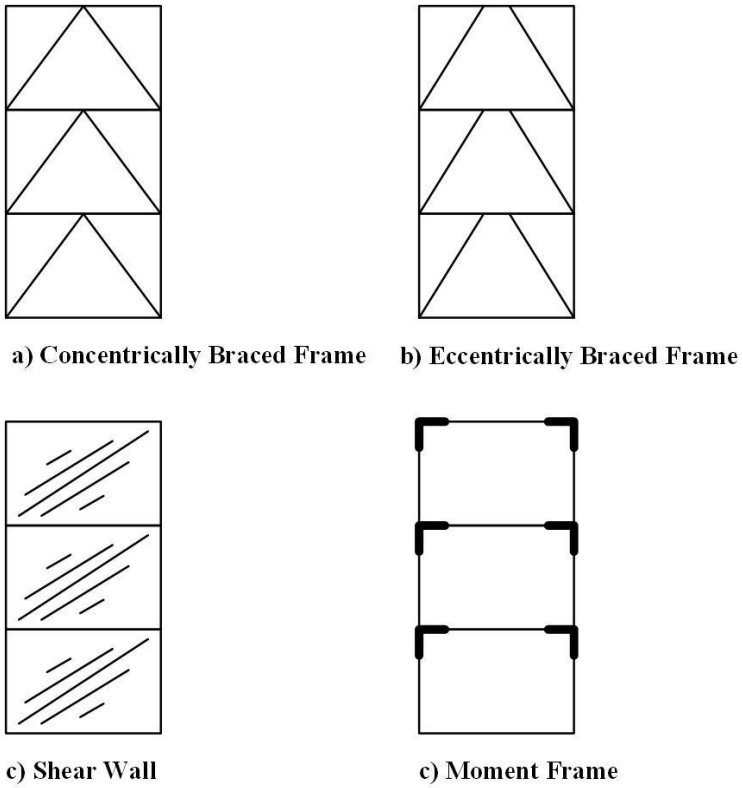

Figure 3-2: Structural Systems: a) Concentrically Braced Frame, b) Eccentrically Braced Frame, c) Shear Wall, d) Moment Frame

3.2.4 Envelope Systems

Envelope systems are being selected by the Department of Building Construction team working on the Thrust 1 of the Resilient and Sustainable building design project. A list of 32

different walls has been developed and are classified in two ways. First walls are distributed into two primary categories: infill walls and curtain walls. After that within each category walls are grouped based on four exterior finishes: Panel (Precast), Masonry, Plaster, and Glazing. Work on the selection of the roof systems in still ongoing.

3.3 Framework

This section provides the framework for the multi-hazard performance based design used in this study. The goal of this framework is to provide an analytical approach to conduct a multi-hazard performance based design. Four sets of relationships are defined for each hazard namely IM to DS, IM to EDP, EDP to DS, and DS to DV. These relationships are used to calculate DVs e.g. repair cost when a structure is subjected to a hazard. Performance based engineering is not very developed for tsunami and hurricane hazard due to which a lot of these relationships have not been developed. Some of the relationships for these hazards are developed using the post-disaster surveys, therefore, there are jumps in the pinch points like for tsunamis IM to DS curves are developed for the whole building and for hurricane IM to DS curves are developed for the building components. This framework shows the most detailed version possible, so that in the future it can incorporate all the sets of relationships. Figure 3-3 shows a flow chart of the framework.

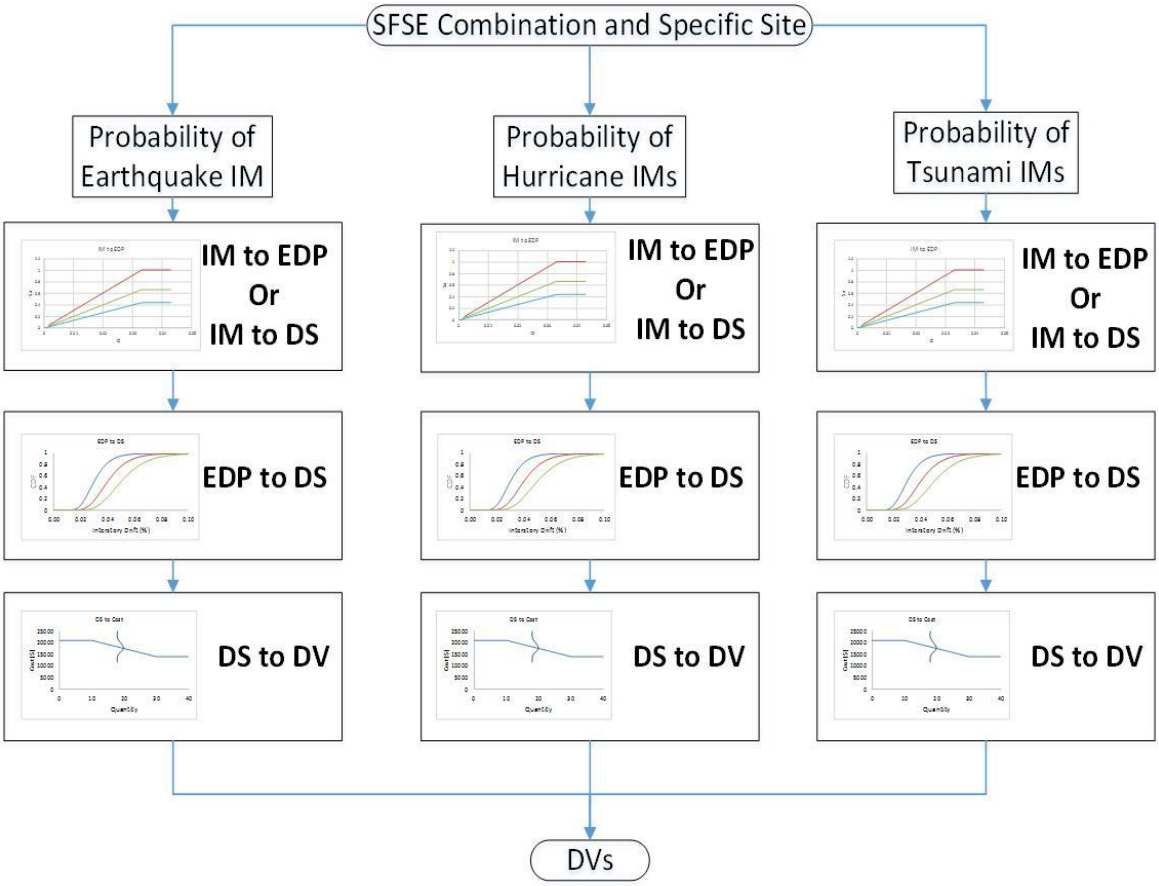

Figure 3-3. Flow chart of the framework.

Chapter 4 Intensity Measure to Engineering Demand Parameter Fragility Curves

4.1 Introduction

This chapter discusses the collection of IM to EDP curves. These curves categorize the buildings and provide a continuous function to calculate the response of building when subjected to an IM. There can be different IMs for each of the hazards e.g. spectral acceleration, wind speed, and tide height etc. Similarly, there can be different EDPs for the building like for structural damage Inter story drift is widely used, but for hospital equipment floor velocity and accelerations are more important.

4.2 IM to EDP for Earthquakes

IM to EDP curves for an earthquake are developed by using Incremental dynamic analysis (IDA). Incremental dynamic analysis (IDA) is an analysis method to estimate the response of structure due to seismic loads. In this method structural model is subjected to multiple scaled ground motions and the response parameters of structure are recorded (Vamvatsikos and Cornell 2002). Each IDA curve is developed by plotting maximum value of response of the structure versus the intensity measure. Usually intensity measure is scaled up until the collapse of the structure occurs. Spectral acceleration and interstory drift are most frequently used as IM and EDP for earthquake respectively. IDA is a computationally expensive process, and it requires detailed modeling of the building. These curves were collected so that SFSE combinations for a building could be optimized at an early stage of design without going through IDA for each system. A mathematical model was developed for the IDA curves to represent them with the least amount of parameters. Curves collected have spectral accelerations as IM and interstory drift as EDP.

Residual drift, floor velocity, and floor acceleration are also important parameters for analyzing the response the buildings, but these curves were not reported in the literature.

IDAs are represented in two ways in the literature. First is that the continuous relationship between the IM and EDP is presented. In the second version, only the collapse fragility curve is presented which gives the median IM at the collapse and the dispersion. Data was not critically reviewed because there were not enough similarities between the studies.

4.2.1 Collapse fragility curves

Collapse fragility is the first set of relationships in performance based design. It is used to calculate the probability of collapse using the IM. It is most frequently represented by a log-normal cumulative density function. Each lognormal curve can be represented by two parameters θ (Median) and β (Dispersion). This relationship is produced by postprocessing of IDA. The dispersion in the curve is due to the variability of the ground motions. Each ground motion is different in terms of frequency content, duration, period, and peak PGA due to which building respond to each ground motion differently, and building can have different drift values for same spectral acceleration due to different ground motions. Figure 4-1 shows a typical collapse fragility curve.

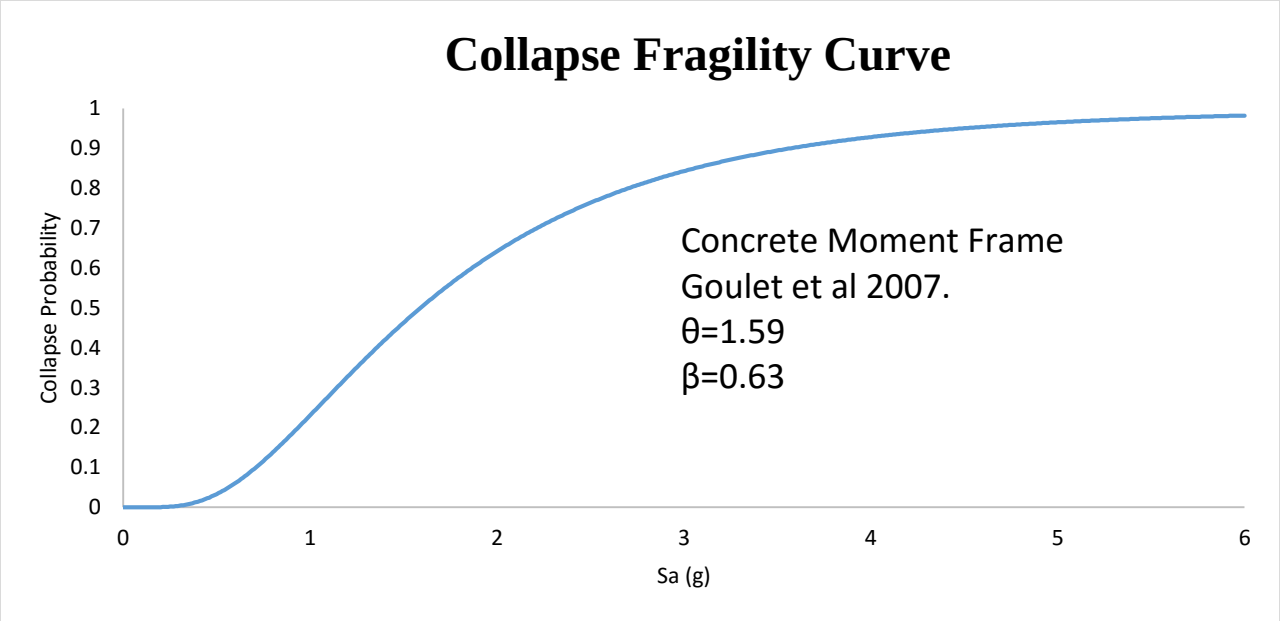

Figure 4-1. Typical Collapse Fragility Curve

4.2.2 Development of Mathematical Model

A mathematical model was necessary to represent IDA curves because it will be difficult to enter curves as raw data into the database. Cornell et al., (2000) developed a model to represent probabilistic assessment of structural demand for a steel moment frame. Later it was rearranged by Padgett, Nielson, & Desroches, (2008) in the form of Equation 1 to be able to perform linear regression analysis. S_D is structural demand which is named as engineering demand parameter in this study. a and b are constants. This model is applied to raw data from IDA results to develop a relationship between IM and EDP. In this study since most of the data is extracted from plots presented in research papers and they only have 16%, 50%, 84% fractile curves to represent the results of IDA, therefore, a mathematical model based on ATC 19 is developed below.

$$\ln(S_D) = b \times \ln(IM) + \ln(a) \qquad \text{Equation 1}$$

ATC 19 was used to develop a theoretical justification for the mathematical model. Based on ATC 19 (Rojahn, Whittaker, & Hart, 1995) structures can be divided into three groups:

1: Short period T < 0.03 sec Infinite Displacement	2: Medium Period 0.12 < T < 0.5 sec Equal Energy	3: Long Period T > 1 sec Equal displacement
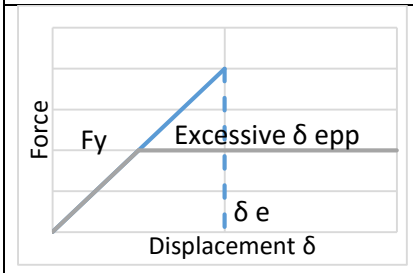	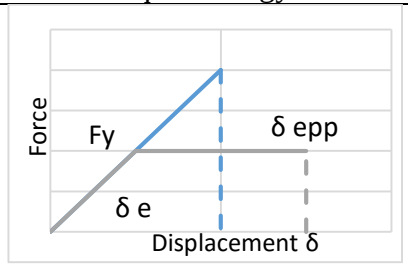	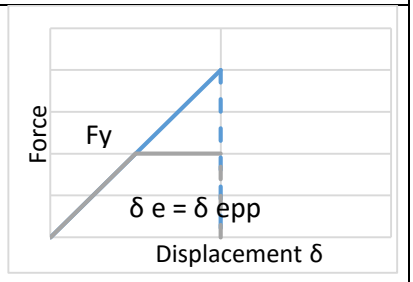
$Sa = \frac{F}{m} \quad \delta e = \frac{F}{k} \quad \delta y = \frac{Fy}{k}$		

The relationship between the Spectral acceleration (S_a) and the drift can be categorized as bi-linear for short and long period structures. For short period structures collapse happens at yield and for long period structures deforms in-elastically based on equal displacement concept until the collapse limit. For medium period structures, the relationship is bi-linear with a transition phase. The transition region starts from the yield point and ends at the collapse point: it is based on the equal energy concept. Most midrise buildings are somewhere in the long and medium period regions. Therefore, for intensity measure to engineering demand parameter curves, there are two sets of equations: one for short and long period buildings, and the second set of equations are based on medium period buildings. Below is the derivation of the equations.

S_a is the spectral acceleration in the equations. F_y is the force at yield point. δ_e is elastic displacement. δ_{epp} is elastic perfectly plastic displacement. $\delta_{collapse}$ is the displacement at collapse. m is the mass of the building. k is the stiffness of the structural system. $C1$ and $C2$ are constant to combine all of the constant values to develop the general equations.

Short and long period: $S_a = \frac{Fy}{m} \rightarrow S_a = \frac{k*\delta}{m} \rightarrow S_a = C1 * \delta \qquad \delta < \delta_{collpase}$

$$S_a = C1 \times \delta \qquad \delta < \delta_{collpase}$$

$$S_a = S_{a_{collpase}} \qquad \delta > \delta_{collpase}$$

Medium period: $S_a = C1 \times \delta \qquad \delta < \delta_y$

$$\delta = \delta y + \frac{F * \delta elastic * 0.5 - Fy * \delta y * 0.5}{Fy} \qquad \delta_y < \delta < \delta_{collpase}$$

$$\delta = \delta y + \frac{S_a * m * \frac{S_a * m}{k} * 0.5 - Fy * \delta y * 0.5}{Fy} \qquad \delta_y < \delta < \delta_{collpase}$$

$$\delta = \delta y + \frac{{S_a}^2 * C1 - C2}{Fy} \qquad \delta_y < \delta < \delta_{collpase}$$

$$\delta = \delta y + {S_a}^2 * C1 - C2 \qquad \delta_y < \delta < \delta_{collpase}$$

$$\delta = {S_a}^2 * C1 + C2 \qquad \delta_y < \delta < \delta_{collpase}$$

$$S_a = \sqrt{\frac{\delta - C2}{C1}} \qquad \delta_y < \delta < \delta_{collpase}$$

$$S_a = S_{a_{collpase}} \qquad \delta > \delta_{collpase}$$

Last part of both formulations is same, but the first part is different. In the first formulation, the first is part is a line representing the long period structures. In the second formulation, the curve is split into three parts. The equation for the transition curve derived from the equal energy concept is following.

$$Sa = \sqrt{\frac{\delta - C2}{C1}}$$

C1 and C2 are constants.

The general way of reporting these curves is to put S_a on the y-axis and drift on the x-axis, therefore, curve fitting will be done based on that same configuration, but spectral acceleration is the independent variable and the drift is the dependent variable. It is more convenient to have functions in the reverse order. Figure 4-2 shows the IDA models for the small, medium and large period buildings.

Short and long period: $\delta = \frac{S_a}{C1}$ $\quad \delta < \delta_{collpase}$

$S_a = S_{a_{collpase}}$ $\quad \delta > \delta_{collpase}$

Medium period: $\delta = \frac{S_a}{C1}$ $\quad \delta < \delta_y$

$\delta = {S_a}^2 \times C1 + C2$ $\quad \delta_y < \delta < \delta_{collpase}$

$S_a = S_{a_{collpase}}$ $\quad \delta > \delta_{collpase}$

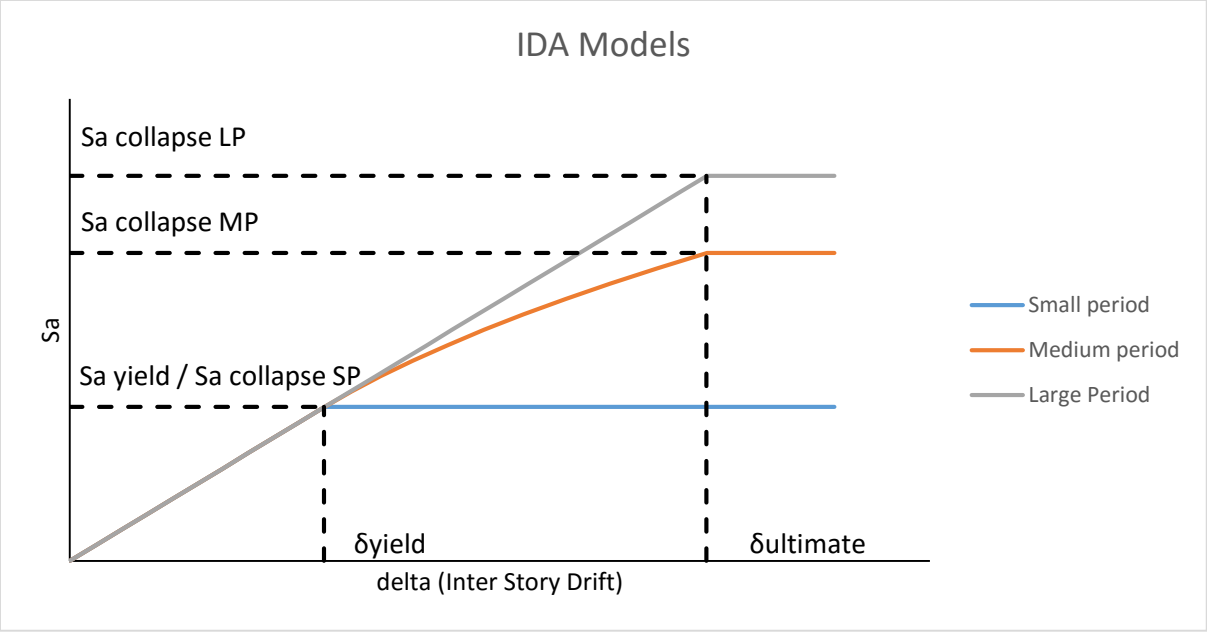

Figure 4-2. Relationship between Spectral acceleration and Inter story drift based on ATC-19 building characterization.

The following 5 models were considered for the IDA simplified model based on the short, medium, and long period equations.

1. Bilinear model using spectral acceleration collapse as a point of change in slope.
2. Bilinear model with regression analysis for the inclined part.
3. Bilinear model with using initial slope for the inclined part.
4. Trilinear model: Inclined part is split into two parts elastic and transition.
5. Model no 3 with transition part represented by a square-root function.

Model 1 and 2 were used based on the amount of information collected in the IDA analyses. Model 2 was preferred if the median curve was reported because it represents the stiffness of the structure between the initial stiffness and the final stiffness. Model 1 was used when the median curve was not reported and the only way to find the transition point was the point where curve becomes flat.

4.2.3 Application of Mathematical Model

Mathematical model number 2, a bilinear model with regression analysis for the inclined part, was fitted to 46 IDA analyses curves from 16 different studies. Three examples are shown below to show the application of the mathematical model. The amount of information provided decreases moving from Example one to three. Example 1 shows when IDA curves were reported with the 16%, 50%, and 84% fractiles. Example 2 shows when only median IDA curve and collapse fragility curve are reported. Example 3 shows when least amount of information is available, that is, collapse fragility curve and IDA curves without fractiles.

4.2.3.1 Example 1:

In this example, IDA curves were reported with the 16%, 50%, and 84% fractiles. First, the curves were digitized using web plot digitizer software. After that curves were split into two parts at the point where curve becomes flat. Regression analysis (minimizing the sum of the square of residuals) was used to find the slope of each of the curves. Figure 4-3 show an example of the regression analysis. After that regression analysis was used again to find the dispersion of the lognormal distribution that fits the data. This analysis was performed using a software developed in this research called Fragility Extractor. After the analysis IDA curve could be represented by three parameters namely slope of the median, median spectral acceleration at collapse, and the dispersion. Figure 4-4 shows the final curves for example 1.

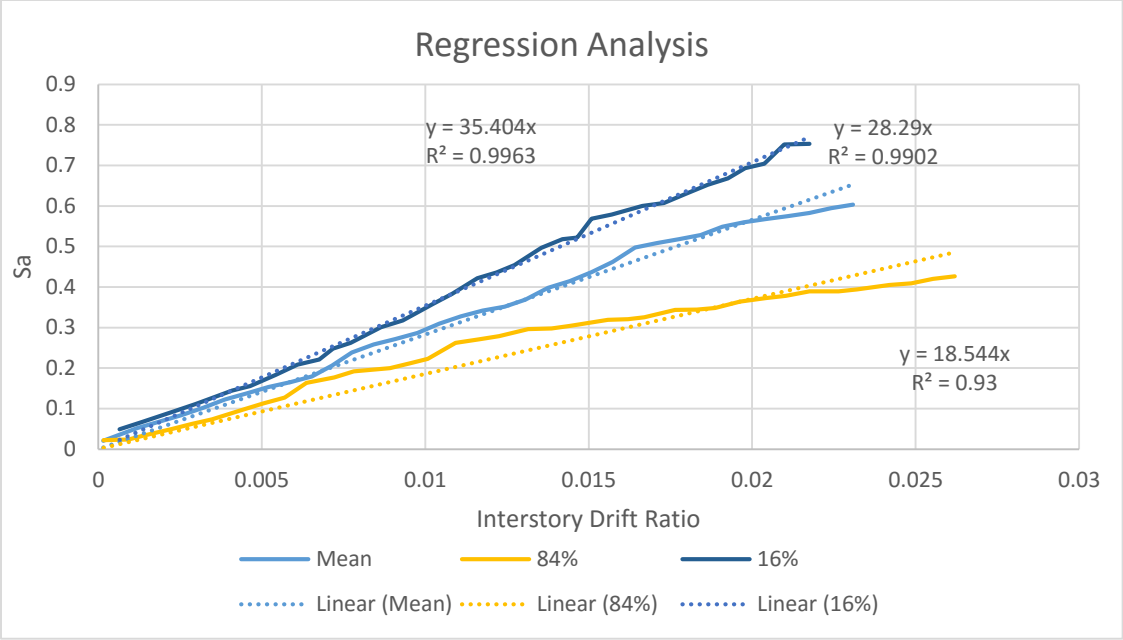

Figure 4-3. Example 1 Regression analysis applied to IDA curve in Pitilakis et al., (2014)

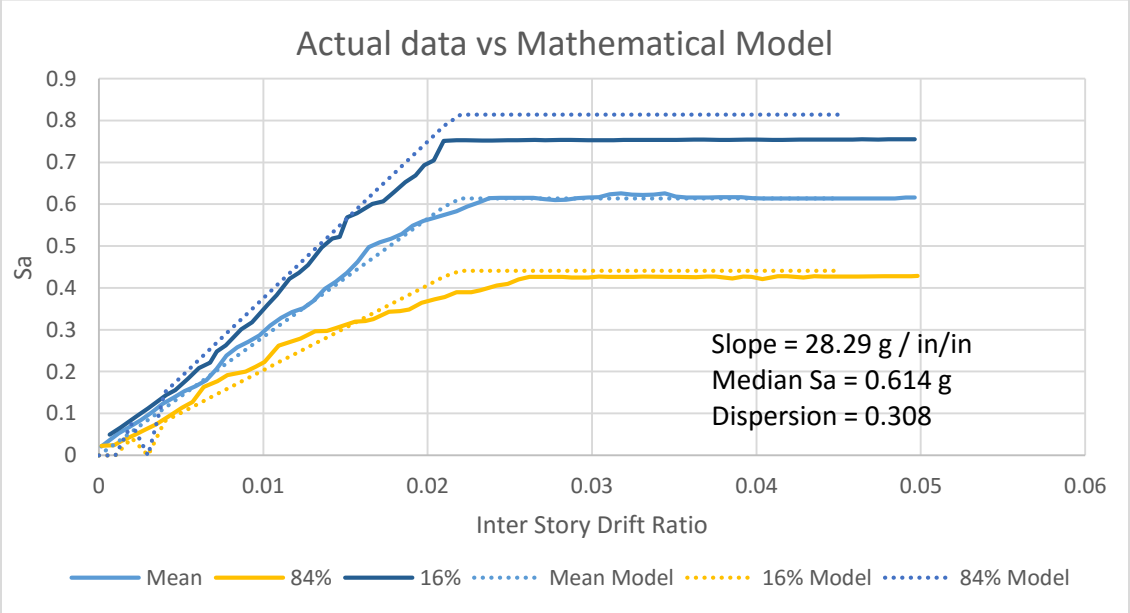

Figure 4-4. Example 1 Actual data vs Mathematical Model applied to IDA curve in Pitilakis et al., (2014)

4.2.3.2 Example 2:

Example 2 gives an example of a case when only the median curve of the IDA was reported with Collapse fragility curve. In this case, median spectral acceleration collapse and dispersion were taken to be the same value as reported for the Collapse fragility curve. However, the slope of the median curve was calculated similarly to example 1. Figure 4-5 compares the IDA curves of a 5 story gate braced frame from the Fanaie & Ezzatshoar, (2014) to the mathematical model. The figure is developed by overlapping the figure from the original article with the model.

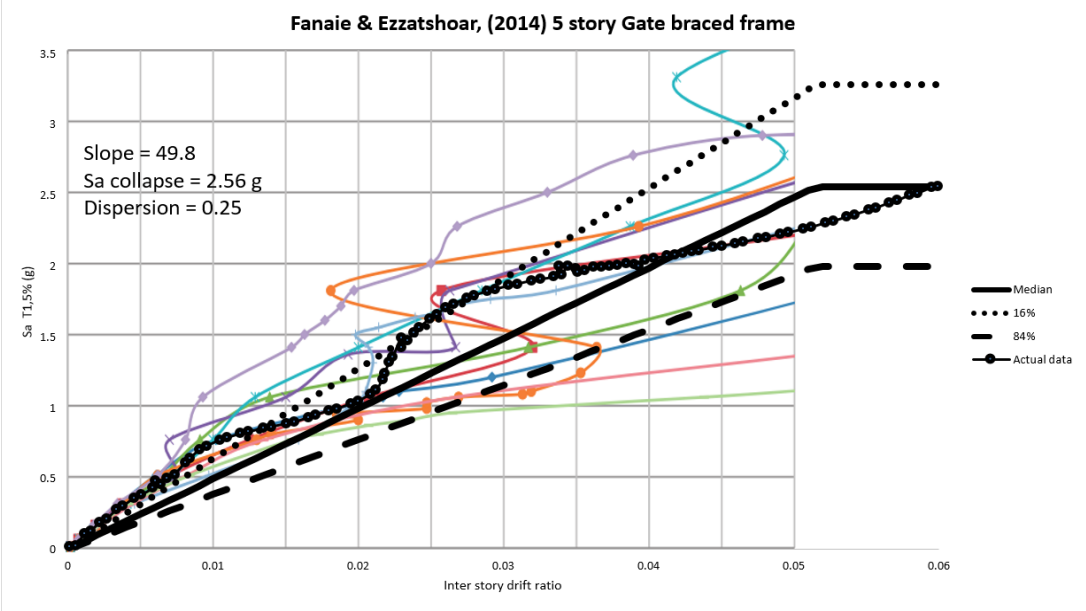

Figure 4-5. Example 2 comparing IDA curve to the mathematical model adapted from Fanaie & Ezzatshoar, (2014)

4.2.3.3 Example 3:

Example 3 gives an example of a case when IDA curves were reported, but the median curve was not specified. Median spectral acceleration collapse and dispersion were taken to be the same value as reported for the Collapse fragility curve, and the slope of the median curve was estimated by finding the interstory drift value at which the curves becomes a flat line by visual inspection. Figure 4-6 compares the IDA curves of a 5 BRKB-TMF frame from the Wongpakdee

et al., (2014) to the mathematical model. The figure is developed by overlapping the figure from the original article with the model.

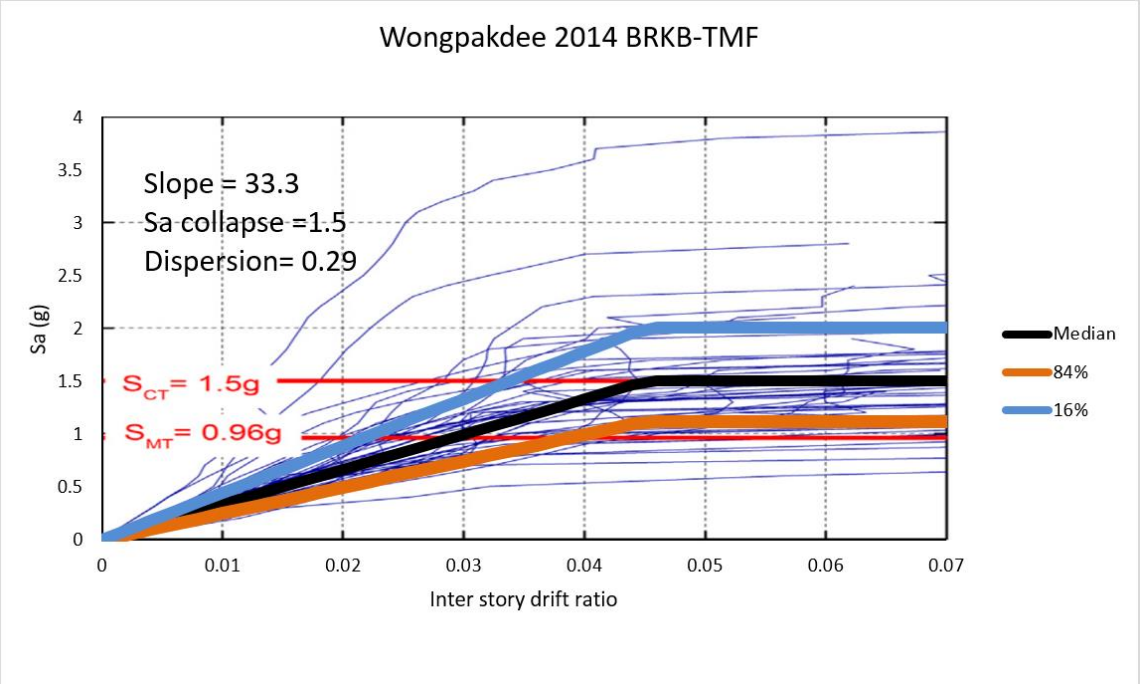

Figure 4-6. Example 3 comparing IDA curve to mathematical model adapted from Wongpakdee et al., (2014)

4.2.4 IDA Analyses

Collapse fragility curve and the IM to EDP curve both are the product of IDA. The summaries of all the studies that reported IDA curves and that were included in the database are provided below. In total 46 IDA curves were collected from 16 independent studies. Data was not critically reviewed because there were not enough similarities in the properties of the specimens and there were not enough curves for each structural system.

Ariyaratana & Fahnestock, 2011

Ariyaratana & Fahnestock, (2011) studied the performance of Chevron Buckling-restrained braced frame (BRBF) with reserve strength. In this study four prototype buildings in

California designed based on ASCE-7-05 were analyzed using IDA. The four types of lateral force system resisting systems are BRBF with no Beam-column moment connections within BRBF, BRBF with Beam-column moment connections within BRBF, BRBF-SMRF and with no Beam-column moment connections within BRBF, BRBF-SMRF and with Beam-column moment connections within BRBF. The frames were designed based on the Equivalent-lateral force method in ASCE-7. 31 ground motions were selected from the PEER center strong motion database. Ground motions were selected based on site class D.

Uriz & Mahin, 2004

Uriz & Mahin, (2004) compared the performance of Chevron CBF and BRBF. In this study two 3 story and two 6 story buildings were analyzed. These buildings were the basis of the Sabelli, Mahin, & Chang, (2003) study. 6400 nonlinear dynamic analysis were performed to analyze the buildings. Twenty ground motions were selected from FEMA/SAC from the 2% probability of exceedance in the 50-year database.

Fanaie & Ezzatshoar, 2014

Fanaie & Ezzatshoar, (2014**)** conducted IDA of Gate concentrically braced frames. In this study 3 frames with a span length of 3 @ 6m and number of stories 3, 5 and 7 were analyzed. Buildings were design based on Iranian national code, which is similar to US code. IDA was conducted in OpenSEES. For the simplified model, median curves were used as it is and the dispersion was calculated based on the Spectral acceleration values reported in Table 4.

Hariri-Ardebili, Zarringhalam, Estekanchi, & Yahyai, 2013

Hariri-Ardebili et al., (2013) analyzed steel moment frame using IDA, Time history and Endurance time analysis method. Seven ground motion defined by the NEHRP and used in FEMA-

440 were selected for IDA. Four buildings were analyzed with 5 m wide 3 bays and number of stories 9, 11, 13 and 15. Buildings were designed to minimize loss of life for an earthquake that has 10% probability of occurrence in 50 years. This also satisfied the life safety condition of the FEMA 365. Instead of Sa PGA is used as Intensity Measure (IM). This lead to higher dispersions. Two states of the building are defined Immediate Occupancy at 2% drift and Collapse Prevention (CP) at 10% drift or when slope of IDA curve reached 20% of the elastic slope. IO and CP are buildings performance levels used to define the state of the building after hazard. IO means building can be occupied after hazard with minor repairs. CP means building did not collapse, but have suffered heavy damage. Data provided for the IO state was used to obtain the slope of the mathematical model and the dispersion. Collapse Prevention Sa was used to find the point of transition.

Jeon, DesRoches, Brilakis, & Lowes, 2012

Jeon et al., (2012) analyzed NONO-Ductile reinforced concrete frames for low-moderate seismic regions. The building was designed only for the gravity loads and without seismic provisions. The building analyzed was a 3 story building with 3 18ft spans. A set of 240 ground motions developed for the eight cities in the Mississippi embayment were used to conduct IDA. Collapse fragility curves are reported for two IMs Sa, T1 and PGA.

Akbas, Sutchiewcharn, Cai, Wen, & Shen, 2013

Akbas et al., (2013) conducted a comparative study of special and ordinary concentrically braced frames. In this study, two building with three and nine stories located in Boston and Los Angeles were analyzed. Buildings at each location were designed for the ground motions of the respective areas. Buildings in Los Angeles had SCBF, and building in Boston had OCBF.

Buildings were designed for seismic and gravity loads estimated with a dead load of 80 psf and live load of 50 psf. IDA was conducted using SAP2000. 20 ground motions for each location were selected with criteria of 2% probability of exceedance in 50 years for Los Angeles and 10% probability of exceedance in 50 years for Boston. IDA curves and spectral acceleration at collapse were reported for all four buildings.

Purba & Bruneau, 2014

Purba & Bruneau, (2014) studied the performance of steel plate shear wall buildings. In this study, fourteen buildings were studied with number of stories being 3, 5 and 10. It also compares buildings designed for low seismic weight versus the buildings designed for high seismic weight. In addition to that two design method are studied. In the first method contribution of boundary moment frames is not included in the lateral force resisting system, and in the second method lateral forces are resisted by both shear wall and moment frame. A set of 44 far field ground motions was selected from PEER database to conduct the IDA. IDA curves were only reported for the two 3 story buildings, and Collapse fragility curves were reported for the remaining 12 buildings with recommended value 0.6 for total dispersion.

Rajeev & Tesfamariam, 2012

Rajeev & Tesfamariam, (2012) studied the seismic response of non-ductile reinforced concrete moment frame with soil structure interaction. In this study IDA of three buildings with number of stories 3, 5 and 9 was performed with fixed base model and The Beam on Nonlinear Winkler Foundation soil structure interaction approach. 30 ground motions were selected from the European strong motion database for the analysis. In addition to aleatory uncertainty from the analysis, the epistemic uncertainty of 0.2 was also recommended based on the FEMA-356

guidelines. IDA results were reported with data points on IM vs. EDP plot and fragility curves for collapse state.

Wongpakdee, Leelataviwat, Goel, & Liao, 2014

Wongpakdee et al., (2014) evaluated a four-story Buckling Restrained Knee Braced Truss Moments Frame. The building was designed using Performance based plastic design approach. The design forces were calculated for the structure using Seismic group 1, Soil type D, S_1=0.6 g, S_s =1.5g. A set of 44 ground motions was selected for IDA based on FEMA P695. IDA was performed on the 2-D model using PERFORM 3D computer software. The results were reported as IDA curves and collapse fragility curve.

Vamvatsikos, 2005

Vamvatsikos, (2005) developed a method for estimating the response of the first mode dominated MDOF using the relationship between Static pushover and IDA. In this study, three different types of building were analyzed to validate the method. The three building are 9 story-Steel moment frame, 5 story concentrically braced frame, and a 20 story steel moment frame. IDA results were reported in the form of 16%, 50%, and 84% fractiles.

Pitilakis, Karapetrou, & Fotopoulou, 2014

Pitilakis et al., (2014) studied the effects of aging and SSI effects on seismic performance of RC buildings. In this study, three RC building with number of stories 3, 4 and 9 were analyzed. Each building was analyzed with fixed based model and SSI model, and for each model two time scenarios: 0 and 50 years were studied. Three main aspects of corrosion were considered in this study namely loss of reinforcement cross-sectional area, degradation of concrete cover and the reduction of steel ultimate deformation. For SSI model, the soil is modeled with a four node plane

strain formulation of a bilinear isoperimetric quadrilateral element. The three-story building was a no code building and was designed only for the gravity loads with no seismic provisions. The four-story building was a high code design and it was designed using the Modern Greek code. The nine-story building was a low code building and designed based on the 1969 Greek seismic code. The IDA was conducted using OpenSees. 15 ground motions were selected from the European strong motion database for conducting the IDA. Results were presented Sa and PGA both as IMs and Inter story drift was used as EDP.

Jalali, Banazadeh, Abolmaali, & Tafakori, 2011

Jalali et al., (2011) studied the seismic performance of steel moment resisting frames with side-plate connections. In this study three buildings with story heights 3, 5 and 7 were analyzed using IDA. Buildings were designed using the UBC-97, AISC 360-05 and AISC 341-05. R=8.5 was used for the design which makes them highly ductile frames and puts them in the category of Special moment resisting frame. IDA was conducted using 44 ground motions specified in FEMA P695. Sa and Inter story drift were used as IM and EDP respectively. The results were reported as IM to EDP curves.

Pang & Ziaei, 2012

Pang & Ziaei, (2012) conducted the nonlinear dynamic analysis of Soft-story Light-frame wood buildings. In this study, a three-story wood building with the soft story was analyzed using 22 far field ground motions. Lateral drifts are concentrated at the first story of the building due to soft story mechanism, therefore, top of the building acts as a rigid box. IDA results were reported in the form of 16%, 50%, and 84% fractiles.

Tehranizadeh & Moshref, 2011

Tehranizadeh & Moshref, (2011) performed an optimization steel moment frame based on two objective criteria: Minimizing Cost (weight) and maximum energy dissipation. A nonlinear dynamic analysis was performed on a five-story three bay moment frame using 22 ground motions. IDA curves were reported for three different cases: minimum weight, intermediate point, and uniform energy dissipation. Sa and Inter story drift were used as IM and EDP respectively. IDA results were reported in the form of 16%, 50%, and 84% fractiles.

Lignos, Zareian, & Krawinkler, 2008

Lignos et al., (2008) studied the response of a 4-story steel moment frame subjected to 40 ordinary ground motions, denoted as LMSR-N (Large Magnitude Small Distance-New) using IDA. The Special steel moment resisting frame was designed using FEMA-350 and AISC seismic provisions. In this study, both aleatory and epistemic uncertainties associated with the plastic rotation capacity and post-capping plastic rotation capacity of moment connection were included. Monte Carlo simulation was used to model the uncertainty in a single structural component. The results were reported in the form of IDA curve and the Collapse probability curve.

Goulet et al., 2007

Goulet et al., (2007) evaluate the performance of code conforming RC moment frame buildings using collapse safety and economic losses. A four-story RC moment frame building designed using 2003 international building code was analyzed in this study. IDA was performed using 64 ground motions chosen for 2%-in-50 years. Eight different design configurations were analyzed, but IDA curves for only Design configuration A were reported. It is a perimeter frame with SCWB ratio of 1.3 and no T-beams. It was designed based on 2003 IBC and ACI 318-02.

Results were reported in the form of IDA curves. Sa and Inter story drift were used as IM and EDP respectively.

NEHRP Consultants Joint Venture, 2010

NEHRP Consultants Joint Venture, (2010) quantifies the building seismic performance factors based on FEMA P-695. This report performs IDA for seven different structural systems named as special reinforced masonry shear wall, ordinary reinforced masonry shear wall, special RC shear wall, ordinary RC shear wall, special steel concentrically braced frame, buckling restrained braced frame, and special steel moment frame. The performance of the structural systems is evaluated by FEMA P695 procedure and for that non-linear dynamic analysis is performed. IDA curves are not reported in the report because the main purpose of the report is to quantify the building seismic performance factors (i.e., R factors). Median spectral acceleration at collapse is reported for each of the systems, but without the dispersion and the IDA curve, neither the collapse fragility curve nor the IM to EDP curve can be developed. Therefore, the information from this study is not included in the database.

4.2.5 IDA Curves collected

This section presents the data collected from the 17 IDA analyses mentioned above. 75 total curves were collected out of which 46 are IDA curves and 29 are collapse fragility curves. To fit the database in this thesis it was split into six small tables. Table 4-1 and Table 4-2 provide the key for the source of the curves and the key for the structural systems respectively. The data is split into four tables based on the type of the curves (i.e. IDA curve and Collapse fragility curve) and the type of data (i.e. source information and curve parameters). Table 4-3 and Table 4-4 give the source information and the curve parameters for the IM to EDP curves. Table 4-5 and Table 4-

6 give the source information and the curve parameters for the IM to DS curves (Collapse fragility curve).

There are 16 different columns in the tables, each signifying a unique field. The **Sr. No.** is the number of the curve in the database and it is unique for each curve. The **Source** field gives the name of the author and year of the research paper from which this curve is obtained. The **System** field defines the structural system of the building. The **period** is the time period of the building that is used for the analysis. Normally it is first mode period of the building and it is measured in seconds. **IM** field describes the intensity measure considered. **EDP** field defines the engineering demand parameter. The **stories** is the number of stories of the building. The **area** gives the total floor plan area of the prototype building in square feet. **Frame** column gives information about the lateral load resisting system. 2 Frames, 3 Bays @ 18' means that there were 2 frames in the building one on each side to resist lateral forces. 3 bays means that there were three bays of lateral force resisting systems and lastly 18’ is the spacing of the bays. The goal of Frame column in the table is to be able to calculate the tributary area for that frame based on the total area and the number of bays that have lateral force resisting system. **Code quality** defines how the building was designed. In general, no code means frame was designed for only gravity loads. Low code means frame was designed for seismic loads and has non ductile behavior, but with minimal seismic detailing. The low code is equivalent to ordinary in ASCE-7. High code means frame has ductile behaviors and designed with seismic detailing. The high code is equivalent to Special in ASCE-7. Any other code quality mentioned is a technique studied by the author, so please see the summary of that paper. **Ground motions** gives the number of ground motions used to conduct the IDA. **IM unit**, **EDP unit** and **Slope unit** field give the units of the number in their respective fields. The **slope** is the slope of the first part of the mathematical model of the IDA curve. **Sa**

median collapse is the median value of the spectral acceleration at which structure collapses and it also defines the pint where the curve becomes flat. The last field is the **dispersion** which gives the lognormal standard deviation of the distribution which is also known as dispersion (β).

Table 4-1. Key for the sources of IDA curves

Source	Symbol
(Pitilakis et al., 2014)	a
(Jalali, Banazadeh, Abolmaali, & Tafakori, 2011)	b
(Pang & Ziaei, 2012)	c
(Tehranizadeh & Moshref, 2011)	d
(Ariyaratana & Fahnestock, 2011)	e
(Uriz & Mahin, 2004)	f
(Fanaie & Ezzatshoar, 2014)	g
(Hariri-Ardebili et al., 2013)	h
(Akbas et al., 2013)	i
(Purba & Bruneau, 2014)	j
(Rajeev & Tesfamariam, 2012)	k
(Wongpakdee et al., 2014)	l
(Vamvatsikos, 2005)	m
(Lignos, Zareian, & Krawinkler, 2008)	n
(Goulet et al., 2007, Haselton et al. 2008a)	o
(Lignos, Zareian, & Krawinkler, 2008)	p
(Jeon et al., 2012)	q

Table 4-2. Key for the structural systems

Structural System	Symbol
Reinforced Concrete Moment Frame	a
Steel Moment Frame	b
Wood Shear Wall	c
Chevron Buckling Restrained Braced Frame	d
Chevron Buckling Restrained Braced Frame w/ Moment Connection	e
Chevron Buckling Restrained Braced Frame with SMRF	f
Chevron Buckling Restrained Braced Frame with SMRF and w/ Moment Connection	g
Chevron Concentrically Braced Frame	h
Gate Concentrically Braced Frame	i
Steel Plate Shear Wall	j
Steel Plate Shear Wall With Contribution Of Boundary Moment Frame	k
Reinforced Concrete Moment Frame with SSI	l
Buckling Restrained Knee Braced Truss Moment Frame	m

Table 4-3. Source information for the IM to EDP curves collected

Sr. no	Source	System	Period (s)	IM	EDP	Stories	Area ft^2	Code Quality	Ground Motions
1	a	a	0.98	Sa (5%,T1)	IDR	3	3888	No	15
2	a	a	0.98	Sa (5%,T1)	IDR	3	3888	No	15
3	a	a	0.89	Sa (5%,T1)	IDR	9		Low	15
4	a	a	0.89	Sa (5%,T1)	IDR	9		Low	15
5	a	a	0.66	Sa (5%,T1)	IDR	4		High	15
6	a	a	0.66	Sa (5%,T1)	IDR	4		High	15
7	b	b	0.87	Sa (5%,T1)	IDR	3	2422	Special	22
8	b	b	1.32	Sa (5%,T1)	IDR	7	2422	Special	22
9	b	b	2.16	Sa (5%,T1)	IDR	15	2422	Special	22
10	c	c		Sa	IDR	3	480	soft story	22
11	d	b	0.69	Sa (5%,T1)	IDR	5		Min Weight	22
12	d	b	0.69	Sa (5%,T1)	IDR	5		Intermediate	22
13	d	b	0.69	Sa (5%,T1)	IDR	5		Uniform Energy Dissipation	22
14	e	d	0.94	Sa (5%,T1)	IDR	7	9475	High	31
15	e	e	0.93	Sa (5%,T1)	IDR	7	9475	High	31
16	e	f	0.9	Sa (5%,T1)	IDR	7	9475	High	31
17	e	g	0.89	Sa (5%,T1)	IDR	7	9475	High	31
18	f	h	0.5	Sa	IDR	3	22816	High	20
19	f	h	0.9	Sa	IDR	6	23716	High	20
20	f	d	0.5	Sa	IDR	3	22816	High	20
21	f	d	0.9	Sa	IDR	6	23716	High	20
22	g	i		Sa (5%,T1)	IDR	3	3481	High	10
23	g	i		Sa (5%,T1)	IDR	5	3481	High	10
24	g	i		Sa (5%,T1)	IDR	7	3481	High	10
25	h	b	1.7	PGA	IDR	15		UBC	7
26	h	b	1.8	PGA	IDR	13		UBC	7
27	h	b	1.62	PGA	IDR	11		UBC	7
28	h	b	1.38	PGA	IDR	9		UBC	7
29	i	h	0.727	Sa, T1	IDR	3	22500	Ordinary	20
30	i	h	2.114	Sa, T1	IDR	9	22500	Ordinary	20
31	i	h	0.457	Sa, T1	IDR	3	22500	Special	20
32	i	h	1.22	Sa, T1	IDR	9	22500	Special	20
33	j	j	0.36	Sa (5%,T1)	IDR	3	21600		44
34	j	k	0.36	Sa (5%,T1)	IDR	3	21600		44
35	k	a	0.64	Sa (5%,T1)	IDR	3		Low	30
36	k	l	0.71	Sa (5%,T1)	IDR	3		Low	30
37	k	a	0.85	Sa (5%,T1)	IDR	5		Low	30
38	k	l	0.88	Sa (5%,T1)	IDR	5		Low	30
39	k	a	1.81	Sa (5%,T1)	IDR	9		Low	30
40	k	l	1.88	Sa (5%,T1)	IDR	9		Low	30
41	l	m	0.94	Sa (,T1)	IDR	4	12000		44
42	m	b	2.3	Sa (5%,T1)	IDR	9	22500		20
43	m	h	1.8	Sa (5%,T1)	IDR	5			20
44	m	b	4	Sa (5%,T1)	IDR	20	12000		20
45	n	b	1.32	Sa (5%,T1)	IDR	4	10800	Special	40
46	o	a	0.94	Sa (2%,T1)	IDR	4	21600		64

Table 4-4. IDA curve parameters for the IM to EDP curves

Sr. no	Frame	Slope (g/in /in)	Sa Median Collapse (g)	Dispersion
1	2 Frames, 3 Bays @ 18'	20.14	0.67	0.42
2	2 Frames, 3 Bays @ 18'	16.98	0.57	0.35
3	2 Frames, 3 Bays @ 13',19.7',13.1'	28.29	0.61	0.32
4	2 Frames, 3 Bays @ 13',19.7',13.1'	22.41	0.52	0.29
5	2 Frames, 3 Bays @ 13',19.7',13.1'	43.49	1.77	0.30
6	2 Frames, 3 Bays @ 13',19.7',13.1'	37.41	1.72	0.53
7	2 Frames, 3 Bay @ 16.4'	36.15	3.47	0.35
8	2 Frames, 3 Bay @ 16.4'	27.91	2.55	0.37
9	2 Frames, 3 Bay @ 16.4'	15.84	1.42	0.46
10	No information	26.69	1.90	0.57
11	2 Frames, 3 Bays @ 30'	25.50	2.01	0.40
12	2 Frames, 3 Bays @ 30'	30.54	2.31	0.18
13	2 Frames, 3 Bays @ 30'	43.15	3.03	0.30
14	2 Frames, 1 Bay @ 25'	36.50	3.34	0.34
15	2 Frames, 1 Bay @ 25'	42.10	3.76	0.31
16	2 Frames, 1 Bay @ 25'	46.90	4.20	0.31
17	2 Frames, 1 Bay @ 25'	50.10	4.44	0.23
18	2 Frames, 2 Bays @ 30'	45.79	2.36	0.15
19	2 Frames, 3 Bays @ 30'	50.06	2.53	0.20
20	2 Frames, 2 Bays @ 30'	63.90	3.07	0.15
21	2 Frames, 3 Bays @ 30'	40.08	3.80	0.20
22	2 Frames, 2 Bay @ 19.7'	79.71	2.88	0.47
23	2 Frames, 2 Bay @ 19.7'	49.69	2.56	0.25
24	2 Frames, 2 Bay @ 19.7'	44.93	2.23	0.28
25	1 Frame, 3 Bay @ 16.4'	57.46	1.72	0.66
26	1 Frame, 3 Bay @ 16.4'	61.19	1.82	0.65
27	1 Frame, 3 Bay @ 16.4'	62.74	2.00	0.60
28	1 Frame, 3 Bay @ 16.4'	56.66	2.09	0.64
29	2 Frames, 2 Bays @ 30'	8.59	0.17	0.16
30	2 Frames, 2 Bays @ 30'	3.06	0.05	0.44
31	2 Frames, 1 Bay @ 30'	62.89	2.53	0.37
32	2 Frames, 2 Bays @ 30'	40.75	1.74	0.30
33	2 Frames, 1 Bay @ 30'	47.37	3.60	0.60
34	2 Frames, 1 Bay @ 30'	39.48	2.29	0.60
35	2 Frames, 3 Bays @ 16.4',16.4',8.2'	19.33	0.96	0.41
36	2 Frames, 3 Bays @ 16.4',16.4',8.2'	19.33	0.92	0.47
37	2 Frames, 3 Bays @ 13.1'	24.34	1.09	0.46
38	2 Frames, 3 Bays @ 13.1'	24.34	1.08	0.46
39	2 Frames, 3 Bays @ 12.6',12.3',11.1'	5.90	0.40	0.48
40	2 Frames, 3 Bays @ 12.6',12.3',11.1'	5.90	0.37	0.51
41	2 Frames, 4 Bays @ 30'	33.33	1.50	0.29
42	2 Frames, 5 Bays @ 30'	11.15	0.91	0.37
43	2 Frames, 1 Bay	48.52	2.26	0.53
44	2 Frames, 5 Bays @ 20'	6.54	0.38	0.34
45	2 Frames, 2 Bays @ 30'	23.86	1.67	0.39
46	2 Frames, 4 Bays @ 30'	38.90	2.80	0.34

Table 4-5. Source information for the collapse fragility curves

Sr. no	Source	System	Period (s)	IM	Stories	Area ft^2	Code Quality	Ground Motions
47	n	b	1.32	Sa (5%,T1)	4	10800		40
48	q	a		Sa (2%,T1)	3	3888	Low	240
49	q	a		PGA	3	3888	Low	240
50	j	j		Sa (5%,T1)	3	21600		44
51	j	j		Sa (5%,T1)	3	21600		44
52	j	j		Sa (5%,T1)	3	21600		44
53	j	j		Sa (5%,T1)	5	21600		44
54	j	j		Sa (5%,T1)	5	21600		44
55	j	j		Sa (5%,T1)	10	21600		44
56	j	k		Sa (5%,T1)	3	21600		44
57	j	k		Sa (5%,T1)	3	21600		44
58	j	k		Sa (5%,T1)	3	21600		44
59	j	k		Sa (5%,T1)	5	21600		44
60	j	k		Sa (5%,T1)	5	21600		44
61	j	k		Sa (5%,T1)	10	21600		44
62	j	k		Sa (5%,T1)	3	21600		44
63	j	k		Sa (5%,T1)	3	21600		44
64	a	a	0.98	PGA	3	3888	No	15
65	a	a	0.98	PGA	3	3888	No	15
66	a	l	0.98	PGA	3	3888	No	15
67	a	l	0.98	PGA	3	3888	No	15
68	a	a	0.89	PGA	9		Low	15
69	a	a	0.89	PGA	9		Low	15
70	a	l	0.89	PGA	9		Low	15
71	a	l	0.89	PGA	9		Low	15
72	a	a	0.66	PGA	4		High	15
73	a	a	0.66	PGA	4		High	15
74	a	l	0.66	PGA	4		High	15
75	a	l	0.66	PGA	4		High	15

Table 4-6. Parameters for the collapse fragility curves

Sr. no	Frame	Sa Median Collapse (g)	Dispersion
47	2 Frames, 2 Bays @ 30'	1.14	0.39
48	2 Frames, 3 Bay @ 18'	0.75	0.73
49	2 Frames, 3 Bay @ 18'	0.75	0.55
50	2 Frames, 1 Bay @ 30'	3.14	0.6
51	2 Frames, 1 Bay @ 30'	3.6	0.6
52	2 Frames, 1 Bay @ 30'	4.08	0.6
53	2 Frames, 1 Bay @ 30'	3.4	0.6
54	2 Frames, 1 Bay @ 30'	4.26	0.6
55	2 Frames, 1 Bay @ 30'	3.4	0.6
56	2 Frames, 1 Bay @ 30'	2.28	0.6
57	2 Frames, 1 Bay @ 30'	2.29	0.6
58	2 Frames, 1 Bay @ 30'	2.32	0.6
59	2 Frames, 1 Bay @ 30'	2.1	0.6
60	2 Frames, 1 Bay @ 30'	2.64	0.6
61	2 Frames, 1 Bay @ 30'	1.92	0.6
62	2 Frames, 1 Bay @ 30'	2.47	0.6
63	2 Frames, 1 Bay @ 30'	2.87	0.6
64	2 Frames, 3 Bays @ 18'	0.73	0.74
65	2 Frames, 3 Bays @ 18'	0.59	0.73
66	2 Frames, 3 Bays @ 18'	0.44	0.65
67	2 Frames, 3 Bays @ 18'	0.37	0.67
68	2 Frames, 3 Bays @ 13',19.7',13.1'	0.68	0.65
69	2 Frames, 3 Bays @ 13',19.7',13.1'	0.59	0.65
70	2 Frames, 3 Bays @ 13',19.7',13.1'	0.28	0.68
71	2 Frames, 3 Bays @ 13',19.7',13.1'	0.26	0.71
72	2 Frames, 3 Bays @ 13',19.7',13.1'	1.31	0.78
73	2 Frames, 3 Bays @ 13',19.7',13.1'	1.13	0.77
74	2 Frames, 3 Bays @ 13',19.7',13.1'	0.75	0.64
75	2 Frames, 3 Bays @ 13',19.7',13.1'	0.67	0.64

4.2.6 Validation of Bi-linear mathematical model for IDA curves

Calculations were performed to validate the bilinear mathematical model developed for the IDA curves and to do the sensitivity analysis for using the mathematical model in PBEE calculations. The first step was to select an IDA curve from the collected data that has all three 16%, 50%, and 84% fractiles. A 9 story steel moment frame from Vamvatsikos, 2005 was used selected for these calculations. The building was designed for soil category D in Los Angeles, CA and has a first mode period of 2.37 sec. Figure 4-7 shows the actual and bilinear model IDA curves. The hazard curve application from USGS website was used to obtain the hazard curve for Los Angeles, CA, soil category D, and T1=2.37 sec. Figure 4-8 shows the hazard curve.

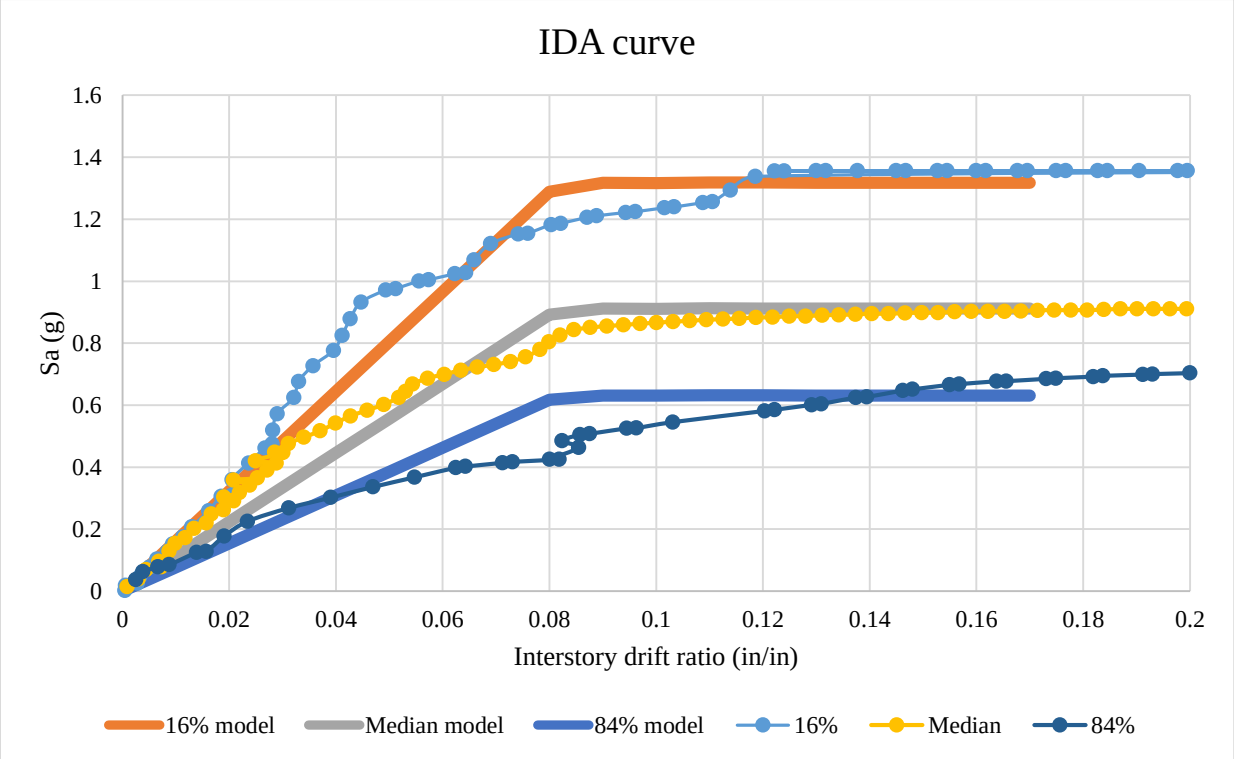

Figure 4-7. Actual IDA Curve and bilinear model of the 9 story steel frame in Los Angeles, CA from Vamvatsikos, 2005.

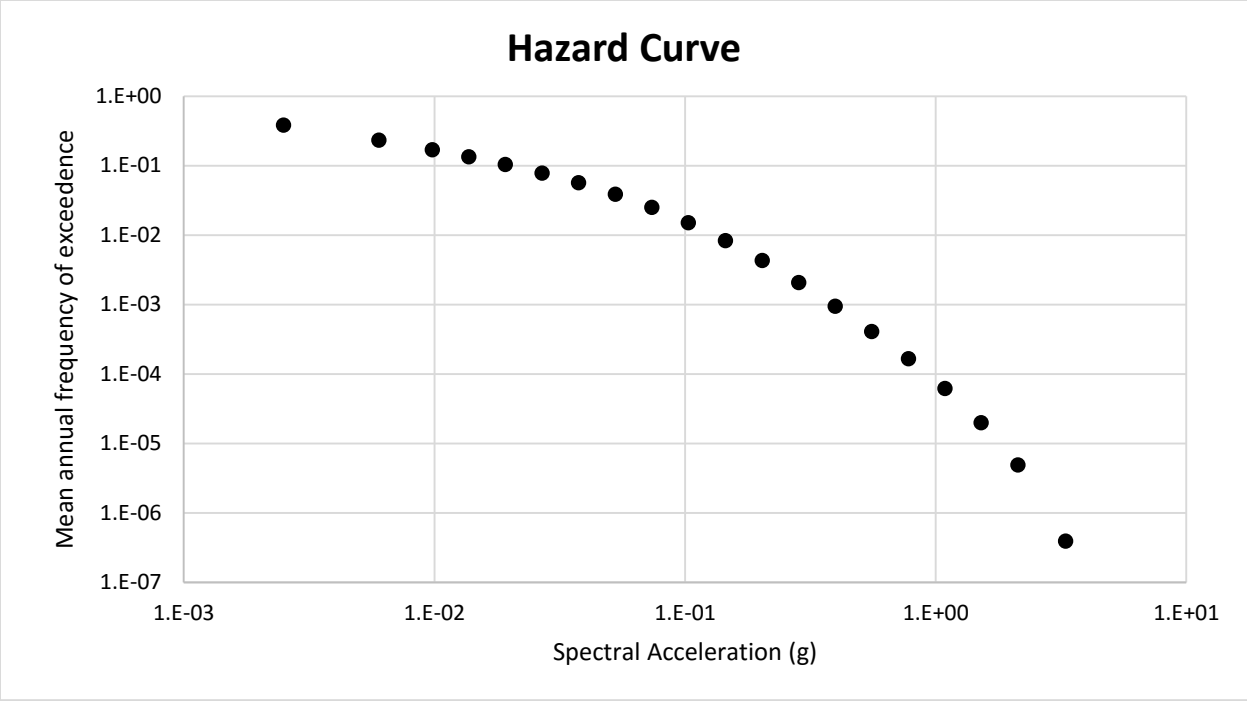

Figure 4-8. Hazard curve for Los Angeles, CA for soil category D and T1=2.37s

A reduced form of the PEER equation was used to calculate the Mean annual frequency of exceedance (MAF) curve for interstory drift ratio. Equation 2 is the PEER equation (cite something). λ (X) is the MAF function and G(X) is the complementary CDF function. The Lowest value of IM (Sa) in the calculation was limited by the smallest value of Sa in the hazard curve. The largest value of IM was limited by the largest value of 84% fractile because the curve becomes a flat line after that point. Equation 3 is the reduced form of PEER equation and was used to calculate the MAF for interstory drift ratio.

$$\lambda(DV) = \iint G(DV|EDP) \times |dG(EDP|IM)| \times |d\lambda(IM)| \quad \text{Equation 2}$$

$$\lambda(EDP) = \int |G(EDP|IM)| \times \frac{d\lambda(IM)}{dIM} \times dIM \quad \text{Equation 3}$$

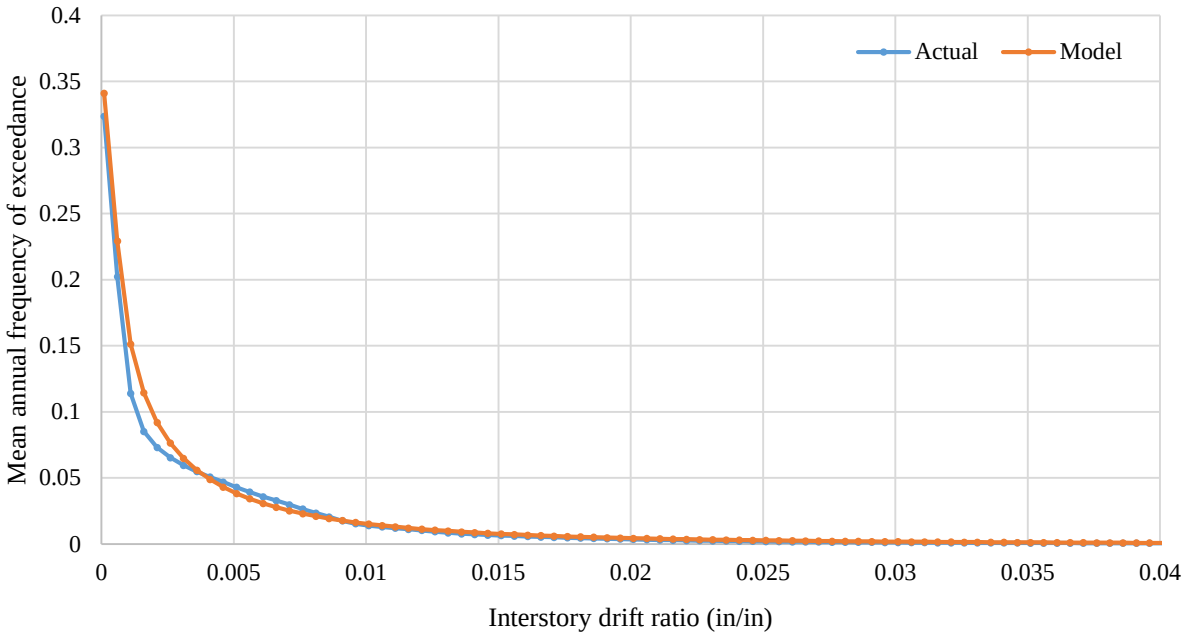

Figure 4-9. Mean annual frequency of Interstory drift ratio for the 9 story steel moment frame

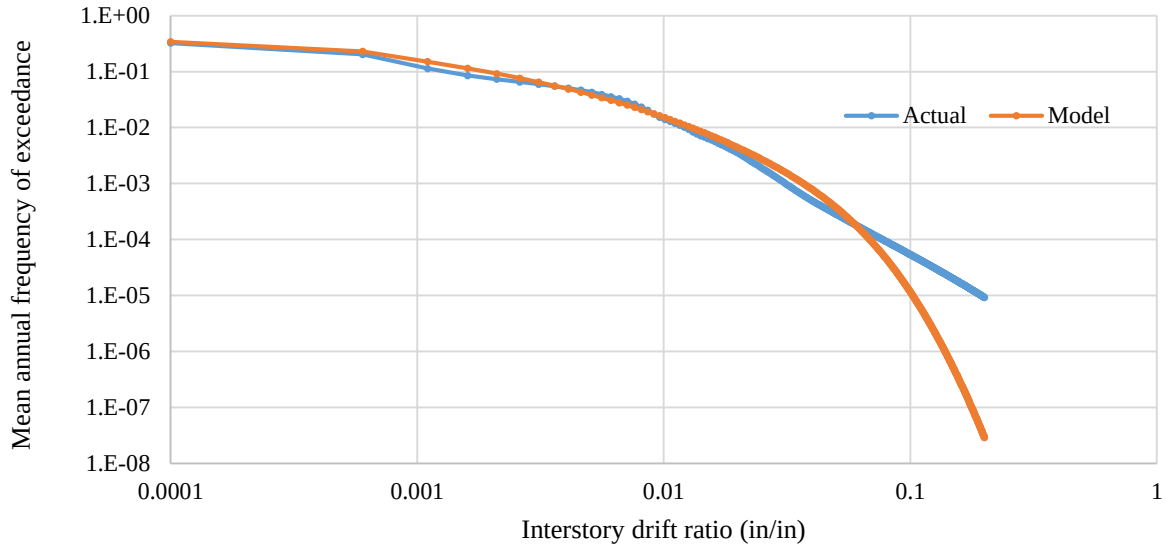

Figure 4-10. Log-Log plot of MAF of Interstory drift ratio for the 9 story steel moment frame

Results of the PBEE calculation were compared by calculating the area under the MAF of interstory drift curves obtained for the actual and the mathematical model to obtain the expected annual engineering demand. Areas were calculated for two domains one starting at 0 interstory drift ratio and the other at a drift ratio of 0.25 inch over 10 feet of story height (0.002). Since drift ratio of 0 is of negligible importance in terms of damage the value using 0.002 drift is considered more realistic. The 4.3% error for representing a nonlinear inelastic analysis of a multi degree of freedom with the bilinear model was considered acceptable.

Table 4-7. Comparison of area under the mean annual exceedance of Interstory drift ratio curves

Area	Actual	Model	Error (%)
Area	0.00071	0.00079	10.3
Area start at 0.002 Interstory drift ratio	0.00041	0.00043	4.3

4.3 IM to DS for Hurricane

Envelopes systems are more affected by hurricanes as compared to structural systems. Therefore, no studies could be found that developed IM to EDP curves for a hurricane. There are no analytical studies found that calculate the response of structure using computer analysis for a hurricane. There have been some studies that utilize post-disaster surveys to develop fragility curves that relate IM to DS like Tomiczek, Kennedy, & Rogers, (2013) and Hatzikyriakou et al., (2015). Tomiczek et al., (2013) developed fragility curves using the buildings affected by the hurricane Ike. The fragility curves developed in this study were limited to one-story wooden houses. Since this study is related to midrise office building these curves were not included in the database. Hatzikyriakou et al., (2015) developed fragility curves for buildings affected by the hurricane Sandy. Although, this study developed fragility curves for structural components, the

Intensity measure used to develop these curves was the distance from the coast. Distance from the coast is not a generalized intensity measure, and it cannot be used in any other scenario because it is very specific to the location and the hurricane.

4.4 IM to DS for Tsunami

No studies could be found that relate IM to EDP for a tsunami. There are no analytical studies that found that perform computer analysis of buildings that are subjected to intensity measure until their collapse. Review of the literature has shown that fragility curves are used to assess the vulnerability of the buildings. These fragility curves are produced using post-disaster survey and satellite imagery. In addition to that numerical modeling and nonlinear shallow water equations are used to model the tsunami. Initial studies only developed the collapse fragility curves, but recent studies have started to develop fragility curves for discrete damage states. These empirical fragility curves are collected instead of the IM to EDP curves and the EDP to DS curves.

4.4.1 Summaries of studies

46 Fragility curves from nine independent studies are collected. These curves are based on five tsunami events ranging from 1993 to 2011. Below are the summaries of the studies.

Charvet, Suppasri, & Imamura, 2014

Charvet et al., (2014) developed fragility curves for buildings affected in Ishinomaki city in 2011 Great East Japan Tsunami. The city was distributed into three regions Plain, Terrain, and River. Buildings were analyzed using flow depth as intensity measure. 20682, 20810, and 13458 buildings were analyzed for the regions respectively. In addition to regions, buildings were grouped into four groups based on their building material Wood, Masonry, RC, and Steel. Fragility

curves for five damage states were produced using ordinal regression analysis and fitting data to the lognormal distribution. Table 4-8 provides the description of the damage states and repair methods.

Table 4-8. Description of damage states for Charvet et al., (2014)

Damage State	Description	Repair Method
DS1	Minor, Flood only	Promptly reusable after floor cleaning
DS2	Moderate, No structural damage	Reusable after minor repair
DS3	Major, Partly damaged walls, but no damage in columns	Maybe reusable after great repair
DS4	Complete, Extensive damage in walls, some damage in columns.	Maybe reusable after great repair only in some cases
DS5	Collapse, More than half of walls were destroyed, most columns were bent or destroyed	Non-repairable

Charvet, Suppasri, Kimura, Sugawara, & Imamura, 2015

Charvet et al., (2015) is the first study that derived multivariate tsunami fragility curves. It also identified the effects of different intensity measures on damage states of the structure. Post-disaster survey of Kesennuma city after the 2011 Great East Japan Tsunami was used to develop the fragility curves. Damage data of 56950 buildings was analyzed using the Ordinal regression analysis. Structures were grouped into four categories: Wood, Masonry, RC, and Steel based on their building material. It was also found the flow depth is not a good predictor of damage in RC and steel buildings. Multivariate fragility curves were reported using flow depth and flow velocity, but enough information was not provided for all damage states to reproduce the curves. Therefore, they were not included in the database. It was also concluded in this study that buildings reach a certain damage state at a lower value of flow depth and flow velocity when looking at them together instead of just using flow depth as intensity measure. Table 4-9 provides the description of the damage states and repair method.

Table 4-9. Description of damage states for Charvet et al., (2015)

Damage State	Description	Repair Method
DS1	Minor damage, No significant structural or non-structural damage, only minor flooding	Possible to use after minor floor and wall clean up
DS2	Moderate damage, Slight damage to non-structural components	Possible to use after moderate repair
DS3	Major damage, Heavy damage to some walls but no damage in columns	Possible to use after major reparations
DS4	Complete damage, Heavy damage to several walls and some columns	Possible to use after complete reparation and retrofitting
DS5	Collapse, Destructive damage to walls (more than half of wall density) and several columns (bent or destroyed)	Loss of functionality (system collapse). Non-repairable or great cost for retrofitting

Koshimura, Oie, Yanagisawa, & Imamura, 2009

Koshimura et al., (2009) developed fragility curves using numerical analysis of tsunami inundation and GIS analysis of post-disaster survey reports of 2004 Sumatra-Andaman tsunami. Damage information of 1000 structures comprised of low-rise wooden houses, timber construction, and non-engineered RC construction with light reinforcement located in the city of Banda Aceh on the northern coast of Sumatra island in Indonesia. Post-disaster data was collected by visual analysis of the pre and post tsunami satellite images. Linear regression analysis was used to fit the normal and lognormal distribution to fragility curves. Collapse fragility curves were produced using inundation depth, current velocity, and hydrodynamic force as intensity measures.

Mas et al., 2012

Mas et al., (2012) developed fragility curves using post-disaster survey of buildings in Dichato, Chile affected by the 2010 Chilean tsunami. More than 80% of the area was affected by the tsunami. Satellite imagery of the area before and after the event was used to determine the condition of the buildings. 915 buildings were visually inspected and used for the development of

the fragility curves. The least square regression analysis was used to fit a lognormal distribution to the fragility curves. Fragility curve for collapse was developed using water depth as intensity measure. It was also compared to the existing fragility developed using data from previous tsunamis.

Murao & Nakazato, 2010

Murao & Nakazato, (2010) developed fragility curves using the post-disaster survey of Sri Lanka after the 2004 Indian Ocean tsunami. A total of 1535 buildings (1202 non-solid, 333 solid) were used for the development of the fragility curves. The data was fitted to the normal distribution. Buildings were classified into two groups: non-solid buildings (brick, block, and wood built; one or two story housing) and solid buildings (RC, steel built; two or more stories; public, commercial, or office use). Fragility curves for three damage: moderate, heavy and complete damage were produced.

Reese et al., 2011

Reese et al., (2011) developed fragility curves using the post-disaster survey of American Samoa and Samoa affected by the 2009 South Pacific Ocean tsunami. Data was collected in four forms; topographic survey, water depth, velocity and direction, structural classification of buildings, and eyewitness reports. Total data from 201 buildings was collected. Fragility curves for five sequential damage states were produced for eight different types of buildings; generic, masonry residential, shielded masonry residential, unshielded masonry residential, debris impacted masonry residential, no debris impacted masonry residential, RC residential, and timber residential. Table 4-10 provides the description of the damage states.

Table 4-10. Description of damage states for Reese et al., (2011)

Damage State	Description
DS1	Light damage -Non-structural damage only
DS2	Minor damage -Significant non-structural damage, minor structural damage
DS3	Moderate damage - Significant structural and non-structural damage
DS4	Severe Irreparable damage - structural damage, will require demolition
DS5	Collapse - Complete structural collapse

Suppasri, Koshimura, & Imamura, 2011

Suppasri et al., (2011) developed fragility curves to categorize the damage in structures located in Thailand after the 2004 Indian Ocean tsunami. Visual inspection of a high-resolution satellite image (IKONOS) was used to develop the fragility curves. Structures were grouped into three categories: wood, Reinforced Concrete, and mixed. Collapse fragility curves were produced by linear regression analysis of data set of 100 building in Phang Nga and 50 in Phuket. A lognormal distribution was used for the fragility curves. Collapse fragility curves were produced using three intensity measures: Inundation depth, Current velocity, Hydrodynamic force. In addition to collapse fragility curve, fragility curves for three damage states: Structural damage in secondary members (roof and wall), Damage in primary members (beam, column, and footings), and the collapse of RC buildings were produced.

Tomiczek, Kennedy, & Rogers, 2013

Tomiczek et al., (2013) developed fragility curves for wood-framed houses using post-disaster surveys of about 2000 houses affected by the hurricane Ike. Since the behavior of the midrise buildings is different from the single story houses these curves were not included in the database.

Valencia, Gardi, Gauraz, Leone, & Guillande, 2011

Valencia et al., (2011) developed fragility curves using the post-disaster survey of Banda Aceh, Indonesia affected by the 2004 Indian Ocean tsunami. Fragility curves for five damage states of buildings category B (Brick unreinforced Cement mortar wall, Fieldstone, Masonry, One story) were reported in the paper. The least square regression analysis was used to fit a lognormal distribution to the curves. Table 4-11 provides the description of the damage states.

Table 4-11. Description of damages states for Valencia et al., (2011)

Damage State	Description
DS1	Light damage
DS2	Moderate damage
DS3	Important damage
DS4	Heavy damage
DS5	Collapse

4.4.2 Collection of data

Collected data is presented by four smaller tables. Table 4-12 and Table 4-13 provide the keys to source and tsunami events respectively. Tables 4-14 and 4-15 present the fragility curve parameters and information about the components. Data is represented by two different distributions: normal and lognormal. In the case of normal distribution, median and dispersion values are normal median and normal standard deviation respectively. In the case of lognormal distribution, median and dispersion values are lognormal median and lognormal standard deviation respectively.

Table 4-12. Key for sources of Tsunami fragility curves

Source	Symbol
(Reese et al., 2011)	a
(Charvet et al., 2015)	b
(Charvet et al., 2014)	c
(Suppasri et al., 2011)	d
(Koshimura et al., 2009)	a
(Murao & Nakazato, 2010)	b
(Mas et al., 2012)	c
(Valencia et al., 2011)	d

Table 4-13. Key for name of Tsunami events

Event	Symbol
2009 South Pacific Tsunami	1
2011 Great East Japan Tsunami	2
2004 Indian Ocean Tsunami	3
1993 Nansei Hokkaido Tsunami	4
2010 Chile Tsunami	5

Table 4-14. Tsunami empirical fragility curves part 1

Sr. No.	Source	Event	Component Name	Location	Intensity Measure	Intensity Measure
1	a	1	Generic Buildings	American Samoa and Samoa	Water depth	meters
2	a	1	Masonry residential	American Samoa and Samoa	Water depth	meters
3	a	1	Shielded masonry residential	American Samoa and Samoa	Water depth	meters
4	a	1	Unshielded masonry residential	American Samoa and Samoa	Water depth	meters
5	a	1	Debris masonry residential	American Samoa and Samoa	Water depth	meters
6	a	1	No debris masonry residential	American Samoa and Samoa	Water depth	meters
7	a	1	RC residential	American Samoa and Samoa	Water depth	meters
8	a	1	Timber residential	American Samoa and Samoa	Water depth	meters
9	b	2	Wood Buildings	Kesennuma City	Water depth	meters
10	b	2	Masonry Buildings	Kesennuma City	Water depth	meters
11	b	2	Reinforced Concrete Buildings	Kesennuma City	Water depth	meters
12	b	2	Steel Buildings	Kesennuma City	Water depth	meters
13	c	2	Wood Buildings	Ishinomaki city, Plain region	Water depth	meters
14	c	2	Masonry Buildings	Ishinomaki city, Plain region	Water depth	meters
15	c	2	Reinforced Concrete Buildings	Ishinomaki city, Plain region	Water depth	meters
16	c	2	Steel Buildings	Ishinomaki city, Plain region	Water depth	meters
17	c	2	Wood Buildings	Ishinomaki city, Terrain region	Water depth	meters
18	c	2	Masonry Buildings	Ishinomaki city, Terrain region	Water depth	meters
19	c	2	Reinforced Concrete Buildings	Ishinomaki city, Terrain region	Water depth	meters
20	c	2	Steel Buildings	Ishinomaki city, Terrain region	Water depth	meters
21	c	2	Wood Buildings	Ishinomaki city, River region	Water depth	meters
22	c	2	Masonry Buildings	Ishinomaki city, River region	Water depth	meters
23	c	2	Reinforced Concrete Buildings	Ishinomaki city, River region	Water depth	meters
24	c	2	Steel Buildings	Ishinomaki city, River region	Water depth	meters
25	d	3	Generic Buildings	Thailand, Khao Lak, Phang Nga	Water depth	meters
26	d	3	Generic Buildings	Thailand, Khao Lak, Phang Nga	Current Velocity	m/s
27	d	3	Generic Buildings	Thailand, Khao Lak, Phang Nga	Hydrodynamic force per width	KN/m
28	d	3	Generic Buildings	Thailand, Kamala/Patong, Phuket	Water depth	meters
29	d	3	Generic Buildings	Thailand, Kamala/Patong, Phuket	Current Velocity	m/s
30	d	3	Generic Buildings	Thailand, Kamala/Patong, Phuket	Hydrodynamic force per width	KN/m
31	d	3	RC building	Thailand (Khao Lak, Phang Nga and Kamala/Patong, Phuket)	Water depth	meters
32	d	3	Generic Buildings	Thailand (Khao Lak, Phang Nga and Kamala/Patong, Phuket)	Water depth	meters
33	d	3	Wood Buildings	Thailand (Khao Lak, Phang Nga and Kamala/Patong, Phuket)	Water depth	meters
34	a	3	Generic Buildings	Indonesia, Sumatra Island, Banda Aceh	Water depth	meters
35	a	3	Generic Buildings	Indonesia, Sumatra Island, Banda Aceh	Current Velocity	m/s
36	a	3	Generic Buildings	Indonesia, Sumatra Island, Banda Aceh	Hydrodynamic force per width	KN/m
37	b	3	Non-solid Buildings	Sri Lanka	Water depth	meters
38	b	3	Solid Buildings	Sri Lanka	Water depth	meters
39	b	3	Generic Buildings	Sri Lanka	Water depth	meters
40	c	4	Wood Buildings	Japan, Okushiri Is. – Aonae	Water depth	meters
41	c	3	Generic Buildings	Indonesia, Sumatra Island, Banda Aceh	Water depth	meters
42	c	3	Reinforced Concrete Buildings	Thailand, Khao Lak, Phang Nga	Water depth	meters
43	c	3	Reinforced Concrete Buildings	Thailand, Kamala/Patong, Phuket	Water depth	meters
44	c	1	Reinforced Concrete Buildings	USA, American Samoa	Water depth	meters
45	c	5	Generic Buildings	Chile, Dichato	Water depth	meters
46	d	3	One story buildings	Indonesia, Sumatra Island, Banda Aceh	Water depth	meters

Table 4-15. Tsunami empirical fragility curves part 2

Sr. No.	Distribution	Median Demand					Data Dispersion				
		DS1	DS2	DS3	DS4	DS5	DS1	DS2	DS3	DS4	DS5
1	Lognormal	0.29	0.48	1.23	1.84	2.77	0.43	0.49	0.58	0.62	0.55
2	Lognormal	0.29	0.46	1.28	1.86	2.49	0.46	0.4	0.35	0.41	0.4
3	Lognormal			1.39	3.11	3.89			0.37	0.49	0.56
4	Lognormal			1.16	1.43	2.25			0.36	0.4	0.42
5	Lognormal			0.92	1.43				0.36	0.32	
6	Lognormal			1.38	1.95				0.32	0.4	
7	Lognormal			1.38	3.45	7.3			0.56	0.54	0.94
8	Lognormal			1.15	1.26	1.62			0.38	0.4	0.28
9	Lognormal	0	0.4	0.67	1.46	1.62	0	0.644	0.593	0.613	0.583
10	Lognormal	0	0.37	0.72	1.91	3.18	0	0.671	0.642	0.633	0.629
11	Lognormal	0	0.37	0.91	2.39	6.03	0	0.593	0.592	0.582	0.574
12	Lognormal	0	0.21	1.11	2.92	6.5	0	0.775	0.487	0.483	0.48
13	Lognormal	0.01	0.61	0.82	1.84	1.84	1.165	0.734	0.578	0.264	0.264
14	Lognormal	0.01	0.43	0.75	1.8	1.8	1.387	1.05	0.678	0.294	0.294
15	Lognormal	0.01	0.41	1.45	2.42	3	0.951	1	0.514	0.324	0.265
16	Lognormal	0.02	0.5	0.99	1.91	2.15	1	1	0.701	0.391	0.352
17	Lognormal	0.02	0.43	0.93	1.87	1.87	0.963	1	0.603	0.292	0.292
18	Lognormal	0.02	0.49	1.01	1.8	1.8	0.63	0.782	0.426	0.237	0.237
19	Lognormal	0.02	0.05	0.84	2.3	4.56	0.688	1	1	0.687	0.374
20	Lognormal	0.02	0.05	0.46	1.53	3.11	0.867	1	1	0.85	0.488
21	Lognormal	0.01	0.01	1.09	2.28	2.28	0.965	1	0.465	0.226	0.226
22	Lognormal	0.01	0.02	1.06	2.13	2.13	0.814	0.618	0.448	0.232	0.232
23	Lognormal	0.01	0.13	1.49	2.35	2.82	0.824	1	0.464	0.311	0.268
24	Lognormal	0.01	0.07	1.4	2.61	3.14	0.88	1	0.521	0.308	0.278
25	Lognormal					1.992					0.903
26	Lognormal					1.914					0.952
27	Lognormal					5.743					1.937
28	Lognormal					2.502					0.642
29	Lognormal					1.422					0.675
30	Lognormal					2.273					3
31	Lognormal			0.355	1.85	5.398			1.0455	1.241	0.66
32	Lognormal					2.111					0.984
33	Lognormal					1.273					0.697
34	Normal					2.99					1.12
35	Lognormal					2.226					0.28
36	Lognormal					4.349					0.75
37	Normal			3.94	2.89	1.82			1.69	1.56	1.45
38	Normal				3.96	2.16				1.31	0.98
39	Normal			4.25	3.19	1.87			1.74	1.6	1.65
40	Lognormal					1.241					0.736
41	Normal					2.985					1.117
42	Lognormal					1.992					0.903
43	Lognormal					2.502					0.642
44	Lognormal					3.222					0.691
45	Lognormal					1.096					1.272
46	Lognormal	2.76	5.26	6.09	6.81	7.57	0.28	0.3	0.27	0.29	0.28

Chapter 5 Engineering Demand Parameter to Damage State Fragility Curves

5.1 Introduction

The third set of relationships collected is the EDP to DS relationship. EDP to DS curves are developed for each component of the building. These curves are also referred as component fragility curves. DS to DV curves are directly related to EDP to DS curves because former are based on the method of repairs required for the damage states. These sets are also the most difficult to obtain because they require actual testing of specimens. Other methods such as computer simulation, the experience of earthquakes, and engineering judgment can also be used to used develop these curves, but curve produced by these methods are not comprehensive, and cannot capture progressive damage occurring in the components in the tests. ATC conducted a ten-year long study to collect EDP to DS curves by collecting data from testing programs of structural components. Curves from FEMA P-58 were included in the database because they also have DS to DV curves associated with them and they are also currently the most comprehensive group of data available in performance based engineering.

5.2 EDP to DS fragility curves for Earthquake

EDP to DS curves in FEMA P-58 are based on 10 background studies. These studies were critically reviewed to determine the quality of the data used to develop the fragility curves. Below are the reviews of each of these studies. The purpose of the reviews is to appreciate the complexity and the amount of effort put in to develop these curves and to identify the actions that could be taken to improve these set of curves. After the reviews all of the studies are compared to each other to identify the issues that authors faced while conducting these studies and what methods were used. Figure 5-1 shows a typical EDP to DS curve in the FEMA P-58 database.

Component fragility curves developed for FEMA P-58 are based on the ATC guidelines. First, test data is collected for the building components. Tests studies were available for most of the structural components. After that, the data from these tests is used to find the trends in the performance of the structural components based on the characteristics of the specimens. Damage states are defined based on three different methods. The first one in based on the visual damage occurring in the specimen, the second method is based on the method of repairs that can be used to repair a group of different types of damage occurring in the specimens, and the last method is to use the backbone curve if enough information about the damage in the specimen is not reported or it is not enough to differentiate between different damage states. The curve for each damage state is defined by a median value of EDP and dispersion. The lognormal distribution is used for the component fragility curves.

Damage states can have three different types of relationships with each other. These relationships are named as Sequential, Mutually exclusive and Simultaneous (Applied Technology Council, 2012). Sequential damage states occur in a sequence and the damage progresses as the damage state number increases. Each damage state occurs only after the previous damage state has occurred. Mutually exclusive damage states are not dependent on each other and they do not have to be in order, but only one of them can happen. One of the cases in which this kind of damage states exist is when damage states are defined based on the damage occurring in the tests and the damage reports from the actual reconnaissance reports and they do not match. Simultaneous damage states are independent and not related to each other. Figure 5-1 shows a typical set component fragility curves for a structural component.

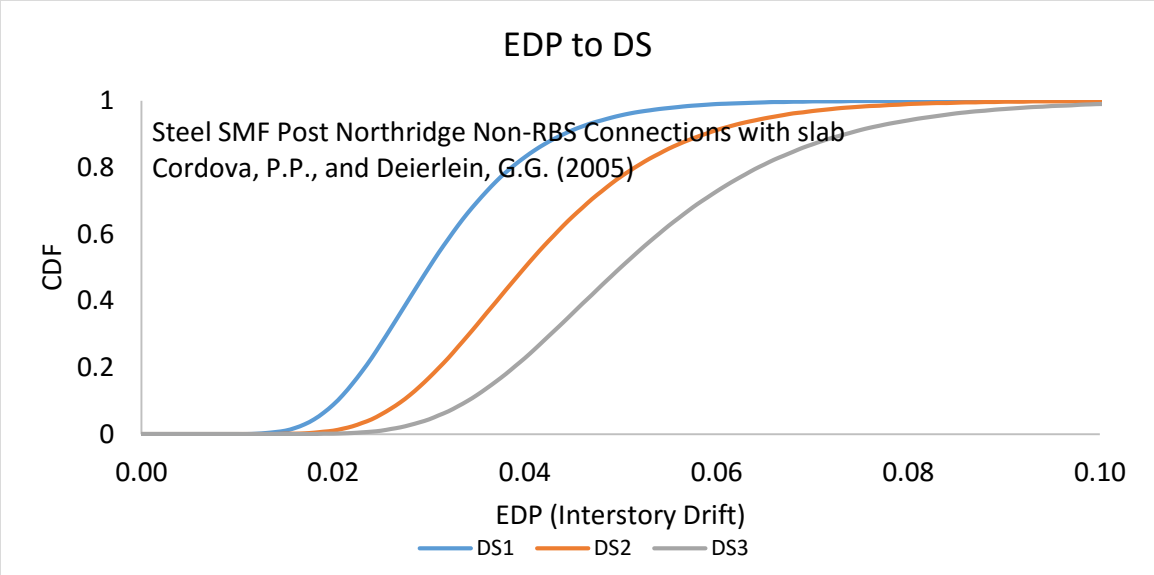

Figure 5-1. A typical set of EDP to DS curves for the building components

5.2.1 Cold-Formed Steel Light-Frame Structural Systems

Grummel & Dolan, (2010) developed fragility functions for three types of Cold-Formed Steel Light–Frame Structural Systems. The Systems are as follows:

1. CFS System #1: CFS light-framed walls with wood structural panel sheathing (plywood or OSB), seismic hold downs and various fastener spacing.
2. CFS System #2: CFS light-framed walls with exterior flat strap X-bracing and seismic hold downs.
3. CFS System #3: CFS light-framed walls with 22 mil or 31 mil exterior steel sheathing, seismic hold downs and various fastener spacing.

Test data from ten independent studies was collected to develop the curves. Inter story drift is used as engineering demand parameter for all of the curves. Pierce's criterion defined in section 3.2 of "Developing Fragility Functions for Building Components for ATC-58" (Porter, Kennedy, &

Bachman, 2007) was used to eliminate the outliers. Table 5-1 and Table 5-2 shows the description of damage states and the fragility curve parameters respectively.

Table 5-1. Description of damage states of Cold-Formed Steel Light-Frame Structural Systems Adapted from (Grummel & Dolan, 2010)

System Type	Damage State Description		
	DS1	DS2	DS3
CFS sys#1-all walls	Fastener Pull through- Removal of contents within 6 feet of wall, Refasten structural panels at locations showing damage (up to 20% of sheathing screws).	Failure of structural panels- Removal of contents within 6 feet of wall; Removal of sheathing panels; Inspect studs and tracks for damage other than local dimpling from previous screws; Replacement/repair of damaged framing, Replacement of sheathing.	Failure of wall and Replace wall.
CFS sys#2steel sheathing	Local buckling of the chord stud occurs. Repair of the buckled chord stud will result in removal contents within 6 feet of the wall, removal of any cladding components (siding, GWB, etc.), and replacement of the buckled stud(s). One should expect to replace both end studs in walls that reach this damage state. Local Buckling of Stud.	At this point, the wall has failed, either due to eccentricities resulting in strong axis bending of studs and tracks or due to yielding of the X-bracing. If DS2 is reached, complete reconstruction of the wall is required.	N/A
CFSsys#3-Xbracing	Complete replacement of steel sheathing at DS1 in addition to the inspection of all framing members for rupture, global and local buckling.	The wall has failed and would need to be torn down and replaced as buckling of studs and tracks will most likely have occurred.	N/A

Table 5-2. Summary of Fragility Curve Parameters of Cold-Formed Steel Light-Frame Structural Systems Adapted from (Grummel & Dolan, 2010)

System Type	Demand Parameter	Median (θ)			Dispersion (β)		
		DS1	DS2	DS3	DS1	DS2	DS3
CFS sys#1-all walls	Inter story Drift (%)	0.4	2.26	2.67	0.4	0.3	0.25
CFS sys#2steel sheathing		1.39	1.79	N/A	0.25	0.25	N/A
CFSsys#3-Xbracing		1.9	2.53	N/A	0.25	0.25	N/A

5.2.2 Concentrically Braced Frames

Rhoeder, Lehman and Lumpkin (2009) used sub-system or system tests to develop the fragility curves for the concentrically braced frames. Concentrically braced frames are complex systems made up of braces, beams, columns, beam-column connections and gusset plate connections (Rhoeder, Lehman and Lumpkin, 2009). Individual tests done on each component of the braced frames e.g. braces, gusset plates, and framing elements were not used to develop the fragility curves because they do not simulate the collective response of the braced frames. These fragility curves are based on the average maximum normalized story drifts calculated using Equation 4. Where h is the story height (Rhoeder, Lehman and Lumpkin, 2009).

$$\Delta = \frac{\Delta_{tension\ max} - \Delta_{comp\ max}}{2\ h} \qquad \text{Equation 4}$$

Rhoeder, Lehman and Lumpkin (2009) produced eight fragility curves for different types of concentrically braced frames using 69 tests. Table 5-3 provides a summary of these fragility curves and their parameters. Fragility curves are defined using four parameters β_γ, θ, β_u, and M. β_γ is the logarithmic standard deviation of the experimental data whereas β_u is to account for the

uncertainty in the test data. M is the number of tests used to develop a certain fragility curve and it is also used to estimate a β_u value for the curve (Rhoeder, Lehman and Lumpkin, 2009).

Rhoeder, Lehman and Lumpkin (2009) have defined 4 sequential damage states for the fragility curves. DS1 is the first damage state and it does not require any repair. Severe inelastic damage to the brace, gusset plates, and members can be seen in the damage states DS2 and DS3. The structure does not lose its integrity in DS2 and DS3, but major repairs and replacements are required. DS4 is the last damage state defined and it represents a reduction of lateral stiffness to 25-40% instead of collapse (Rhoeder, Lehman and Lumpkin, 2009). They have also defined observable damage and appropriate repairs corresponding to each damage state for each component of the braced frame i.e. braces, gusset plates, and framing elements.

Table 5-3. Fragility, damage measures, and consequences for Concentrically Braced Frames [Adapted from (Roeder et al., 2009)]

Concentrically Braced Frames	DS	M	β_γ	β_u	θ
Concentrically Braced Frame With No Seismic Detailing	DS1	0	NA	0.25	0.0042
	DS2				
	DS3				
	DS4				
Ordinary Concentrically Braced Frames	DS1	4	0.6604	0.25	0.159
	DS2				
	DS3	4	0.1466	0.25	1
	DS4	4	0.4248	0.25	1.776
Special Concentrically Braced Frames With Min. Standards	DS1	10	0.1694	0.1	0.377
	DS2	6	0.288	0.1	0.735
	DS3	9	0.2383	0.1	1.209
	DS4	13	0.3417	0.1	1.524
Special Concentrically Braced Frames With Tapered Gusset Plates	DS1	6	0.2637	0.1	0.373
	DS2	5	0.2642	0.1	0.753
	DS3	6	0.216	0.1	1.452
	DS4	6	0.358	0.1	1.989
Special Concentrically Braced Frames With Rectangular Gusset Plates And Improved Balanced Design	DS1	14	0.1878	0.1	0.3804
	DS2	14	0.3174	0.1	0.9152
	DS3	14	0.0962	0.1	1.668
	DS4	14	0.0939	0.1	2.2331
Special Concentrically Braced Frames With Wide Flange Braces	DS1	3	0.3879	0.25	0.346
	DS2	3	0.5781	0.25	0.584
	DS3	3	0.4271	0.25	1.415
	DS4	3	0.0478	0.25	2.832
Special Concentrically Braced Frames With Double Angle Braces	DS1	8	0.2827	0.1	0.256
	DS2	6	0.297	0.1	0.485
	DS3				
	DS4	9	0.4897	0.1	1.124
Special Concentrically Braced Frames With Double Angle Braces And X-Bracing	DS1	3	0.414	0.25	0.226
	DS2	3	0.489	0.25	0.748
	DS3	4	0.0803	0.25	1.446
	DS4	6	0.265	0.25	1.854

Note:

Median values for the seismic concentric braced frame with double angle was wrongly reported for the DS2 and DS3 in the FEMA database.

5.2.3 Reinforced Concrete Moment Frames

ATC 58 collected data on following eight different types of concrete moment frames.

1. ACI Special Moment Frames (SMF)
2. ACI Intermediate Moment Frames (IMF)
3. ASCE Category 1 Frames (ASCE1)
4. ASCE Category 2 Frames (ASCE2)
5. ACI Non-Compliant Frames (NCF/ASCE3)
6. ACI Ordinary Moment Frames Controlled by Flexure-Shear or Shear Response of Beams (OMF-BYS/ASCE4).
7. ACI Ordinary Moment Frames Controlled by Flexure-Shear or Shear Response of Columns with Moderate Axial Loads (OMF-CYSM/ASCE5).
8. ACI Ordinary Moment Frames Controlled by Flexure-Shear or Shear Response of Columns with High Axial Loads (OMF-CYSH/ASCE6).

Data was collected from two types of tests: subassembly tests and cantilever column tests. A total of 106 sub-assembly tests from 24 different programs and a total of 35 cantilever column tests from 19 different programs were collected. Subassembly tests were primarily used to develop the fragility functions because they were a better model of an actual building except they were missing slabs.

Six damage states were identified to categorize the damage in the moment frame. These damage states are based on concrete crushing, concrete cracking, reinforcement yielding,

reinforcement buckling and lateral load resistance. Eventually, data was collected to develop fragility functions for 3 damage states.

There are two parts of the dispersion in the fragility functions. β_γ represents the test data and β_u represents the uncertainty in the actual building. A range of 0.1 to 0.4 of β_u was used to calculate the total dispersion depending upon the consistency and size of data. Equation 5 gives the relation between the dispersions. Table 5-4 provides the fragility curve parameters for the RC moment frames.

$$\beta = \sqrt{\beta_\gamma^2 + \beta_u^2} \qquad \text{Equation 5}$$

Table 5-4. Proposed fragility parameters for the RC moment frames [Adapted from (Lowes & Li, 2009)]

Moment Frames	Ductility	Damage State 1		Damage State 2		Damage State 3	
		θ	β	θ	β	θ	β
SMF	High	2.00	0.40	2.75	0.30	5.00	0.30
ASCE 1	High	2.00	0.40	2.50	0.30	4.00	0.30
IMF	Moderate	2.00	0.40	2.50	0.30	3.50	0.40
ASCE 2 / OMF-BYJS	Moderate	1.75	0.40	2.25	0.30	3.25	0.40
ASCE4 / ASCE 5	Low	1.50	0.40	2.00	0.30	2.50	0.40
NCF / ASCE3	Low	1.50	0.40			2.00	0.40
ASCE 6	No	0.25	0.40			0.50	0.50

Notes:

1. **Damage state 1 (Epoxy Inject Concrete):** Crack's width is greater than 0.06 in and there is no significant spalling. Remove furnishings, ceilings and mechanical, electrical and plumbing systems (as necessary) 5 feet either side of damaged area to repair. Clean area adjacent to the cracks. Prepare cracks, as necessary, to receive the epoxy injection. Inject cracks. Replace and repair finishes. Replace furnishings, ceilings and mechanical, electrical and plumping systems as necessary.
2. **Damage state 2 (Patch Concrete):** Crack's width is greater than 0.06 in and spalling has exposed the transverse steel. Remove furnishings, ceilings and mechanical, electrical and plumbing systems (as necessary) 8 feet either side of damaged area. Clean area adjacent to

the damaged concrete. Prepare spalled concrete and adjacent cracks, as necessary, to be patched and to receive the epoxy injection. Patch concrete with grout. Replace and repair finishes. Replace furnishings, ceilings and mechanical, electrical and plumping systems as necessary).

3. **Damage state 3 (Replace Concrete):** Crack's width is greater than 0.06 in and spalling has exposed the longitudinal steel and there is no fracture or buckling of reinforcement. Remove furnishings, ceilings and mechanical, electrical and plumbing systems (as necessary) 15 feet either side of damaged area. Shore damaged member(s) a minimum of one level below (more levels may be required). Remove damaged concrete at least 1 inch beyond the exposed reinforcing steel. Place concrete forms. Place concrete. Remove forms. Remove shores after one week. Replace and repair finishes. Replace furnishings, ceilings and mechanical, electrical and plumping systems (as necessary).

5.2.4 Link Beams in Eccentrically Braced Frames

Gulec, Gibbons, Chen, and Whittaker (2011) developed the fragility curves for the link beams in the eccentrically braced frames. Eccentrically braced frames are used in the moderate to high seismic zones to provide higher stiffness to control drift and greater ductility to meet larger deformation demands (Gulec, Gibbons, Chen, & Whittaker, 2011). Most of the inelastic action occurs in the link beams, therefore, most of the damage occurs in these link beams. As a consequence, seismic performance of a building depends on the inelasticity of the link beams. AISC 341-05 [AISC (2005)] has defined three modes in which EBFs can perform depending upon the normalized link length ρ: 1 shear yielding occurs for ρ less than 1.6, 2) flexural yielding occurs for ρ greater than 2.6, and 3) both shearing force and moment are the part of the response if ρ is between 1.6 and 2.6. Gulec, Gibbons, Chen, and Whittaker (2011) developed a database of 110 link beams test results. 107 test were subjected to reverse cyclic loading and only 3 to monotonic loading. Gulec, Gibbons, Chen, and Whittaker (2011) also reported that 71 out of the 110 tests were controlled by shear, 11 controlled by flexure and 28 were controlled by a combination of shear and flexure based on the AISC definitions. The normalized length of specimens varied from 0.57 to 3.95 (C. K. Gulec et al., 2011).

Plastic link rotation was chosen by the Gulec, Gibbons, Chen, and Whittaker (2011) as engineering demand parameter for the development of the fragility curves. Plastic link rotation is a product of a nonlinear response history analysis and it can be calculated using Equation 6.

$$\gamma_p = \gamma_T - \gamma_E \qquad \text{Equation 6}$$

Where γ_T is defined as the total rotation that is equal to the ratio of the relative total displacements of the end of the links to the length of the link, and γ_E is the elastic rotation. Table 5-5 shows the relation between damages states and method of repairs (MOR), and these are based on expert opinion. Monotonically loaded tests were not used in the fragility curve development because they achieve significantly higher inelastic rotations as compared to tests with cyclic loading. MOR1 for the shear links is based on the theory since no data was available for that. Four data sets were developed for the MOR-2 and MOR-3 of the shear critical links: 1) Links comply with ASCE 341-05 [AISC (2005)] to achieve a minimum elastic rotation of 0.05 rad, 2) Links comply with ASCE 341-05 [AISC (2005)] to achieve a minimum elastic rotation of 0.08 rad, 3) Similar to dataset 1, but excluding D-braced EBFs that fractured at link-column joint, 4) Similar to dataset 1, but excluding all shear critical links connected at one end to a column (C. K. Gulec et al., 2011)**.** The results of these data sets are in Table 5-6 and they are not very different from each other, therefore, only a single value of median and dispersion was reported for the Shear links. In the case of flexural links fragility curves for MOR 2 and MOR 3 were developed. Table 5-6 also shows the fragility parameters calculated by Gulec, Gibbons, Chen, and Whittaker (2011). Epistemic uncertainty was not included in any of the dispersions because sufficient test data was available to develop the fragility curves (C. K. Gulec et al., 2011)**.**

Gulec, Gibbons, Chen, and Whittaker (2011) did not report any final values for the shear and flexural links, therefore, the FEMA fragility database was checked to determine what final

value were chosen. In the FEMA fragility database, flexural links are not mentioned at all. Table 5-7 shows the fragility parameters for the shear links in the FEMA fragility database.

Table 5-5. Damage States of Link Beams in eccentrically braced frames (C. K. Gulec et al., 2011)

ID	Damage States	Applicable link type			Method of Repair (MoR)
DS0.1	Web yielding	Shear	Int.	Flexural	Cosmetic repair (MoR-0)
DS0.2	Flange yielding	Shear	Int.	Flexural	
DS0.3	Yielding in intermediate stiffeners	Shear	Int.	Flexural	
DS1.1	Damage to concrete slab above the link	Shear	Int.	Flexural	Concrete replacement (MoR-1)
DS2.1	Web local buckling	Shear	Int.		Heat straightening (MoR-2)
DS2.2	Flange local buckling	Shear	Int.	Flexural	
DS3.1	Web fracture	Shear	Int.		Link replacement (MoR-3)
DS3.2	Flange fracture	Shear	Int.	Flexural	
DS3.3	Lateral torsional buckling		Int.	Flexural	

Table 5-6. Calculated Fragility curve parameters for Flexure and Shear critical link beams [Adapted from (C. K. Gulec et al., 2011)]

Failure Mode	Data Set	MoR	lognormal	
			θ	β
Flexure Critical	**1**	**1**	NA	NA
		2	0.010	0.58
		3	0.018	0.48
Shear Critical	**1,2,3,4**	**1 (Theoretical)**	0.04	0.3
	1	**2**	0.060	0.30
		3	0.079	0.32
	2	**2**	0.056	0.30
		3	0.076	0.34
	3	**2**	0.060	0.30
		3	0.083	0.27
	4	**2**	0.062	0.28
		3	0.083	0.26

Table 5-7. Fragility parameters in the FEMA database

Failure Mode	MoR	lognormal	
		θ	β
Flexure Critical (Not Reported in FEMA)	**1**	NA	NA
	2	0.010	0.58
	3	0.018	0.48
Shear Critical	**1**	0.04	0.30
	2	0.06	0.30
	3	0.08	0.30

5.2.5 Low Aspect Ratio Reinforced Concrete Walls

A set of 434 tests was collected to develop the fragility curves for the low aspect ratio reinforced concrete walls, but most of these tests were conducted to measure the maximum strength and the initial elastic stiffness of the walls, and very little information was recorded about the progression of damage (Gulec, Whittaker, & Hooper, 2009). Experiment data from only 111 squat walls was used to develop the fragility curves and all of these walls had five things common: 1) no openings; 2) symmetric bar layout; 3) no diagonal rebar; 4) aspect ratios less than or equal to 2; and 5) cantilever test fixture (Gulec, Whittaker, & Hooper, 2009). The walls are separated into three types Rectangular, Barbell, and Flanged. Out of 111 tests, 28 walls are Flanged walls, 32 are Barbell walls and 51 were rectangular walls. Loading mechanism for these test was also different 81 test used cyclic loading and 21 used monotomic loading.

Gulec, Whittake and Hooper (2009) have defined damages states based on methods of repairs instead of damage metrics such as concrete crack width, concrete crushing, reinforcement yielding and reinforcement buckling, because repairs methods are monetarily quantifiable. Table 5-8 shows the summary of the damage states and the method of repairs of the walls. In the performance based design framework, each method of repair will become one damage state. Gulec

Whittake and Hooper (2009) used four different distributions namely: Lognormal, Gamma, Weidbull and Beta for statistical analysis. Fragility curves based on lognormal distribution will only be used in this study. Fragility curves were produced using two different methods, one by using multiple damage states for each MOR and another by using the damage state corresponding to the lowest drift value for each MOR. Method 1 produced higher median values. Gulec Whittake and Hooper (2009) could not find a clear relationship between the strength or stiffness of the wall and the aspect ratio, horizontal and vertical web reinforcement ratio, axial load, web thickness and the number of reinforcement curtains. Damage characteristics of the 3 types of walls were different from each other. Table 5-9 shows a summary of the recommended values of the fragility curves by the Gulec Whittake and Hooper (2009).

Table 5-8. Damage states and Method of repairs (K. Gulec, Whittaker, & Hooper, 2009)

ID	Damage States	Method of Repair (MoR)
DS1.1	Initiation of cracking	Cosmetic repair (MoR-1)
DS1.2	Initiation of flexural cracking	
DS1.3	Initiation of shear cracking	
DS1.4	Maximum measured crack widths less than 0.02 in. (0.5 mm)	
DS2.1	Initiation of yielding in horizontal web reinforcement	Epoxy injection (MoR-2)
DS2.2	Initiation of yielding in vertical web reinforcement	
DS2.3	Initiation of yielding in vertical boundary element reinforcement	
DS2.4a	Maximum measured shear crack widths larger than 0.02 in (0.5 mm) but less than 0.12 in. (3 mm)	
DS2.5a	Maximum measured flexural crack widths larger than 0.02 in (0.5 mm) but less than 0.12 in. (3 mm)	
DS2.4b	Maximum measured shear crack widths larger than 0.04 in (1.0 mm) but less than 0.12 in. (3 mm)	
DS2.5b	Maximum measured flexural crack widths larger than 0.04 in (1.0 mm) but less than 0.12 in. (3 mm)	
DS3.1	Concrete crushing at the compression toes / initiation of crushing in the wall web	Partial wall replacement (MoR-3)
DS3.2	Vertical cracking in the toe regions of the web	
DS3.3	Buckling of boundary element vertical reinforcement	
DS3.4	Flexural crack widths exceeding 0.12 in. (3 mm)	
DS4.1	Initiation of sliding	Wall replacement (MoR-4)
DS4.2	Wide diagonal cracks	
DS4.3	Widespread crushing of concrete	
DS4.4	Reinforcement fracture	
DS4.5	Shear crack widths exceeding 0.12 in (3 mm)	

Table 5-9. Fragility curves for Low aspect ratio walls (K. Gulec, Whittaker, & Hooper, 2009)

Walls	MOR	Damage State	θ	β
Rectangular	**1**	DS1	0.07	0.79
	2	DS2	0.55	0.34
	3	DS3	1.09	0.27
	4	DS4	1.30	0.35
Barbell	**1**	DS1	0.03	0.31
	3	DS3	0.33	0.33
	4	DS4	0.87	0.18
Flanged	**1**	DS1	0.05	0.76
	3	DS3	0.76	0.33
	4	DS4	1.34	0.45

5.2.6 Reinforced Masonry Shear Wall

Identification of damage states for reinforced masonry shear walls is based on maximum applied loads instead of physical conditions like cracking because cracks can close after the lateral loads are removed due to gravity loads. Using maximum applied loads to develop fragility curves does not follow the practice of other structural background reports, but it is necessary since the physical damage is undetectable after the loads are removed.

Sixty-nine tests from eight different studies were collected to develop the fragility curves for the reinforced masonry shear walls. Some tests resulted in only one of the damage states. These tests covered the effects of different Vertical reinforcement ratios, wall aspect ratios, and axial compressive loads. Seventeen walls out of sixty-nine were partially grouted and rest were fully grouted.

Murcia-Delso & Shing (2012) produced two different sets of fragility curves. Class A curves are for simplified analysis based on only story drift ratio, whereas Class B curves are based on flexural deformation for DS1, DS2 and DS3 because these damage states relate to flexural

failure. DS4, DS5, and DS6 are based on shear force demand because these damage states are brittle and sudden. Since in this research interstory drift ratio is being used as an engineering demand parameter Class A curves will be used to determine the damage state.

As discussed previously, there are two parts of the dispersion in the fragility functions. β_γ represents the test data and β_u represents the uncertainty in the actual building. β_u is assumed to be 0.25 for Class A curves and 0.1 for Class B curves. Equation 5 gives the relation between the dispersions.

Flexure (DS1, DS2, DS3), shear (DS4, DS5), and sliding (DS6) damage states are mutually exclusive. For a wall to be flexure critical its nominal shear strength and sliding shear resistance should be 1.25 times the shear corresponding to the nominal flexural strength of the wall (Murcia-Delso & Shing, 2012).

Fragility curves for the fully grouted walls are based on the experimental data, but there was not enough data for the partially grouted walls, therefore, curves for the first four damage states were derived using engineering judgment by decreasing the median value and increasing the dispersion value of the corresponding curve of the fully grouted wall. The median value is assumed to be 57% of the fully grouted wall and a factor of 0.3 was added to β_γ for the partially grouted walls. DS6 is not included in the Class A fragility curves.

Table 5-10. Description of damage states for the masonry shear walls (Murcia-Delso & Shing, 2012)

Damage State	Description	Repair Measures (Fully-grouted)	Repair Measures (Partially-grouted)
DS1 Slight Flexure Damage	- A few flexural and shear cracks with hardly noticeable residual crack widths. - Slight yielding of extreme vertical reinforcement. - No spalling. - No fracture or buckling of vertical reinforcement. - No structurally significant damage.	- Cosmetic repair. - Patch cracks and paint each side.	- Cosmetic repair. - Patch cracks and paint each side.
DS2 Moderate Flexure Damage	- Numerous flexural and diagonal cracks. - Mild toe crushing with vertical cracks or light spalling at wall toes. - No fracture or buckling of reinforcement. - Small residual deformation.	- Epoxy injection to repair cracks. - Remove loose masonry. - Patch spalls with non-shrink grout. - Paint each side.	- Remove loose masonry. - Patch spalls with non-shrink grout. - Grout wall cavities. - Grout injection into remaining cracks. - Paint each side.
DS3 Severe Flexure Damage	- Severe flexural cracks. - Severe toe crushing and spalling. - Fracture or buckling of vertical reinforcement. - Significant residual deformation.	- Shore. - Demolish existing wall. - Construct new wall.	- Shore. - Demolish existing wall. - Construct new wall.
DS4 Moderate Shear Damage	- First occurrence of major diagonal cracks. - Cracks remain closed with hardly noticeable residual crack widths after load removal.	- Epoxy injection. - Paint each side.	- Grout wall cavities. - Grout injection into remaining cracks. - Paint each side.
DS5 Severe Shear Damage	- Wide diagonal cracks with typically one or more cracks in each direction. - Crushing or spalling at wall toes.	- Shore. - Demolish existing wall. - Construct new wall.	- Shore. - Demolish existing wall. - Construct new wall.
DS6 Severe Sliding Shear	- Large permanent wall offset. - Spalling and crushing at the wall toes due to dowel action and flexure. - Shear fracture of vertical reinforcement or dowels.	- Shore. - Demolish existing wall. - Construct new wall.	- Shore. - Demolish existing wall. - Construct new wall.

Table 5-11. Summary of Class A Fragility Parameters for Fully-Grouted RM Shear Walls (Murcia-Delso & Shing, 2012)

Damage State	Demand Parameter	Median θ	Total Dispersion β	Derivation Method
DS1	Story-drift ratio	0.31%	0.45	Actual demand data
DS2	Story-drift ratio	0.87%	0.35	Actual demand data
DS3	Story-drift ratio	1.51%	0.30	Actual demand data
DS4	Story-drift ratio	0.36%	0.60	Actual demand data
DS5	Story-drift ratio	0.59%	0.50	Actual demand data

Table 5-12. Summary of Class A Fragility Parameters for Partially-Grouted RM Shear Walls (Murcia-Delso & Shing, 2012)

Damage State	Demand Parameter	Median θ	Total Dispersion β	Derivation Method
DS1	Story-drift ratio	0.18%	0.75	Authors' opinion
DS2	Story-drift ratio	0.51%	0.60	Authors' opinion
DS3	Story-drift ratio	0.86%	0.55	Authors' opinion
DS4	Story-drift ratio	0.20%	0.85	Authors' opinion
DS5	Story-drift ratio	0.33%	0.75	Actual demand data

5.2.7 Slab Column Connections

Gogus & Wallace, (2008) developed fragility function for three types of slab-column connections: (1) reinforced concrete slab-column connections without shear reinforcements, (2) reinforced concrete slab-column connections with shear reinforcements, (3) post-tensioned slab-column connection without shear reinforcements, (4) post-tensioned slab-column connection with shear reinforcements, and (5) Reinforced concrete slab-column connections with shear capitals and/or drop panels. Inter story drift was used as engineering demand parameter, and connection types were grouped based on the Gravity Shear Ratio (GSR). Gravity Shear Ratio is defined to be the ratio of the factored gravity shear force acting on the slab critical section divided by the nominal concrete shear strength of the slab critical section defined by ACI 318- 08 Chapter 11 for

connections without slab shear reinforcement (Gogus & Wallace, 2008). Gogus & Wallace, (2008) considered two ranges of GSR based on the available data: (1) $0.2 \leq GSR < 0.4$, (2) $0.4 \leq GSR < 0.6$. GSR range of 0 to 0.2 was included for the reinforced concrete connection without shear reinforcements because sufficient data was available, but for other connection types fragility functions developed for the GSR 0.2 to 0.4 provide a conservative estimate of damage for GSR less than 0.2. Fragility functions are developed based on seventy-one tests collected from twenty-seven individual studies. Test data include geometry, reinforcement and material properties. Tests specimens that were constructed with light weight, or high strength concrete, or subjected to monotonic loading were not included.

Gogus & Wallace, (2008) defined two repair states for the connections, one related to modest repair requiring epoxy injection, and the other related to major repair requiring shoring, removing damaged concrete, possibly jacking and placing new concrete. These damage states rarely occur in literature, therefore, yielding of the specimen and Immediate /gradual drop in the lateral load capacity were used to formulate the fragility functions. No crack patterns for DS1 were available in the literature. Therefore, DS1 crack patterns were estimated based on DS2 cracks. Fragility function for connection type 1, 2, and 3 are based on the test data, but fragility function for connection type 4 and 5 are based on engineering judgment due to insufficient data. Table 5-13 provide the summary of the recommended parameters for the fragility functions. Table 5-14 provides the description of the damage states and the procedure to repair walls.

Table 5-13. Summary of Fragility Functions adapted from (Gogus & Wallace, 2008)

No.	Connection Type	GSR	Parameters	DS1	DS2	Basis
1	Reinforced Concrete Specimens without Shear Reinforcement	$0 < V_g/V_0 < 0.2$	x_m	2.5	4	Test Data
			β	0.4	0.4	
		$0.2 < V_g/V_0 < 0.4$	x_m	2	3.5	
			β	0.4	0.4	
		$0.4 \leq V_g/V_0 < 0.6$	x_m	1.2	1.5	
			β	0.4	0.4	
2	Reinforced Concrete Specimens with Shear Reinforcement	$0.2 < V_g/V_0 < 0.4$	x_m	3	4.8	
			β	0.4	0.5	
		$0.4 \leq V_g/V_0 < 0.6$	x_m	2.2	3	
			β	0.4	0.5	
3	Post-Tensioned Specimens without Shear Reinforcement	$0.2 < V_g/V_0 < 0.4$	x_m	1.8	3	
			β	0.4	0.4	
		$0.4 \leq V_g/V_0 < 0.6$	x_m	1.25	1.9	
			β	0.4	0.5	
4	Post-Tensioned Specimens with Shear Reinforcement	$0.2 < V_g/V_0 < 0.4$	x_m	2.8	4	Engineering Judgment
			β	0.5	0.5	
		$0.4 \leq V_g/V_0 < 0.6$	x_m	2.3	3.2	
			β	0.5	0.5	
5	Reinforced Concrete Specimens with Shear Capitals/Drop Panels	$0.2 < V_g/V_0 < 0.4$	x_m	2.5	4.2	
			β	0.5	0.5	
		$0.4 \leq V_g/V_0 < 0.6$	x_m	1.7	2.3	
			β	0.5	0.5	

Table 5-14. Description of damage states for slab column connections (Gogus & Wallace, 2008)

Damage state	Damage state characteristics	Associated repair method	Details of repair activity
DS1	Yield strain of the slab flexural reinforcement has been exceeded, spalling of concrete may/may not occur, slab exhibits sufficiently large crack widths to allow epoxy injection.	Epoxy injection	Remove furnishings, ceilings, mechanical, electrical and plumbing systems as necessary, 5 feet either side of the damaged area. Prepare work area for epoxy injection, inject epoxy, and replace and repair finishes. Replace furnishings, ceilings, mechanical, electrical, and plumping systems.
DS2	Slab punching failure occurs, causing significant spalling of concrete. Epoxy injection is no longer expected to be sufficient to restore the required strength and stiffness to the slab and the slab-column connection.	Major repair	Remove furnishings, ceilings, mechanical, electrical and plumbing systems as necessary, 15 feet either side of the damaged area. Shore damaged area a minimum of one level below (more levels if necessary). Remove damaged concrete at least 1 inch beyond the exposed reinforcing steel. Place concrete forms, and then concrete. Remove forms, replace and repair finishes. Replace furnishings, ceilings, mechanical, electrical, and plumbing systems. Significant drop of the slab relative to column would be expected; 1) if no shear reinforcement is provided, and 2) if the slab punches outside the shear reinforced zone. This case requires floor leveling prior to major repair (and more shoring), and slab flexural reinforcement may need to be removed, and new reinforcement spliced to existing reinforcement.

5.2.8 Slender Reinforced Concrete Walls

Birely, Lowes, & Lehman, (2011) developed fragility functions for slender reinforced concrete walls. Slenderness ratio of walls was defined as shear span ratio, and walls with shear span ratio greater than or equal to 2.0 were considered slender. Data on 66 wall tests were collected from 18 individual studies. Walls with openings or missing damage and load-displacement relationship were not included. The data comprised of 42 rectangular, 13 barbell, 5 C-shaped, 2 H-shape, and 4 T-shape walls. Fifty walls were tested with cyclic, uni-directional loading, 11 with monotonic uni-directional loading, and 5 with bi-directional loading. For each test the following

information was collected: 1) material properties, 2) specimen geometry and reinforcement layout, 3) positive and negative load –displacement envelopes, and 4) damage information.

Three types of engineering demand parameters—specimen drift, effective drift, and hinge rotation—were considered by the Birely, Lowes, & Lehman, (2011). Fragility functions were developed for four method of repairs (MOR). Each MOR included damages states that could be repaired using the corresponding MOR. Table 5-15 provides details about each MOR. The dataset of tests was reduced to eliminate the outliers based on Pierce's criterion, and tests subjected to monotonic loading were also removed. The impact of five design parameters on fragility function was also studied. The following parameters were considered: 1) shape, 2) shear span ratio, 3) axial load ratio, 4) shear stress demand, and 5) shear demand/capacity ratio. Trends were found in median values of the fragility functions due to change in shape, shear span ratio, and axial load ratio, but due to lack of enough experiments separate fragility functions could not be produced. The difference in shear stress demand and shear/demand capacity ratio had no effect on the fragility functions. There are two parts of the dispersion in the fragility functions. B_d represents the test data and β_u represents the uncertainty in the actual building. Based on ATC 58 guidelines β_u was assumed to be 0.25 when the number of specimens was greater or equal to five, otherwise, it was 0.1. Equation 5 gives the relation between the dispersions.

Final fragility functions were presented in terms of rotation demand as required by the ATC 58. Fragility functions based on effective drift are also reported in the Table 5-16 because in this study interstory drift is one of the engineering demand parameters considered.

Table 5-15. Description of Damage States of slender RC walls (Birely et al., 2011)

Method of Repair	Damage State	Description
Cosmetic repair	DS1a	Initial cracking
	DS1b	Initial flexural cracking
	DS1c	Initial shear cracking
	DS1d	Tensile yield of extreme longitudinal steel
	DS1e	Compression yield of longitudinal steel
	DS1f	Tensile yield of horizontal reinforcement
Epoxy injection and concrete patching	DS2a	Spalling of boundary region cover concrete
	DS2b	(not revealing longitudinal reinforcement) Spalling of patched concrete
	DS2c	Spalling of web concrete
	DS2d	Vertical cracks/splitting
Replace concrete	DS3a	Spalling revealing longitudinal reinforcement
Replace wall	DS4a	Core crushing (boundary element) Bar buckling
	DS4b	Compressive failure of boundary element
	DS4c	Failure by core crushing (boundary element)
	DS4d	Bar fracture
	DS4e	Failure due to bar buckling
	DS4f	Failure due to bar fracture
	DS4g	
	DS4i	Shear failure
	DS4k	Web crushing
	DS4m	Failure due to web crushing
	DS4o	Failure by bond slip
	DS4p	Core crushing in confined boundary element of flange tips (bi-directional tests only)
	DS4q	Confining reinforcement open or fractured

Table 5-16: Fragility Curve Parameters for slender RC shear walls (Birely et al., 2011)

EDP	Damage State	θ	β_d	β_u	β
Effective drift	DS1	0.118	0.755	0.1	0.762
	DS2	0.927	0.465	0.1	0.476
	DS3	1.28	0.326	0.1	0.326
	DS4	1.86	0.43	0.1	0.43
Hinge Rotation	DS1	0.00087	0.9	0.1	0.9
	DS2	0.0084	0.5	0.1	0.5
	DS3	0.012	0.4	0.1	0.4
	DS4	0.019	0.45	0.1	0.45

5.2.9 Special Moment Frame systems (SMF)

ATC 58 collected data on following four components of the SMF systems.

1. Beam-to-column moment connections
2. Beam-to-column gravity beam shear connections
3. Moment resisting column base plate connections
4. Welded column splices

It is assumed that the columns, joint panel zones, and beam-column connections in the SMF systems are strong enough to develop inelastic action at the beam hinges and column base plates. Almost all of the tests were done on isolated subassemblies; therefore, they could not capture additional effects of full frames on the connections. Cordova and Deierlein (2005) explains the benefits of frame continuity and suggests that subassemblies tests over-estimate the damage. Laboratory tests do not cover the variation in the field; therefore, dispersion of the test underestimates the actual dispersion of the fragility curves (Deierlein & Victorsson, 2008).

Reduced beam section (RBS) connections were developed after the 1994 Northridge, CA earthquake. During the earthquake most of the steel moment connections failed at much lower load and drift levels. Most of the inelasticity is focused at the connections in the steel moment frame. Pre- Northridge connections did not had enough ductility to sustain inelastic deformations due to which they failed and led to the development of the RBS connections. In RBS connections steel beam flanges are cut a little away from the connections to reduce the size of the section and focus the inelasticity at the reduced section instead of the connection.

5.2.9.1 Beam-to-column moment connections:

Beam to column moment connection are further subdivided into three types of connection:

1. Pre-Northridge Connections
2. Post-Northridge RBS Connections with Slab and strong panel zones
3. Post-Northridge Non-RBS connections with Slab

5.2.9.1.1 Pre-Northridge Connections

Twenty-two laboratory tests from four different investigations were used to develop fragility curve for these connections. Damage states were developed by expert judgment of damage in tests and damage in buildings after the Northridge earthquake. Dispersion of the damage states was increased to 0.4 to account for the variations not covered in the tests. Some of the damage states only had one or two tests in them, so it was necessary to account for the increased variability. Table 5-17 summarizes the fragility curve parameters for the Pre-Northridge connections.

Table 5-17. Fragility, damage measures, and consequences for Steel SMF Pre-Northridge Beam-Column Moment Connections [Adapted from (Deierlein & Victorsson, 2008)]

Component category:	Structural				
Basic composition:	Fully restrained beam-column connection with welded flanges and bolted webs. Flange welds are of the pre-Northridge type with non-notch toughness electrodes and backing bars left in place.				
Units:	Number of connections				
Demand parameter:	Story Drift Ratio				
Number of damage states:	5 (DS-1A/B; DS-2A/B, DS-3)				
If multiple damage states:	DS 1 and DS 2 are ordered, and within each of these the A/B variants are mutually exclusive of each other. DS 3 is mutually exclusive of DS 1 and 2.				
Damage states, fragilities, and consequences					
	DS 1 & DS2: Weld Fractures				**DS 3**
	DS 1A	**DS 1B**	**DS 2A**	**DS 2B**	**DS 3**
Description:	Note 1A	Note 1B	Note2A	Note2B	Note 3
Median demand (θ):	0.017	0.017	0.025	0.025	0.03
Dispersion (β):	0.40	0.40	0.40	0.40	0.40
Repairs required:	Note 1A	Note 1B	Note2A	Note2B	Note 3

Notes:

1A) **DS-1A:** Fracture of lower beam flange weld and failure of web bolts (shear tab connection), with fractures confined to the weld region. Repair will typically require gouging out and re-welding of the beam flange weld, repair of shear tab, and replacing shear bolts.

1B) **DS-1B:** Similar to DS-1A, except that fracture propagates into column flanges. In addition to measures for DS-1A, repairs to column will be necessary that will involve replacing a portion of the column.

2A) **DS-2A:** Fracture of upper beam flange weld, either alone or combined with DS-1 type damage. Fracture is confined to beam flange region. Repairs will be similar to those required for DS-1A, except that access to weld will likely require removal of a portion of the floor slab above the weld.

2B) **DS-2B:** Similar to DS-2A, except that fracture propagates into column flanges. In addition to measures for DS-2A, repairs to column will be necessary that will involve replacing a portion of the column.

3) **DS-3:** Ductile fracture initiating at weld access hole and propagating through beam flange, possibly accompanied by local buckling deformations of web and flange. Repair is similar to that for DS-1A except that a portion of the beam web and flange may need to be heat straightened or replace.

5.2.9.1.2 Post-Northridge RBS Connections with Slab and strong panel zones

Twenty-one tests from four different studies were considered for fragility curves. Out of twenty-one tests eight has stiff panel zones. The performance of Tests without stiff panel zones was different than the tests with stiff panels. They were susceptible to lateral torsional buckling and local web/flange buckling. Only eight Tests with stiff panel zones were used to create the fragility curves. Damage states were developed by the observations done during tests only. No real building damage was available for these connections. Table 5-18 summarizes the fragility curve parameters for the steel SMF Post-Northridge RBS connections with slab and strong panel zones.

Table 5-18. Fragility, damage measures, and consequences for the steel SMF Post-Northridge RBS connections with slab and strong panel zones [Adapted from (Deierlein & Victorsson, 2008)]

Component category:	Structural		
Basic composition:	Fully restrained beam-column connection with welded flanges, bolted webs, and reduced beam section (RBS) in the plastic hinge region. Welding details utilize electrodes with high notch-toughness and other modifications to minimize potential for weld root fractures.		
Units:	Number of connections		
Demand parameter:	Story Drift Ratio		
Number of damage states:	3		
If multiple damage states:	DS 1, 2 and 3 are ordered.		
Damage states, fragilities, and consequences			
	DS 1	**DS 2**	**DS 3**
Description:	Note 1	Note2	Note 3
Median demand (θ):	0.03	0.04	0.05
Dispersion (β):	0.30	0.30	0.30
Repairs required:	Note 1	Note 2	Note 3

Notes:

1) **DS-1:** Local beam flange and web buckling. The likely repair state is heat straightening of the buckled web and flanges

2) **DS-2:** DS1 plus lateral-torsional distortion of beam in hinge region. Repair by heat straightening may be possible, but it is likely that the distorted portions of the beam may need to be replaced.

3) **DS-3:** Low-cycle fatigue fracture of beam flanges in buckled region of RBS. The fracture is usually precipitated by DS-1 and possibly DS-2. Repair will necessitate removal and replacement of distorted and fractured portion of beam.

5.2.9.1.3 Post-Northridge Non-RBS connections with Slab

Fragility curves were developed from twenty-seven tests from five different studies. They were less susceptible to local buckling than RBS connections. Damage states were developed by the observations done during tests only. No real building damage was available for these connections. The dispersion was increased to 0.3 because the number of tests was significantly less than the range of member sizes and bracing configurations. Table 5-19 summarizes the fragility curve parameters the steel SMF Post-Northridge Non-RBS connections with the slab.

Table 5-19. Fragility, damage measures, and consequences for steel SMF Post-Northridge Non-RBS connections with slab [Adapted from (Deierlein & Victorsson, 2008)]

Component category:	Structural		
Basic composition:	Fully restrained beam-column connection with welded flanges, bolted webs, and other non-RBS post-Northridge connection details. Welding Details utilize electrodes with high notch-toughness and other modifications to minimize potential for weld root fractures.		
Units:	Number of connections		
Demand parameter:	Story Drift Ratio		
Number of damage states:	3		
If multiple damage states:	DS 1, 2 and 3 are ordered.		
Damage states, fragilities, and consequences			
	DS 1	**DS 2**	**DS 3**
Description:	Note 1	Note2	Note 3
Median demand (θ):	0.03	0.04	0.05
Dispersion (β):	0.30	0.30	0.30
Repairs required:	Note 1	Note 2	Note 3

Notes:

1) **DS-1:** Local beam flange and web buckling. The likely repair state is heat straightening of the buckled web and flanges

2) **DS-2:** DS1 plus lateral-torsional distortion of beam in hinge region. Repair by heat straightening may be possible, but it is likely that the distorted portions of the beam may need to be replaced.

3) **DS-3:** Low-cycle fatigue fracture of beam flanges in buckled region of RBS. The fracture is usually precipitated by DS-1 and possibly DS-2. Repair will necessitate removal and replacement of distorted and fractured portion of beam.

4) Damage state DS-2 was evident in only some connections and is judged to have a 25% chance of occurrence when the demand parameter for DS-2 is reached.

5.2.9.2 Gravity Beam Shear Connections:

Thirteen test from a single study were used to form the fragility curves for gravity beam shear connections. Damage states were made by observations of the tests. Median and dispersion were not adjusted to account for increased variability in actual buildings. Table 5-20 summarizes the fragility curve parameters the gravity beam shear connections.

Table 5-20. Fragility, damage measures, and consequences for Gravity Beam Shear Connections [Adapted from (Deierlein & Victorsson, 2008)]

Component category:	Structural		
Basic composition:	Gravity shear connection consisting of vertical shear tab plate that is welded to column and bolted to the supported beam web.		
Units:	Number of connections		
Demand parameter:	Story Drift Ratio		
Number of damage states:	3		
If multiple damage states:	DS 1,2 and 3 are ordered.		
Damage states, fragilities, and consequences			
	DS 1	**DS 2**	**DS 3**
Description:	Note 1	Note2	Note 3
Median demand (θ):	0.04	0.08	0.11
Dispersion (β):	0.40	0.40	0.20
Repairs required:	Note 1	Note 2	Note 3

Notes:

1) **DS-1:** Yielding of shear tab and elongation of bolt holes, possible crack initiation around bolt holes or at shear tab weld. Careful inspection and welded repair to any cracks and possible replacement of shear tab if bolt hole deformations are excessive (possible for deeper 6-bolt or deeper shear tabs).
2) **DS-2:** Partial tearing of shear tab and possibility of bolt shear failure (6-bolt or deeper connections). Repairs will include either welded repair of shear tab or possible complete replacement of shear tab and installation of new bolts. Repairs may require shoring of beam.
3) **DS-3:** Complete separation of shear tab, close to complete loss of vertical load resistance. Repair will include complete replacement of shear tab and installation of new bolts. Repairs will require shoring of beam.

5.2.9.3 Column Base plates:

Sixteen tests from four different studies were used to develop the fragility curves for column base plates. It was assumed that the anchor rods and the base plates are strong enough to allow development of plastic hinge at the column base and the failure will be due to failure of the column hinging and weld fracture (Deierlein & Victorsson, 2008). Table 5-21 summarizes the fragility curve parameters the column base plates.

Table 5-21. Fragility, damage measures, and consequences for Column Base Plates [Adapted from (Deierlein & Victorsson, 2008)]

Component category:	Structural		
Basic composition:	Column base plates – welded to steel column and anchored to concrete footing to create fixed condition.		
Units:	Number of connections		
Demand parameter:	Story Drift Ratio		
Number of damage states:	3		
If multiple damage states:	DS 1,2 and 3 are ordered.		
Damage states, fragilities, and consequences			
	DS 1	**DS 2**	**DS 3**
Description:	Note 1	Note2	Note 3
Median demand (θ):	0.04 (strong axis) 0.01 (weak axis)	0.07 (strong axis) 0.025 (weak axis)	0.10 (strong axis) 0.05 (weak axis)
Dispersion (β):	0.40	0.40	0.40
Repairs required:	Note 1	Note 2	Note 3

Notes:

1) **DS-1:** Initiation of ductile fracture at the fusion line between the column flange and the baseplate weld. The repair will involve gouging out material surrounding the fracture initiating and re-welding.
2) **DS-2:** Propagation of brittle crack into column and/or base plate. Depending on the crack trajectory, the repair will range from replacement of a portion of the column or base plate to full replacement of the column base. Replacement will require shoring of column, torch cutting to remove damaged material, and fabrication and field welding to install replacement material.
3) **DS-3:** Complete fracture of the column (or column weld) and dislocation of column relative to the base plate. Repair may not be feasible depending on the extent of dislocation, which is likely to be accompanied by large residual story drift. If feasible, repair would likely involve replacing the entire base plate assembly and most of the column in the story above the base plate.

5.2.9.4 Welded Column Splices:

No test data was used to develop the fragility curves for welded column splices. Damage states and fragility curves are developed using exceedance of stress from a nominal weld stress and sufficient deformations. Stress is calculated from the nonlinear time history analysis. Table 5-21 summarizes the fragility curve parameters welded column splices.

Table 5-22. Fragility, damage measures, and consequences for Column Base Plates [Adapted from (Deierlein & Victorsson, 2008)]

Component category:	Structural	
Basic composition:	Welded column splice consisting of partial penetration groove welds of the column flanges and a web splice plate.	
Units:	Number of connections	
Demand parameter:	Stress Trigger and Story Drift Ratio	
Number of damage states:	3	
If multiple damage states:	DS 1 and 2 are ordered.	
Damage states, fragilities, and consequences		
	DS 1	**DS 2**
Description:	Note 1	Note2
Median demand (θ):	Stress Trigger (Note 3), 0.02	0.05
Dispersion (β):	0.40	0.40
Repairs required:	Note 1	Note 2

Notes:

1) ***DS-1*:** Ductile fracture of the groove weld flange splice. Repair would involve gouging out the material adjacent to the fracture and repairing with a new groove weld.
2) ***DS-2*:** *DS-1* following by complete failure of the web splice plate and dislocation of the two column segments on either side of the splice. Repair may not be practically feasible, but would require either realignment or replacement of adjacent column segments and rewelding of splice.
3) The stress trigger on DS-1 is to be evaluated as follows: $\sigma_{applied} < 1.5f_u$, where fu is the minimum specified strength of the weld metal and $\sigma_{applied}$ is the maximum *tensile* stress induced by the combination of major- and minor-axis bending and axial load. The stress check could either be made based on forces calculated during the nonlinear time history analysis or by simplified calculations to relate the imposed story drifts to the induced stresses, taking into account the structural configuration and member sizes.

5.2.10 Wood Light-Frame Structural Systems

Ekiert & Filiatrault, (2008) developed fragility curves for the wood light –frame structural walls. Walls systems were selected from the ATC guidelines. Following are the six systems selected for the fragility curve development.

1. System #47: Structural panel sheathing (plywood or OSB) shear walls with interior gypsum Wallboard, basic strength design.
2. System #48: Structural panel sheathing with stucco exterior and gypsum Wallboard interior, basic strength design.
3. System #49: Stucco on gypsum wallboard.

4. System #50: Structural panel sheathing (plywood or OSB) shear walls with interior gypsum Wallboard, strength design with seismic tie downs and nail/screw details.
5. System #51: Structural panel sheathing (plywood or OSB) shear walls with stucco exterior and gypsum Wallboard interior, strength design with seismic tie downs and nail/screw details.
6. System #52: Light Wood Frame, Diagonal Strut Bracing

Fragility curves are developed for the wall Gypsum wallboard, # 50 and # 51 were developed using actual test data from six, five, and five tests respectively. Test studies included cyclic tests of wall assemblies and shake table testing of wood light frame buildings. # 49 was not considered because it is not a common practice in North America. Fragility curves for the #52 wall were developed based on the tests done in Japan. The fragility curve of the #47 wall was developed by multiplying the median value of the # 50 wall by 2/3 and increasing the dispersion to 0.4. The Fragility curve of the #48 wall was developed by multiplying the median value of the # 51 wall with 2/3 and increasing the dispersion to 0.4. Only the tests performed according to the CUREE-Caltech loading protocol were used in the development of the fragility curves because it was found that the CUREE-Caltech protocol is more realistic than the Sequential Phased Displacement or ISO loading protocols. Lilliefors test was used to check the goodness of fit. Lilliefors test is used to computes the normality of a give data. It is used to test if the lognormal distribution is acceptable to represent the data. Table 5-23 and Table 5-24 summarize the fragility curve parameters and the damage state description for the wood shear walls respectively.

Table 5-23: Fragility Curve Parameters for Wood Light Frames [Adapted from (Ekiert & Filiatrault, 2008)]

System Number/Type	Demand Parameter	Median % (θ)			Dispersion (β)			Data Type*
		DS_1	DS_2	DS_3	DS_1	DS_2	DS_3	
Gypsum Wallboard***	Interstory Drift (%)	0.33	0.56	-	0.55	0.56	-	A,A
Wall System #50***		1.50	2.62	3.69	0.40	0.16	0.17	E,A,A
Wall System #47***		1.00	1.75	2.50	0.40	0.40	0.40	E,E,E
Wall System #51***		0.25	0.52	2.52	0.43	0.28	0.12	A,A,A
Wall System #48***		0.17	0.35	1.70	0.50	0.40	0.40	E,E,E
Braced Wall System #52		1.00	-	-	0.30	-	-	E

*A – Actual Data (Method A), E – Expert Judgment (Method E)

***For wall piers with aspect ratios between 2:1 and 3.5:1, median value should be multiplied by 2bs/h

Table 5-24: Damage State Discerptions for Wood Light Frame Structures [(Ekiert & Filiatrault, 2008)]

System Number/ Type	Damage States (DS1)	Description of Damage State
Gypsum Wall board	DS1	Cracking of paint over fasteners or joints
	DS2	Local and global buckling out-of-plane and crushing of gypsum wallboard
System # 50 and # 47	DS1	Slight separation of sheathing or nails come loose
	DS2	Permanent rotation of sheathing, tear out of nails or sheathing tear out
	DS3	Fracture of studs, major sill plate cracking
System # 51 and # 48	DS1	Cracking of Stucco
	DS2	Spalling of stucco, separation of stucco and sheathing from studs
	DS3	Fracture of studs, major sill plate cracking
System # 52	DS1	Failure of Diagonal Bracing

5.2.11 Comparison and Results

The review of the 10 structural background reports that are the basis of the development of the component fragility curve database in the FEMA P-58 led to the identification of the different techniques used to develop the curves and the identification of the problems faced by the authors while developing theses curves. Overall all of the reports attempted to develop the component

fragility curves from the test data, but in the case of insufficient information, engineering judgment was also used. In total fragility curves for 41 different structural components were produced, and only seven of them were entirely based on the engineering judgment.

The first common issue that authors had to face was that the test studies used for the fragility curve development were not conducted for this specific purpose. Test studies done on structural subassemblies are primarily done to calculate the maximum capacity of the specimens, therefore, most of the data till the collapse point is not often reported or recorded, especially at low applied loads when there is only cosmetic damage data. DS1 in the case of insufficient data points was developed based on the engineering judgment.

The second issue was that the subassembly tests have lower stiffness as compared to when they are part of a full system. Authors recognized this issue in the reports, but no adjustments were made to the median values. In the case of Pre-Northridge connections, damage observations from the test data and the post-disaster reports were available, and the comparison of these damage states showed that the type of damage occurring in the test setups was not same as in the post-disaster reports (cite).

There were three main methods used to identify the damage states. The first method was to use visual observation to define the damage state and afterward the method of repairs were defined. The second method was used when several different types of damage could occur in the specimen, but they were grouped based on the method of repairs required to repair them. Then these groups were used as damage states. The last method was to use backbone curves if the damage observation were not consistent. In this method, points corresponding to each damage state were defined on the backbone curve to get more consistent results.

Dispersion in the test data was reported for all of the curves, but some authors did not include the uncertainty due to different construction qualities. ATC guideline recommended a β_u factor be added to the dispersion based on the number tests used to develop the fragility curves.

In conclusion, all of the reports were well documented and utilized the full potential of the test studies. The biggest problem was the intent of the test studies. None of the test studies were specifically conducted to develop fragility curves. In the future, test studies should be conducted to develop the fragility curves instead of just determining the final strength of the component because not in only it captures the strength of the specimens, but also the progression of damage in the specimens. The other way to solve this problem would be to include the video recording of the damage progression as standard procedure in all of the tests.

5.3 EDP to DS Fragility Curves for Hurricane and Tsunami

According to data found in the literature, the convention for hurricane and tsunami is to go directly from IM to DS. These curves were collected and reported in Chapter 4. No EDP to DS curves were found in the literature for structural components.

Chapter 6 Damage State to Decision Variable Fragility Curves

6.1 Introduction

The last set of relationships required in performance based design is the DS to DV curve. They are also called consequence functions. These curves convert all of the analysis into the form that can be used to make decisions and can also be interpreted by the building owners. For each DS of the component of the structure, there is a corresponding consequence function relating it to each of the DVs. The method of repair is defined for the DS and then based on it the consequence function is developed.

6.2 DS to DV curves for the Earthquakes

In the case of earthquakes FEMA-P58 (Applied Technology Council, 2012) includes a database of the consequence functions for each of the component fragility curves produced. These curves are defined by five values, namely, max value, min value, max quantity, min quantity, and dispersion. Max value is the value of the DV per unit quantity when the economies of scale and efficiencies in operation are excluded. Min value is the value of DV per unit quantity when the economies of scale and efficiencies in operation are included. Min quantity defines the quantity till which max value of DV is applicable, and max quantity defines the value after which the Min value of DV is applicable. Linear interpolation can be used between the max and min quantity. Dispersion accounts for the uncertainty in the values of the DV. The database includes dispersion values for both normal and lognormal distribution. Figure 6-1 shows a typical consequence function in FEMA P-58. The values in the database are calculated for Northern California as a reference location and the reference time is 2011. Currently, it has consequence functions for two

decision variables repair cost and repair time. These curves were not critically reviewed because there was no background information available regarding their development.

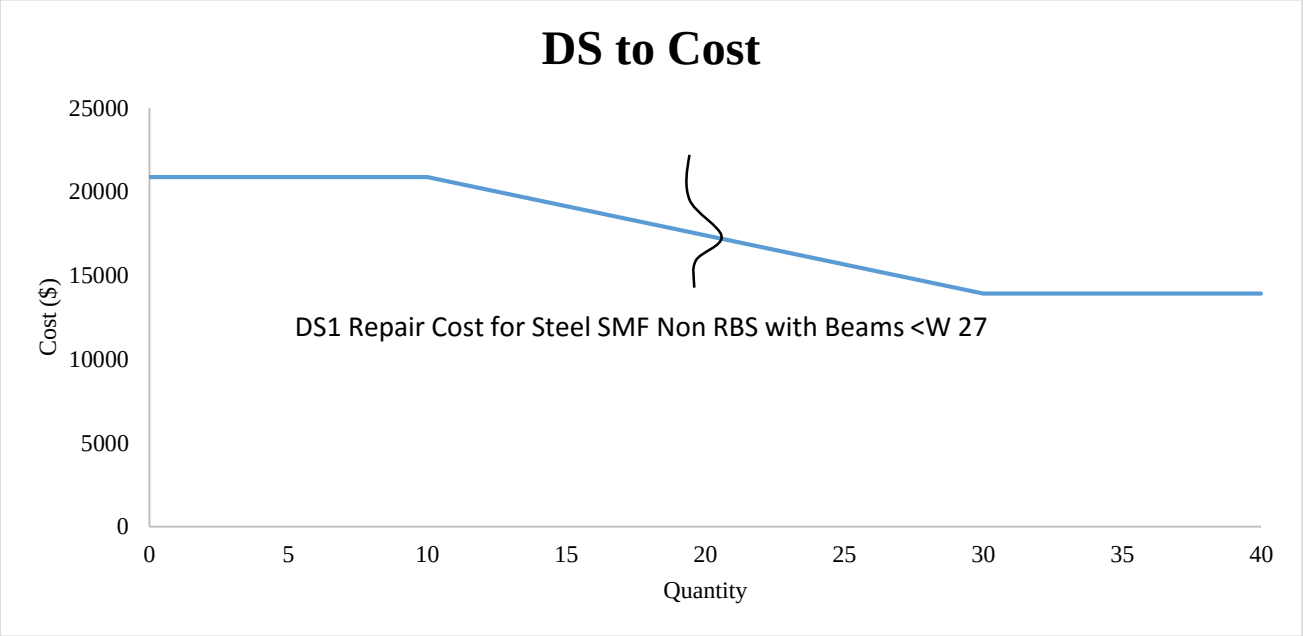

Figure 6-1. A typical DS to DV curve in FEMA P-58

6.3 DS to DV curves for the Hurricanes

Consequence functions are based on the damage state of the building components. In the case of hurricanes very few component fragility curves (EDP to DS) are developed and their authors do not define the corresponding consequence functions. The functions in FEMA P-58 can be used for the hurricanes as long the method of repair is same for the damages incurred due to the hurricane. Although, there is one significant difference between the damage from earthquakes and hurricane that is the water damage.

6.4 DS to DV curves for the Tsunami

DS to DV curves were not found in the literature because there were not EDP to DS curves for the components of the building. Similarly to hurricanes, if the method of repair for damage

incurred due to the tsunami is same as in FEMA P-58, then those curves can also be used for the tsunami. Water damage is also a separate issue for tsunamis and new consequence function will need to be developed to account for that kind of damage.

Chapter 7 Identification of Gaps and Methods for Filling

7.1 Introduction

In this chapter gaps in the collected data are identified and possible methods are recommended to fill those gaps. Figure 3-3 in chapter 3 was developed on the basis of the available information in the literature. The goal of that flow chart was to lay out the plan for the collection of the existing relationships between pinch points. The flow chart provided a general idea about what relationships between pinch points are required for PBEE calculation. Figure 7-1 was developed after the collection of data from the literature to graphically represent the gaps in the data. Each blue arrow shows the relationship required, and each green arrow represents the relationships collected from the literature. Green arrows do not necessarily indicate that relationship for all of the structural systems has been collected from the database, only that some information has been collected. Figure 7-1 also shows the framework for performing PBEE calculations for each SFSE combination. There are five points in Intensity Measure (IM), Load combination (LC), Engineering demand parameter (EDP), Damage state (DS), and Decision variable (DV). There are four sets of relationships required to connect these points and they are discussed below.

7.2 IM to LC

In the case of earthquake ground acceleration is the only intensity measure considered, so there is no need of load combinations. In the case of a hurricane, there are several intensity measures to which building is subjected during an event like wind speed, water depth, flow velocity etc. These intensity measures are needed to be combined into one LC because the response of the building may go into inelastic range and results from each intensity measure cannot be combined by superposition. This same reason is applicable to tsunami because it also has multiple intensity measures.

Vector-based intensity measure is a well-developed and widely used way to combine multiple intensity measures. Vector-based intensity measure can be used to skip the load combination step.

7.3 LC to EDP

IDA curves collected for earthquake comes in this category, but the curves collected do not include all the structural systems, and do not have enough curves for each of the systems that a generalized curve for each of the system could be developed. IDA analysis could be performed to develop these relationships. Another issue with the curves is that the relationships only relate spectral acceleration to interstory drift ratio. Different components are sensitive to different EDP, e.g., structural components are sensitive to interstory drift ratio and non-structural components are sensitive to peak floor accelerations and velocities. IDA analysis of more structures will solve this issue also.

Response of the structure is dependent upon the attributes of the structure like location, design intensity measure, number of stories, structural system, and design code etc. It is essential while conducting analysis to keep attributes of structure similar as many as possible so that sole effect on response of structure is due to the structural system. Structures at different locations are designed for different levels of design intensity measures e.g. design loads for a building designed in Los Angeles would be different than the building in Boston, and it would not be acceptable to compare the response of these two structures. Comparison of two structural systems designed for same location is acceptable. The other issue is that some structural systems are more efficient for higher loads and some for lower loads, so it will not be affair to represent a structural system by a response of structure at a specific location. It is essential to design and analyze buildings for multiple locations or multiple design intensity measures.

IM to DS fragility curves collected for the tsunami from post-disaster survey partially come in this category. There are third issues with these curves. The first issue is that they relate IM to DS of the whole building instead of components, therefore, detailed PBEE calculations are not possible. The second issue is that these curves are for individual IMs and do not account for their combined effects. The last issue is that most of these curves are based on non-engineered buildings and do not differentiate between structural systems. The only way to solve these issue would be to use computer analysis because post-disaster surveys do not show the combined effects of intensity measures.

There is no data collected for a hurricane that corresponds to these relationships, therefore, computer analysis of structures is required to categorize the response of structures.

7.4 EDP to DS

Component fragility curve collected from FEMA P-58 provide a good source of EDP to DS curves for earthquakes. FEMA P-58 (Applied Technology Council, 2012) also provides guidelines for developing these curves by five methods: 1. Actual demand data (using actual test data from sufficient data and specimens reach a damage state at a certain value.), 2.Bounding demand data (Using test data or post-earthquake survey report and damage state occurred in some specimens), 3) Capable demand data (Using test data or post-earthquake survey report and damage state did not occur in any of the specimens), 4)Derivation (Using analytical models to estimate the demand at which damage state occurs), and 5) Expert Opinion (No data is available and analysis is not possible then engineering judgement can be used).

Building level fragility curves are good substitute for component fragility curves for generic structures. They require a lot less testing and mostly based upon post disaster surveys. Building

level curves also help to produce consequence functions at building level instead of component level. They decrease the accuracy of the performance based calculation with the decrease in the complexity, but for generic buildings it is used to compare SFSE combinations so it is acceptable.

There are no EDP to DS curves available for tsunami and hurricane. Guidelines mentioned above could also be used to develop fragility curves for tsunami and hurricane.

7.5 DS to DV

The last set of relationships is DS to DV. These curves are directly related to EDP to DS curves because Damage state determines the method of repair and decision variables like repair cost and repair time are directly related to the method of repair. These relationships are developed by obtaining quotes from contractors or engineering judgment. Consequence function collected from FEMA P-58 also provide a good source of these curves for earthquakes. Component-level DS to DV curves for tsunami and hurricane are not present in literature because the EDP to DS state has not been characterized for those hazards.

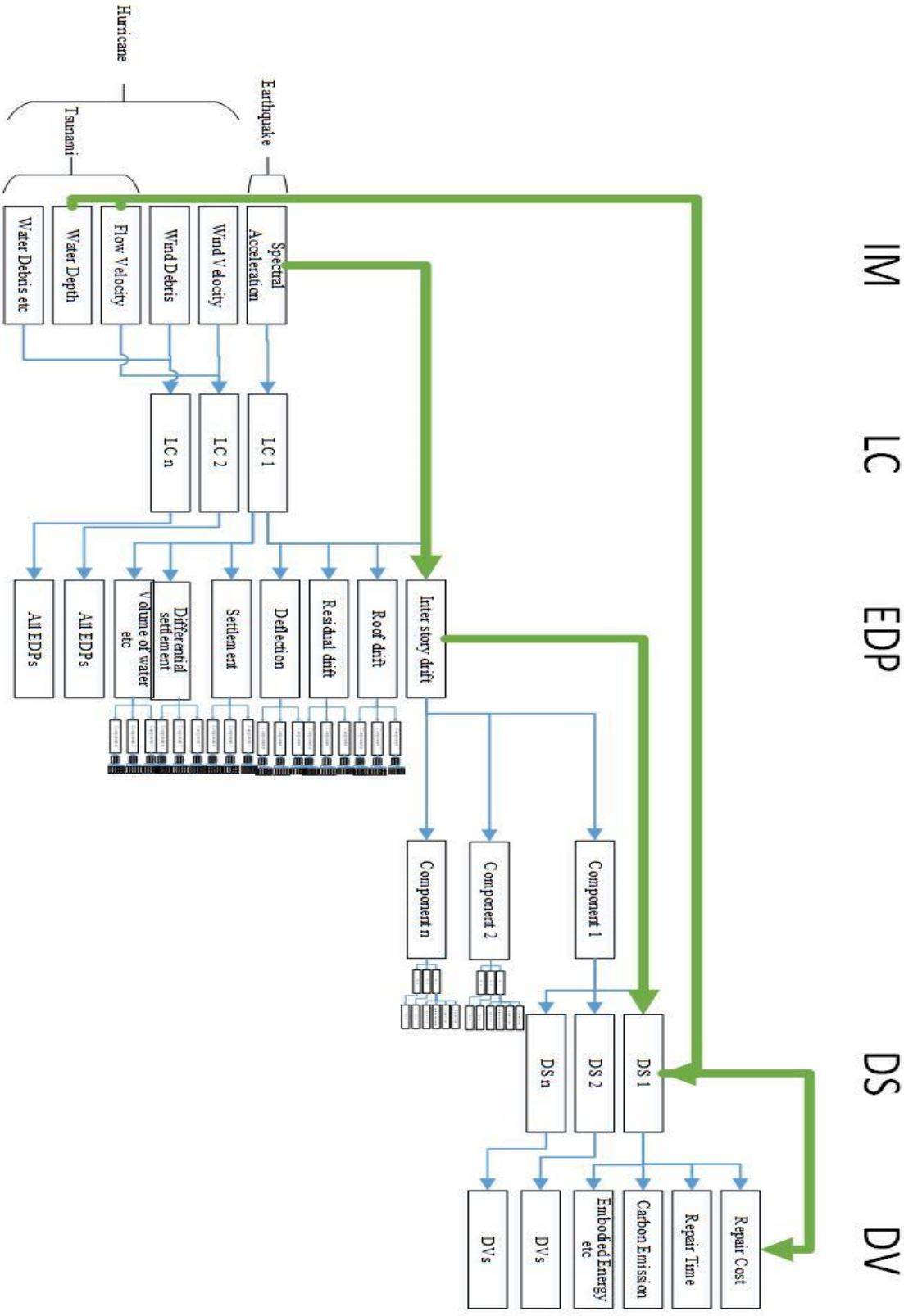

Figure 7-1. Collected data and Gaps

7.6 Screening of SFSE combinations

The motivation of the database was to be able to perform preliminary performance based engineering calculations for each of the SFSE combinations, and reduce the number of combination based on these calculations. Allowing the next part of this study to have a feasible number of combination for which detailed analysis can be performed. SFSE combinations were reduced on the basis of engineering judgment. Table 8-1 summarizes the reduction in the combinations. There were 4224 combinations possible based upon 3 soil systems, 4 foundation systems, 11 structural systems, and 32 envelope systems. Combinations were divided into two categories. In first category envelope systems are recognized as a variable which is important for Performance based engineering calculations. In the second category, envelope systems are not taken as a variable because computer analysis of structures is usually assumed not to depend on envelope systems, but envelopes can be included in the analysis if they are heavy/stiff enough to affect the response of the structure.

In addition to categories, three checks were employed based on engineering judgment to reduce the number of combinations. Check 1 did not allow single footing with structural systems that use the shear wall as lateral force resisting system. Check 2 did not allow deep footings with improved soil because they are alternative ways of solving poor soil conditions. Check 3 was used to allow only selective envelope systems for wood shear wall structures and cold-formed steel shear wall system because these structural systems do not have a large load carrying capacity and it does not make sense to use certain envelope systems with them. Only 5 out of 32 systems were allowed for wood shear wall and cold-form steel shear wall structural systems: Curtain Wall Glazing - w/out Cavity, Infill Wall SS: Masonry - w/ Cavity, Infill Wall SS: Masonry - w/out Cavity, Infill Wall SS: Plaster - w/ Cavity, and Infill Wall SS Plaster - w/out Cavity.

Table 7-1 summarizes the results of the screening of the SFSE combinations based on engineering judgement. Two categories of SFSE combination with and without envelopes are screened based on three checks mentioned above. Each entry in front of checks represent the number of combination eliminated by that check. Reduced combinations show the final number of combinations left after screening in each category.

Table 7-1. Reducing number of SFSE combinations based on engineering judgment

Combinations	Combination with envelope systems	Combination without envelope systems
Total	4224	132
Check 1(No single footing with shear wall)	576	18
Check 2 (No deep footing with improved soil)	704	22
Check 3 (selective envelopes with wood and cold-formed steel systems)	648	NA
Reduced combinations	2566	92

Chapter 8 Conclusion

In conclusion, a preliminary database of fragility curves, structural analysis, and consequence functions was developed, although the database is far from completion due to very limited amount of data available in the literature. Chapter 7 explained the gaps in the data and the procedures to fill in the gaps. Contrary to original expectations, the amount of data collected was more like small patches, and gaps were a lot bigger than those patches. 46 IDA curves and 29 collapse fragility curves were collected from 16 independent studies covering 6 out of 11 structural systems selected for this study. Review of ten FEMA P-58 structural background reports accumulated EDP to DS fragility curves and DS to DV consequence functions for 41 structural components, out of which only seven were based on engineering judgments. For tsunami 46 IM to DS curves were collected from 9 independent studies based upon post-disaster surveys. Curves collected for tsunami were mainly for non-engineered structures and they did not differentiate between the 11 structural systems. These curves were based on tsunami events ranging from 1993 to 2011. Taken together, these curves are a good start for the development of the database, however, these curves are collected from independent studies which do not have many similarities. IM to EDP curves cannot be compared with each other for same components because the number of studies on each component is not sufficient enough to develop a general curve for that component. The above mentioned reasons lead to the conclusions that a systematic analysis of structural systems is required to develop curves to represent generic structural systems, while keeping other variables constant like floor plan, story height, location, design code and ground motions etc.

The data collected in this study is not sufficient for conducting multi-hazard PBEE calculation. There is therefore a huge potential for future work on this topic. Accumulation of relationships

between pinch points for all of the structural systems is necessary and for that analysis and testing of these systems is required. Further study is required to attain the final goal of optimizing the SFSE combination for multi-hazard resilient and sustainable building design.

References

Akbas, B., Sutchiewcharn, N., Cai, W., Wen, R., & Shen, J. (2013). Comparative study of special and ordinary braced frames Bulent. *The Structural Design of Tall and Special Buildings*, *24*(January 2012), 989–1022. http://doi.org/10.1002/tal

Applied Technology Council. (2012). FEMA P-58-1: Seismic Performance Assessment of Buildings. Volume 1 – Methodology, *1*(September).

Ariyaratana, C., & Fahnestock, L. A. (2011). Evaluation of buckling-restrained braced frame seismic performance considering reserve strength. *Engineering Structures*, *33*(1), 77–89. http://doi.org/10.1016/j.engstruct.2010.09.020

B. F. Howell, J. (1997). Patterns of Seismic Activity after Three Great Earthquakes in the Light of Reid's Elastic Rebound Theory, *87*(1).

Benjamin, J. R., & Cornell, C. A. (2014). *Probability, Statistics, and Decision for Civil Engineers*. Courier Corporation. Retrieved from https://books.google.com/books?hl=en&lr=&id=Gqm-AwAAQBAJ&pgis=1

Birely, A. C., Lowes, L. N., & Lehman, D. E. (2011). Background Document Fragility Functions for Slender Reinforced Concrete Walls, 1–191.

Bisadi, V., & Padgett, J. E. (2015). Explicit Time-Dependent Multi-Hazard Cost Analysis Based on Parameterized Demand Models for the Optimum Design of Bridge Structures, *30*, 541–554. http://doi.org/10.1111/mice.12131

Charvet, I., Suppasri, A., & Imamura, F. (2014). Empirical fragility analysis of building damage caused by the 2011 Great East Japan tsunami in Ishinomaki city using ordinal regression,

and influence of key geographical features. *Stochastic Environmental Research and Risk Assessment*, *28*(7), 1853–1867. http://doi.org/10.1007/s00477-014-0850-2

Charvet, I., Suppasri, A., Kimura, H., Sugawara, D., & Imamura, F. (2015). A multivariate generalized linear tsunami fragility model for Kesennuma City based on maximum flow depths, velocities and debris impact, with evaluation of predictive accuracy. *Natural Hazards*, *79*(3), 2073–2099. http://doi.org/10.1007/s11069-015-1947-8

Chock, G., Robertson, I., & Riggs, R. (2011). TSUNAMI STRUCTURAL DESIGN PROVISIONS FOR A NEW UPDATE OF BUILDING CODES AND PERFORMANCE-BASED ENGINEERING, 1–5.

Cornell, C. A., Asce, M., Jalayer, F., Hamburger, R. O., Asce, M., Foutch, D. A., & Asce, M. (2000). Management Agency Steel Moment Frame Guidelines, (May 2010).

Deierlein, G., & Victorsson, V. (2008). Background Document Fragility Curves for Components of Steel SMF Systems, 1–64.

Ekiert, C., & Filiatrault, A. (2008). Background Document Fragility Curves for Wood Light-Frame Structural Systems, 1–54.

Fanaie, N., & Ezzatshoar, S. (2014). Studying the seismic behavior of gate braced frames by incremental dynamic analysis (IDA). *Journal of Constructional Steel Research*, *99*, 111–120. http://doi.org/10.1016/j.jcsr.2014.04.008

Gogus, A., & Wallace, J. W. (2008). Background Document Fragility Curves for Slab-Column Connections, 1–56.

Goulet, C. a., Haselton, C. B., Mitrani-reiser, J., Beck, J. L., Deierlein, G. G., Porter, K. a., &

Stewart, J. P. (2007). Evaluation of the seismic performance of a code-conforming reinforced-concrete frame building—from seismic hazard to collapse safety and economic losses. *Earthquake Engineering & Structural Dynamics*, *41*(11), 1549–1568. http://doi.org/10.1002/eqe

Grummel, A., & Dolan, D. D. (2010). Background Document Fragility Curves for Cold- Formed Steel Light-Frame Structural Systems, 1–50.

Gulec, C. K., Gibbons, B., Chen, A., & Whittaker, A. S. (2011). Damage states and fragility functions for link beams in eccentrically braced frames. *Journal of Constructional Steel Research*, *67*(9), 1299–1309. http://doi.org/10.1016/j.jcsr.2011.03.014

Gulec, K., Whittaker, A., & Hooper, J. (2009). Background Document Damage States and Fragility Curves for Low Aspect Ratio Reinforced Concrete Walls, 1–71.

Hariri-Ardebili, M. A., Zarringhalam, Y., Estekanchi, H. E., & Yahyai, M. (2013). Nonlinear seismic assessment of steel moment frames using time-history, incremental dynamic, and endurance time analysis methods. *Scientia Iranica*, *20*(3), 431–444. http://doi.org/10.1016/j.scient.2013.04.003

Hatzikyriakou, A., Lin, N., Gong, J., Xian, S., Hu, X., & Kennedy, A. (2015). Component-Based Vulnerability Analysis for Residential Structures Subjected to Storm Surge Impact from Hurricane Sandy. *Natural Hazards Review*, *17*(1), 05015005. http://doi.org/10.1061/(ASCE)NH.1527-6996.0000205

Jalali, S. a., Banazadeh, M., Abolmaali, a., & Tafakori, E. (2011). Probabilistic seismic demand assessment of steel moment frames with side-plate connections. *Scientia Iranica*, *19*(1), 27–40. http://doi.org/10.1016/j.scient.2011.11.036

Jeon, J. S., DesRoches, R., Brilakis, I., & Lowes, L. N. (2012). Modeling and Fragility Analysis of Non-Ductile Reinforced Concrete Buildings in Low-to-Moderate Seismic Zones. *Structures Congress 2012*, 2199–2210. http://doi.org/10.1061/9780784412367.193

Kameshwar, S., & Padgett, J. E. (2014). Multi-hazard risk assessment of highway bridges subjected to earthquake and hurricane hazards. *ENGINEERING STRUCTURES*. http://doi.org/10.1016/j.engstruct.2014.05.016

Kareem, A., & McCullough, M. . (2011). A Framework for Performance-Based Engineering in Multi-Hazard Coastal Environments M., *1020*, 2862–2873.

Koshimura, S., Oie, T., Yanagisawa, H., & Imamura, F. (2009). Developing Fragility Functions for Tsunami Damage Estimation Using Numerical Model and Post-Tsunami Data From Banda Aceh, Indonesia. *Coastal Engineering Journal*, *51*(03), 243–273. http://doi.org/10.1142/S0578563409002004

Lignos, D. G., Zareian, F., & Krawinkler, H. (2008). Reliability of a 4-Story Steel Moment-Resisting Frame against Collapse Due to Seismic Excitations. *Structures 2008: Crossing Borders*, 243–243. http://doi.org/10.1061/41016(314)243

Lowes, L., & Li, J. (2009). Fragility Functions for Reinforced Concrete Moment Frames, 1–191.

Mas, E., Koshimura, S., Suppasri, A., Matsuoka, M., Matsuyama, M., Yoshii, T., … Imamura, F. (2012). Developing Tsunami fragility curves using remote sensing and survey data of the 2010 Chilean Tsunami in Dichato. *Natural Hazards and Earth System Science*, *12*(8), 2689–2697. http://doi.org/10.5194/nhess-12-2689-2012

Moehle, J., & Deierlein, G. G. (2004). Vision 2000 — A Framework for Performance Based

Earthquake Engineering, (January 2004).

Murao, O., & Nakazato, H. (2010). Vulnerability Functions for Buildings Based on Damage Survey Data in Sri Lanka After the 2004 Indian Ocean Tsunami. *International Conference on Sustainable Built Environment (ICSBE-2010) Kandy,* (December), 371–378. http://doi.org/10.3130/aijs.75.1021

Murcia-delso, J., & Shing, P. B. (2009). Background Document Damage States and Fragility Curves for Reinforced Masonry Shear Walls, 1–108.

Murcia-Delso, J., & Shing, P. B. (2012). Fragility Analysis of Reinforced Masonry Shear Walls. *Earthquake Spectra*, *28*(4), 1523–1547. http://doi.org/10.1193/1.4000075

NEHRP Consultants Joint Venture. (2010). Evaluation of the FEMA P-695 Methodology for Quantification of Building Seismic Performance Factors (NIST GCR 10-917-8). *NaTional InsTiTuTe of sTandards and TeChnology, …*. Retrieved from http://scholar.google.com/scholar?hl=en&btnG=Search&q=intitle:Evaluation+of+the+FEMA+P-695+Methodology+for+Quantification+of+Building+Seismic+Performance+Factors#0

Oommen, T., Drive, T., & Baise, L. G. (2013). Documenting Earthquake-Induced Liquefaction Using Satellite Remote Sensing Image Transformations, *XIX*(4), 303–318.

Padgett, J. E., Nielson, B. G., & Desroches, R. (2008). Selection of optimal intensity measures in probabilistic seismic demand models of highway bridge portfolios, (December 2007), 711–725. http://doi.org/10.1002/eqe

Pang, W., & Ziaei, E. (2012). Nonlinear Dynamic Analysis of Soft-Story Light-Frame Wood

Buildings. *Structures Congress 2012*, 1767–1777. http://doi.org/10.1061/9780784412367.156

Pitilakis, K. D., Karapetrou, S. T., & Fotopoulou, S. D. (2014). Consideration of aging and SSI effects on seismic vulnerability assessment of RC buildings. *Bulletin of Earthquake Engineering*, *12*(4), 1755–1776. http://doi.org/10.1007/s10518-013-9575-8

Porter, K., Kennedy, R., & Bachman, R. (2007). Developing Fragility Functions for Building Components for ATC-58, 1–39.

Purba, R., & Bruneau, M. (2014). Seismic Performance of Steel Plate Shear Walls Considering Two Different Design Philosophies of Infill Plates . II : Assessment of Collapse Potential. *Journal of Structural Engineering*, *141*(6), 1–12. http://doi.org/10.1061/(ASCE)ST.1943-541X.0001097.

Rajeev, P., & Tesfamariam, S. (2012). Seismic fragilities of non-ductile reinforced concrete frames with consideration of soil structure interaction. *Soil Dynamics and Earthquake Engineering*, *40*, 78–86. http://doi.org/10.1016/j.soildyn.2012.04.008

Reese, S., Bradley, B. A., Bind, J., Smart, G., Power, W., & Sturman, J. (2011). Empirical building fragilities from observed damage in the 2009 South Pacific tsunami. *Earth-Science Reviews*, *107*(1-2), 156–173. http://doi.org/10.1016/j.earscirev.2011.01.009

Roeder, C. W., Lehman, D. E., & Lumpkin, E. (2009). Background Document Fragility Curves for Concentrically Braced Steel Frames with Buckling Braces, 1–169.

Rojahn, C., Whittaker, A., & Hart, gary. (1995). *ATC 19 Structural Response Modifictaion factors*.

Sabelli, R., Mahin, S., & Chang, C. (2003). Seismic demands on steel braced frame buildings with buckling-restrained braces. *Engineering Structures*, *25*(5), 655–666. http://doi.org/10.1016/S0141-0296(02)00175-X

Suppasri, A., Koshimura, S., & Imamura, F. (2011). Developing tsunami fragility curves based on the satellite remote sensing and the numerical modeling of the 2004 Indian Ocean tsunami in Thailand. *Natural Hazards and Earth System Science*, *11*(1), 173–189. http://doi.org/10.5194/nhess-11-173-2011

Tehranizadeh, M., & Moshref, A. (2011). Performance-based optimization of steel moment resisting frames. *Scientia Iranica*, *18*(2), 198–204. http://doi.org/http://dx.doi.org/10.1016/j.scient.2011.03.029

Tomiczek, T., Kennedy, A., & Rogers, S. (2013). Collapse Limit State Fragilities of Wood-Framed Residences from Storm Surge and Waves during Hurricane Ike. *Journal of Waterway, Port, Coastal, and Ocean Engineering*, *140*(February), 130521221218007. http://doi.org/10.1061/(ASCE)WW.1943-5460.0000212

Unnikrishnan, V. U., Barbato, M., Petrini, F., Ciampoli, M., & Rouge, B. (2013). Probabilistic Performance Based Risk Assessment Considering the Interaction of Wind and Windborne Debris Hazard, *2*(Porter 2003), 1183–1193.

Uriz, P., & Mahin, S. a. (2004). SEISMIC PERFORMANCE ASSESSMENT OF CONCENTRICALLY BRACED STEEL FRAMES, (1639).

Valencia, N., Gardi, A., Gauraz, A., Leone, F., & Guillande, R. (2011). New tsunami damage functions developed in the framework of SCHEMA project : application to European-Mediterranean coasts, 2835–2846. http://doi.org/10.5194/nhess-11-2835-2011

Vamvatsikos, D. (2005). Seismic Performance, Capacity and Reliability of Structures as Seen Through Incremental Dynamic Analysis, (151), 1–172.

Vickery, P. J., Lin, J., Skerlj, P. F., Twisdale, L. a., & Huang, K. (2006). HAZUS-MH Hurricane Model Methodology. I: Hurricane Hazard, Terrain, and Wind Load Modeling. *Natural Hazards Review*, *7*(2), 82–93. http://doi.org/10.1061/(ASCE)1527-6988(2006)7:2(82)

Wongpakdee, N., Leelataviwat, S., Goel, S. C., & Liao, W. C. (2014). Performance-based design and collapse evaluation of buckling restrained knee braced truss moment frames. *Engineering Structures*, *60*, 23–31. http://doi.org/10.1016/j.engstruct.2013.12.014

Appendix A: Lognormal Distribution

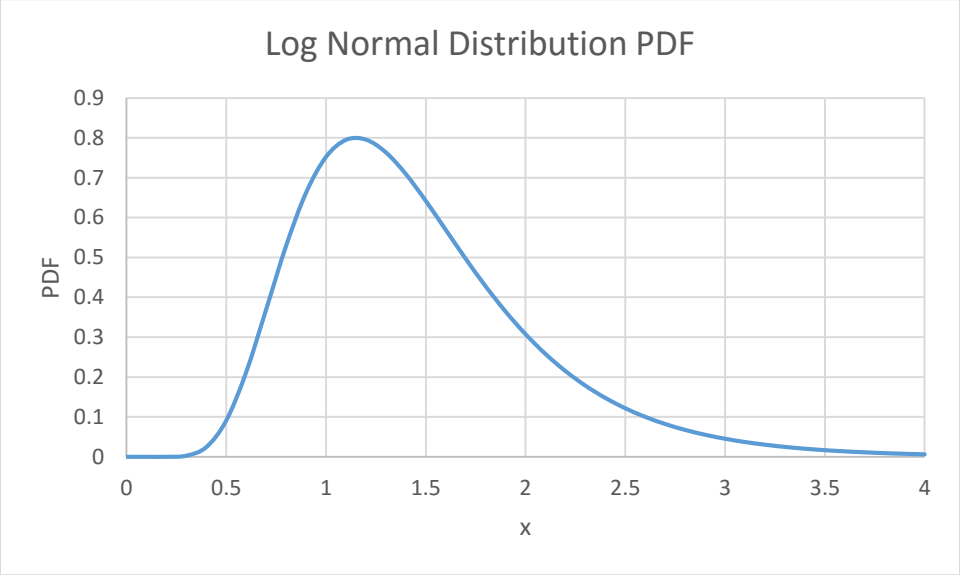

Figure A-1. Typical probability density function of lognormal distribution

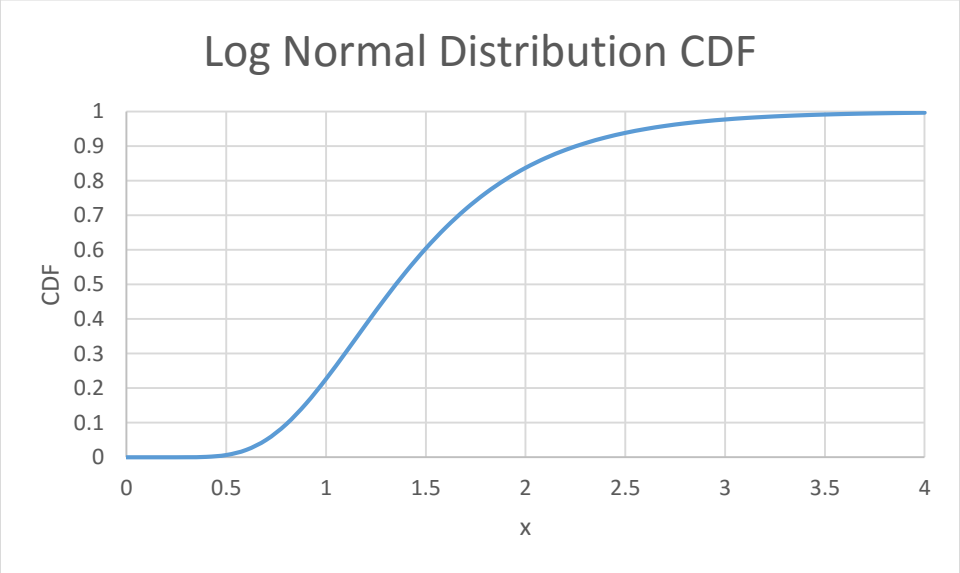

Figure A-2. Typical cumulative density functions for lognormal distribution

Variables:

1. Mean (m)
2. Variance (v)
3. Lognormal Mean (mu)
4. Lognormal Standard deviation (sigma) / Dispersion (β)
5. Median (θ)

   Following equations are obtained from (Benjamin & Cornell, 2014) for the conversion of the variables.

$$\mu = ln\left(\frac{m}{\sqrt{1+\frac{v}{m^2}}}\right)$$

$$\sigma = \sqrt{\ln\left(1+\frac{v}{m^2}\right)}$$

$$\theta = \frac{m}{\sqrt{e^{\sigma^2}}}$$

$$\theta = e^{\mu}$$

Appendix B: Pinch Point Terminology

Hazard

Hurricane:	"A tropical cyclone in which the maximum sustained surface wind (using the U.S. 1-minute average) is 64 kt (74 mph or 119 km/hr) or more" (noaa.gov)
Earthquake:	"A sudden and violent shaking of the ground, sometimes causing great destruction, as a result of movements within the earth's crust or volcanic action" (google.com)
Tsunami:	An aspect of an earthquake, but for this study will it will be treated as a separate hazard defined as "a long high sea wave caused by an earthquake, submarine landslide, or other disturbance" (google.com)

Hazard Aspects

Wind Pressure:	The positive (pushing) and negative (pulling) pressures produced by the wind that are exerted on the building exterior and interior components
Uplift:	Wind flow over the top of the roof system that creates negative pressure greater than below it, which can cause the roof to lift off of the structure
Windborne Debris:	Debris that enters a wind stream becoming airborne and travels at a portion of the wind velocity with the potential to impact a building
Wind-Driven Rain:	Rain forced into exterior enclosure openings and joints as a result of wind occurring simultaneously
Rain:	Precipitation in the form of liquid water
Standing Water:	A large body of standing that partially or completely inundates typically dry building interior and/or exterior areas and exerts hydrostatic loads
Waterborne Debris:	Debris that enters a water stream becoming waterborne and travels at a portion of the water flow velocity with the potential to impact a building
Wave:	Moving water across the surface of large bodies of water that can break on and strike a building that exerts hydrodynamic loads
Erosion:	Loss of ground surface area primarily due to flood and/or wave loads

Scour:	Loss of soil surrounding obstructions such as foundation elements due to flood and/or wave forces
Ground Motion:	Movement of the ground
Liquefaction:	The conversion of solid soil into quick sand under the following conditions: loose granular soil, ground motion, and saturated soil
Landslide:	Movement of land due to its unstable slope

Intensity Measures

Wind Velocity:	The distance at which wind moves over time
Exposure:	Local surroundings, building characteristics, and topography influences on wind velocity
Debris Class:	The shape, mass, and origin of debris
Debris Velocity:	The distance at which debris travels over time
Rainfall Intensity:	The amount of rainfall over time
Standing Water Elevation:	The height of standing water above ground level
Standing Water Duration:	The amount of time the standing water persists
Wave Height:	The distance at which a wave rises above the water surface as a result of wave energy gained from the wind
Wave Period:	The time between consecutive wave crests
Wave Velocity:	The distance at which the wave moves over time
Ground Accelerations:	Acceleration of the ground that is normally measured in g's

Engineering Demand Parameters

Deflection:	Amount of movement or displacement of a building element under a load (e.g. wall panel)

Interstory Drift Ratio:	The drift of one level of a multistory building relative to the level below divided by the height of that level
Roof Drift Ratio:	The drift of the roof of the building divided by the height of the building
Residual Drift:	A measure that shows how plumb is the building after the hazard has passed
Volume of water:	Amount of water intrusion into a building enclosure component
Settlement:	The downward movement of the entire building to a point below its original position
Differential Settlement:	When different parts of the building have different settlements
Floor Acceleration:	Acceleration of floors when the building is subjected to ground motion
Floor Velocity:	Velocity of floors when the building is subjected to ground motion

Damage States

Peel/Detachment:	Separation or loosening of cladding materials, sealants, joints, or connections
Deformation:	Permanent material shape distortion
Break/Crack/Tear:	Initial split or puncture of an enclosure material or complete component that does not lead to a separation into multiple pieces
Crack Displacement:	Long-term crack – change in crack width over time
Collapse:	Falling down of cladding materials or complete components
Wetting:	Moisture intrusion and/or saturation of building materials and components

Performance Parameters - Enclosure

Moisture Control:	Rainscreens and cladding materials used to provide moisture resistance surfaces and to control bulk water through the process of either drainage, evaporation, or diffusion

Air Control:	Airtight materials and the use of sealants to completely close joints and connections to prevent air infiltration
Vapor Control:	The use of permeability to control vapor diffusion through materials
Thermal Control:	Insulating materials used to control heat loss
Structure:	Supports the building structure and cladding materials, as well as load transfer (load paths)

Decision Variables

Casualties:	Number of fatalities due to the hazard.
Repair Cost:	Total cost to repair the building.
Repair Time:	Total time to repair the building.
Carbon Emission:	The total amount of greenhouse gas emissions from a building.
Embodied Energy:	It is the total energy consumed in the development of a building.
Building Lifetime:	The total service life of a building.

Appendix C: Guide to Database

The database is distributed into following five tables.

1. Initial Parameters
2. IM to EDP
3. EDP to DS
4. DS to DV
5. IM to DS

Table C-1 to C-5 describes the column fields in the corresponding tables.

Table C-1. Guide for Initial parameters table

Column Field	Description
System	Name of the system e.g. soil, foundation, structure, and envelope
Sub Category	Subcategory of the system e.g. concrete, infill walls
Name	Name of component
Description	Detailed description of the component
Initial Cost ($/ft2)	Initial cost includes estimates for labor and material
Initial EE (MJ/m2)	Initial embodied energy (EE) is total primary energy
Initial EE in (Btu/ft2)	Initial embodied energy (EE) is total primary energy
Initial Energy (BTUh/ft2)	Initial energy is currently based upon heat transfer rate only (loss of energy)

Table C-2. Guide for IM to EDP table

Column Field	Description
Sr. no	Serial number of entry
Source	Author name and year of research paper e.g. (Fanaie & Ezzatshoar, 2014)
Type	Type of curves e.g. IM to EDP, Collapse fragility curve
Hazard	Name of hazard e.g. Earthquake, Tsunami
Material	Construction material of frame e.g. steel, concrete
Structural system	Name of structural system e.g. steel moment frame
Period (s)	First mode period of building
Period description	Information about period e.g. calculation method either analysis or ASCE 7 equation
IM Description	Name of IM e.g. Sa (5%,T1)
IM Unit	Units of IM e.g. g
Area	Total floor plan area of building in ft^2
Mass	Total mass of building or dead and live loading used for design
Frame	Information about lateral force resisting system e.g. 2 Frames, 3 Bays @ 18' means 2 frames in the direction of loading applied, 3 bays in each frame spaced at 18’
Code	Code used for the design of building e.g. ASCE (2005) and ANSI/AISC341-05 (2005)
Ground Motion Description	Information about how ground motions for IDA were collected e.g. FEMA 440 ground motions related to Soil Class B
Site Class	USGS site class e.g. D,B
EDP Description	EDP name e.g. Inter story drift
EDP Unit	Units of EDP e.g. in/in
Slope Unit	Units of the slope of the bilinear approximation of IDA curve
Slope	Slope of the bilinear approximation of IDA curve
Sa Median Collapse	Median spectral acceleration collapse of the bilinear approximation of IDA curve
Dispersion	Lognormal dispersion
Components of dispersion	Name of sources of uncertainty included in the dispersion e.g aleatory, epistemic
Analysis	Name of analysis e.g. IDA
Age (Years)	Normally it is 0, but when deterioration and aging effects are considered it will have the age of structure at the time of analysis
Code Quality	Quality of code e.g. Special, ordinary
Number of Ground Motions	Number of ground motions used in IDA
Location	Location of Prototype building
Other	Any other significant information

Table C-3. Guide for EDP to DS table

Column Field	Description
Sheet Names	Name of sheet in fragility specifications in FEMA P-58
Run this Line?	YES or NO to include this line in PACT
File	File number in FEMA P-58
Type	Material type e.g. steel, concrete
Source	Author name and year of research paper e.g. FEMA P-58
Basis	How curves are developed e.g. test data , engineering judgment
Duplicate Names or Numbers?	Any duplicates
NISTIR Classification	FEMA P-58 naming convention
Component Name	Name of component
Component Description	Description of component
Construction Quality:	Quality of construction if specified
Seismic Installation Conditions:	Specific requirements for seismic installation if any
Normative Quantity (value):	Quantity to measure component e.g. each
Normative Quantity (unit):	Unit of normative quantity
Demand Parameter (value):	Engineering demand parameter on which fragility curves are based e.g. interstory drift ratio, peak floor accelerations
Demand Parameter (unit):	Unit of Demand parameter e.g. unit less, g
Number of Damage States:	Number of damage states of component
DS 1 to DS 5	Names of damage states normally DS1 to DS5
DS 1 to DS 5 Type	Type of DS e.g. Sequential, Mutually exclusive and Simultaneous see section 5.2 for definition of terms
DS Hierarchy	Order of DS e.g. DS1,DS2,DS3
Line Number	Line number in database
Costing Normative Unit	Quantity used for costing
Round to Integer Unit?	Whether to round costing quantity to integer or not.
Multi-Occupancy Fragility, allow summation by Floor or Building?	Typically NO.
DS 1 to DS 5, Description	Description of damage in a component related to DS
DS 1 to DS 5, Probability	The probability of DSs occurring for sequential is 1 and for other types it depends on the data.
DS 1 to DS 5, Median Demand	Median value of IM for fragility curves of DSs
DS 1 to DS 5, Data Dispersion	Dispersion of IM for fragility curves of DSs. It is due to uncertainty in the data.
DS 1 to DS 5, Uncertainty	Uncertainty accounts variability in construction quality of the component.
DS 1 to DS 5, Total Dispersion (Beta)	Vector sum of data dispersion and uncertainty is equal to total dispersion
Correlated?	Yes means all member of the performance group will have same damage state for each realization and NO means they will have different damage state

Column Field	Description
Directional?	Yes if component is sensitive to direction of shaking e.g. walls are vulnerable to in plane shaking otherwise NO
Data Quality	The quality of data on which fragility curves are based.
Data Relevance	The relevance of data on which fragility curves are based.
Documentation Quality	Documentation quality of the fragility curves development
Rationality	Level of Rationality in the development of fragility curves
DS 1 to DS 5, Repair Description	Method of repair for the corresponding damage state
DS 1 to DS 5, Long Lead Time	Time to procure specialized equipment and materials for building.
DS 1 to DS 5, Potential non-collapse casualty?	Potential of non-collapse casualty
DS 1 to DS 5 - Casualty Affected Area	Causality affected Area for corresponding damage states
DS 1 to DS 5 Serious Injury Rate - Median	Median value of EDP for serious injury rate
DS 1 to DS 5 Serious Injury Rate - Dispersion	Dispersion of EDP for serious injury rate
DS 1 to DS 5, Unsafe Placard Trigger Flag	Yes means the component at corresponding damage state can cause unsafe placard. Unsafe placard in a rating based on a post-earthquake survey whether it is safe to enter building or not.
DS 1 to DS 5, Unsafe Placard Damage Median	Median value of EDP for unsafe placard
DS 1 to DS 5, Unsafe Placard Damage Dispersion	Dispersion of EDP for unsafe placard
Comments / Notes	Any comments
Date Created	Date of creation
Approved	Name of person who approves
Official	official
Author	Who developed fragility curves
DS1 to DS 5, Illustrations	Name of files that have pictures of damage states
Demand Location (use floor above? Yes/No)	Typically it is no for structural components
Revision History	Information about revision history
Component Sub Types?	Yes If there are sub types of component.

Table C-4. Guide for DS to DV table

Column Field	Description
Sheet Names	Name of sheet in fragility specifications in FEMA P-58
Run this Line?	YES or NO to include this line in PACT
File	File number in FEMA P-58
Type	Material type e.g. steel, concrete
Source	Author name and year of research paper e.g. FEMA P-58
Basis	How curves are developed e.g. test data , engineering judgment
NISTIR Classification	FEMA P-58 naming convention
Component Name	Name of component
Repair Cost, p10, DS1 to DS5	Value of repair cost at 10% probability
Repair Cost, p50, DS1 to DS5	Value of repair cost at 50% probability
Repair Cost, p90, DS1 to DS5	Value of repair cost at 90% probability
Repair Cost Best Fit, DS1 to DS5	Type of distribution either lognormal or normal
Repair Cost Mean Value, DS1 to DS5	Mean value of repair cost
Repair Cost CV / Dispersion, DS1 to DS5	Dispersion of repair cost
Repair Cost Lower Qty. Cutoff, DS1 to DS5	Quantity at which repair cost starts to decrease linearly. See Figure 6-1
Repair Cost Lower Qty. Mean, DS1 to DS5	Mean repair cost value before the lower quantity. See Figure 6-1
Repair Cost Upper Qty. Mean, DS1 to DS5	Mean repair cost value after the upper quantity. See Figure 6-1
Repair Cost Upper Qty. Cutoff, DS1 to DS5	Quantity at which repair cost become constant. See Figure 6-1
Repair Cost Quantity Unit, DS1 to DS5	Unit in which number of components are measured
Time, p10, DS1 to DS5	Value of repair time at 10% probability
Time, p50, DS1 to DS5	Value of repair time at 50% probability
Time, p90, DS1 to DS5	Value of repair time at 90% probability
Time Best Fit, DS1 to DS5	Type of distribution either lognormal or normal
Time Mean Value, DS1 to DS5	Mean value of repair time
Time CV / Dispersion, DS1 to DS5	Dispersion of repair time
Time Lower Qty. Cutoff, DS1 to DS5	Quantity at which repair time starts to decrease linearly. See Figure 6-1
Time Lower Qty. Mean, DS1 to DS5	Mean repair time value before the lower quantity. See Figure 6-1
Time Upper Qty. Mean, DS1 to DS5	Mean repair time value after the upper quantity. See Figure 6-1
Time Upper Qty. Cutoff, DS1 to DS5	Quantity at which repair time become constant. See Figure 6-1
Time Quantity Unit, DS1 to DS5	Unit in which number of components are measured

Table C-5. Guide for IM to DS table

Column Field	Description
Sr. No.	Serial number of entry
Hazard	Name of hazard e.g. Earthquake, Tsunami
Source	Author name and year of research paper e.g. (Fanaie & Ezzatshoar, 2014)
Basis	How fragility curves are developed e.g. empirical, analysis, testing
Component Name	Name of component
Component Description	Detailed description of the component
Event	Name and year of hazard event
Location	Location of the buildings used to develop fragility curves
Intensity Measure	Name of IM e.g. water depth
Intensity Measure (unit):	Units of IM e.g. meters
Number of Damage States:	Number of damage states e.g. 5,2
Distribution	Type of distribution e.g. lognormal, normal
DS 1 to DS 5, Type	Type of DS e.g. Sequential, Mutually exclusive and Simultaneous see section 5.2 for definition of terms
DS 1 to DS 5, Description	Description of damage in a component related to DS
DS 1 to DS 5, Median Demand	Median value of IM for fragility curves of DSs
DS 1 to DS 5, Data Dispersion	Dispersion of IM for fragility curves of DSs
DS 1 to DS 5, Repair Description	Method of repair for the corresponding damage state

Appendix D: Software Utility for Extracting Fragility Curves

A set of tools was developed to extract fragility curves from the research papers using graphs. In total seven tools were developed MATLAB and later on Visual studio was to combine these tools into one program and to develop a graphical user interface. All tools use least squares approach to fit lognormal CDF function to given data. There are two main tabs: cumulative density function (CDF) and probability density function (PDF). Cumulative density function tab is further divided into following six sub tabs.

1. 2-Point Method
2. Theta and Beta
3. Mean and Variance
4. Mean and COV
5. Data Points
6. IDA Curve

2-Point Method can be used when coordinates of two points on a lognormal CDF are known. It is not a good tool if points are not from a CDF function because as the difference between CDF and the data points increases it becomes less reliable. In that case, it is more appropriate to use the Data points tab because it allows to input coordinates of more than two points. Range min and Range max are used to define the bounds of the variable on x-axis and it is also crucial that the median of CDF lies within this range. Interval defines the interval of variables on x-axis at which values of cumulative probability are calculated. Theta and Beta tab can be used to draw the CDF and calculate probability at intervals of x values given theta and beta values. Mean and Variance and Mean and COV tabs work similar to Theta and Beta and they also calculate theta and beta values of the CDF. Data points tab work similar to 2-point method except multiple points can be used in it. It is best to use this tool when data points are not on a smooth CDF that can be represented by one theta and beta. IDA Curve tab is used to find lognormal dispersion values for

IDA curves at regular intervals of x-axis values. Slope and Spectral acceleration at collapse values for 16%, 50%, and 84% fractiles are input into the program. The last tool is the Probability Density Function tab. It works similar to the 2-point method except the coordinates entered into this tool are from a probability density function. All tools show the results in the form of plot and give output in a table format. Figure D-1 to D-7 shows the screen shots of the tools.

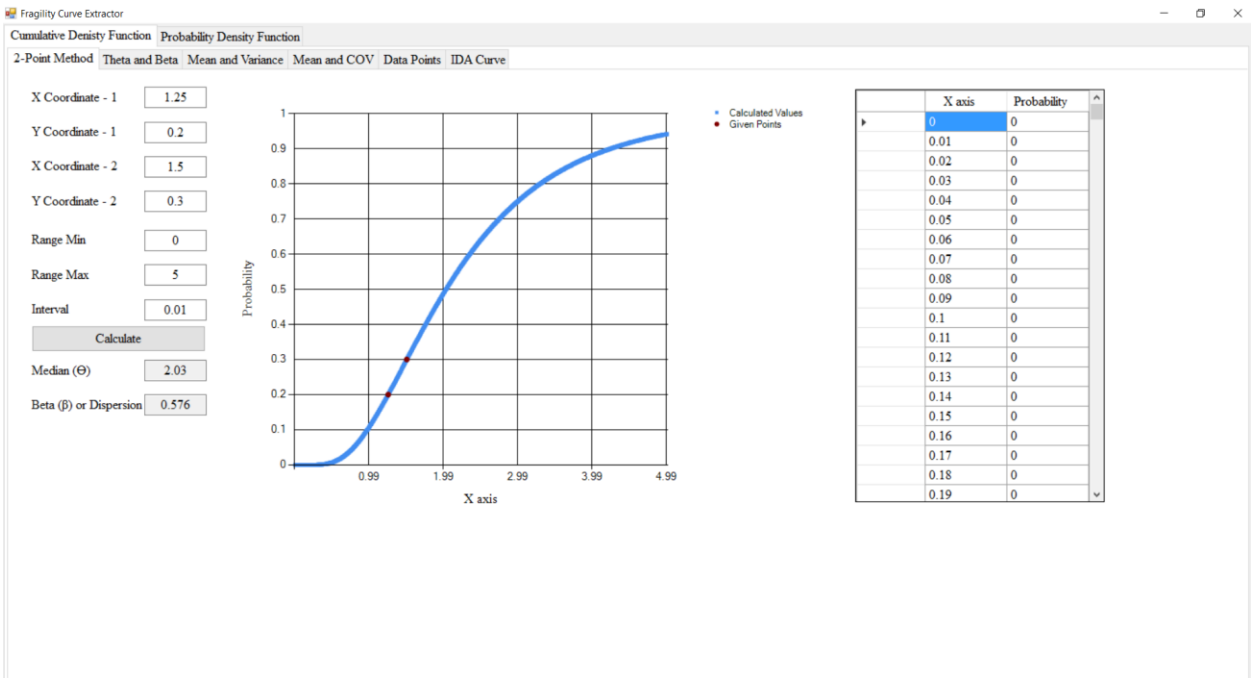

Figure D-1. 2-Point Method tab screen shot

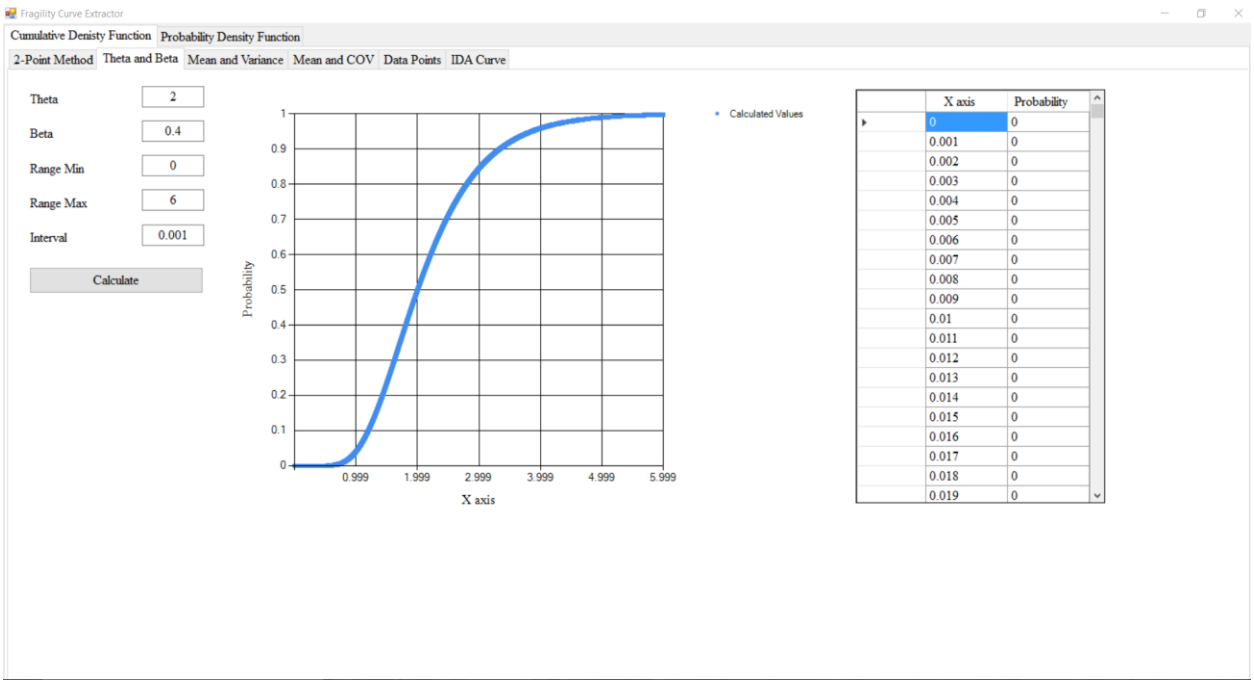

Figure D-2. Theta and Beta tab screen shot

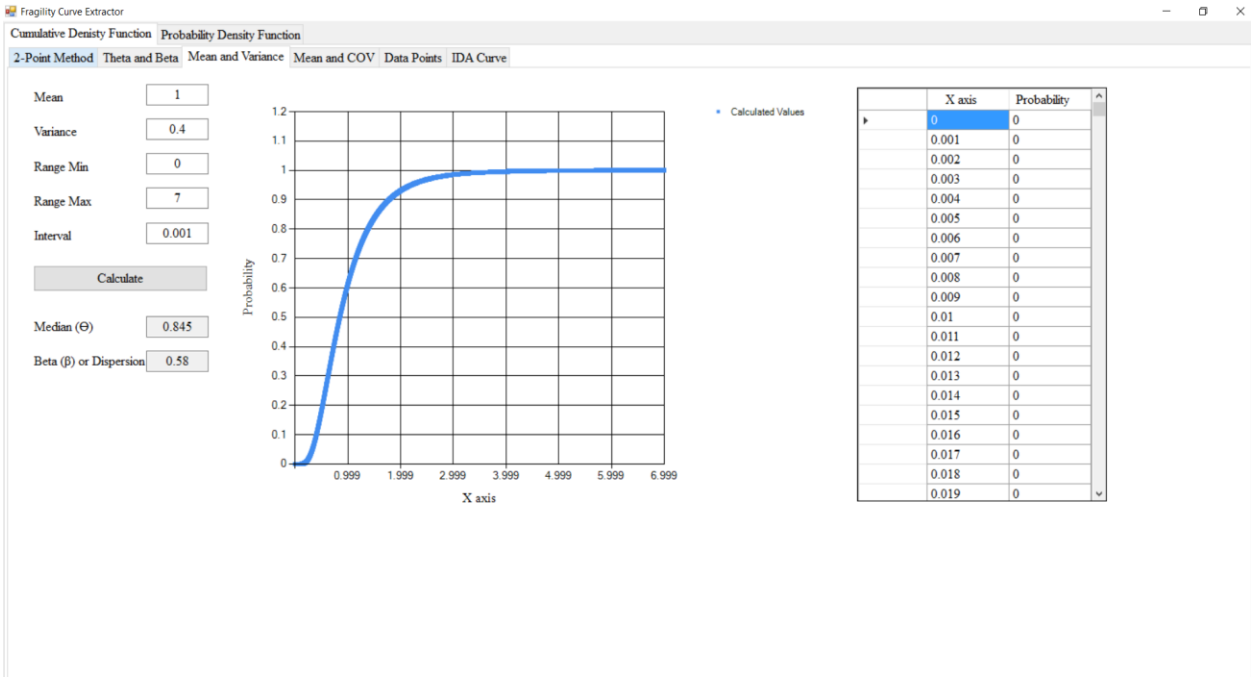

Figure D-3. Mean and Variance tab screen shot

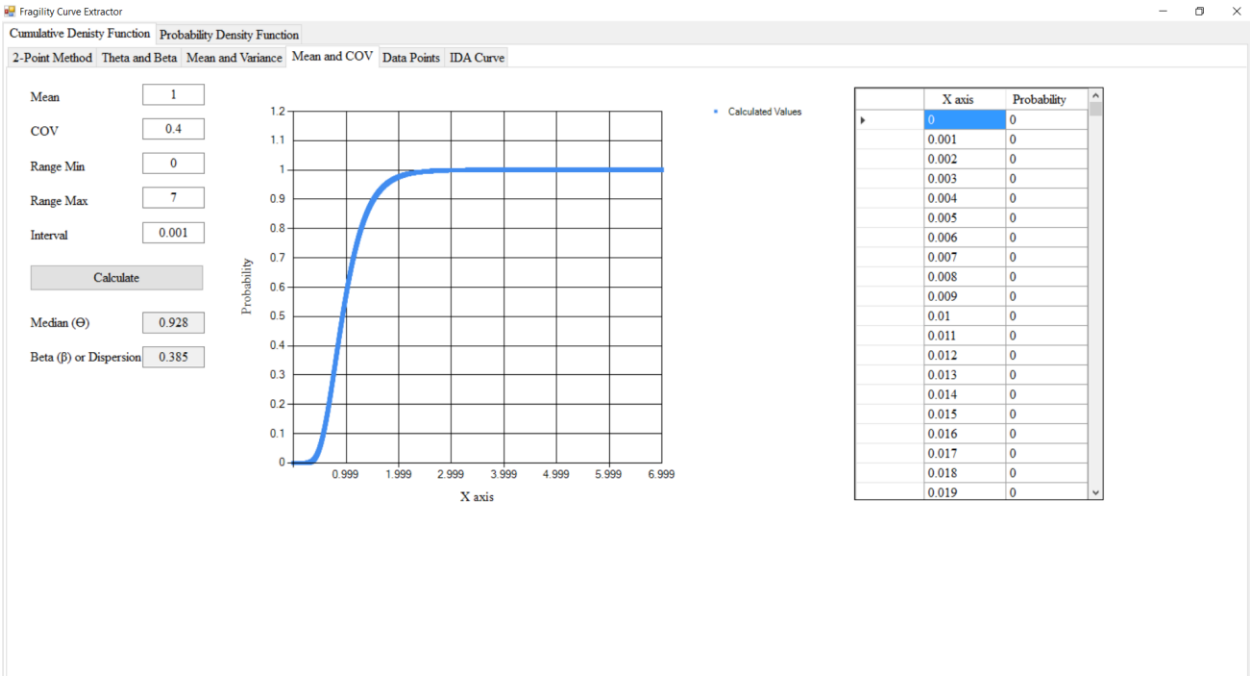

Figure D-4. Mean and COV tab screen shot

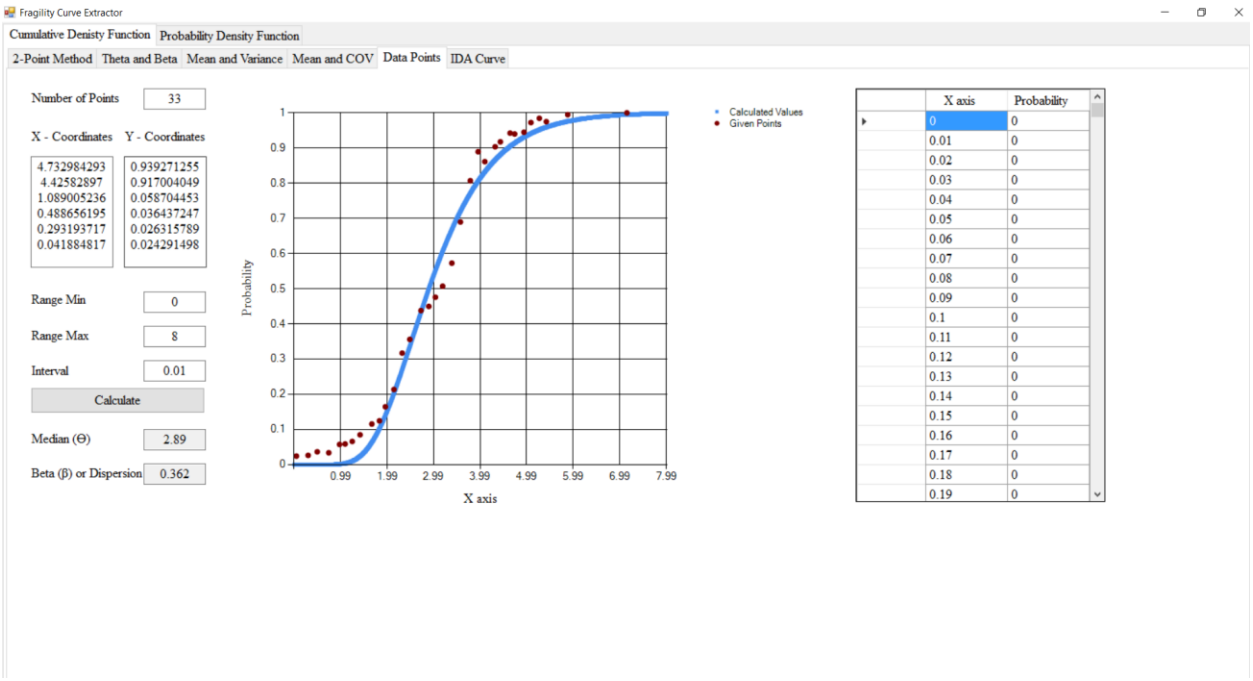

Figure D-5. Data Points tab screen shot

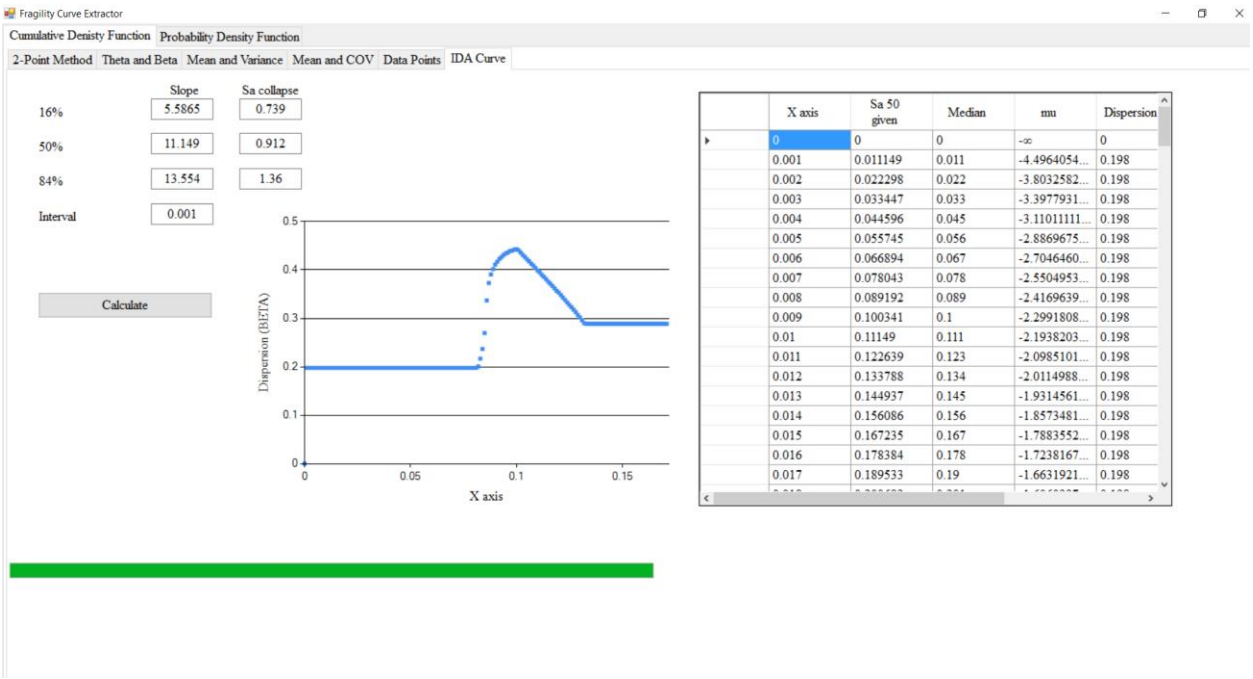

Figure D-6. IDA Curve tab screen shot

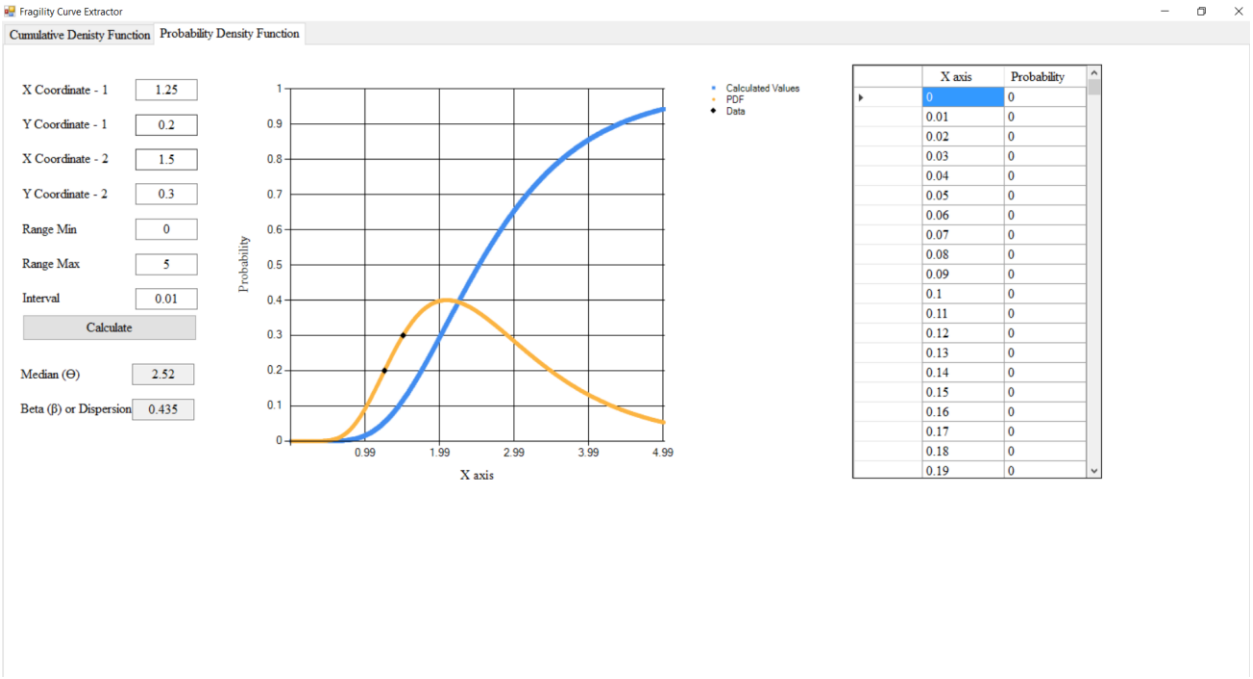

Figure D-7. Probability Density Function tab screen shot